

**EFFECTS OF MICROMECHANICAL FACTORS
IN THE STRAIN INVARIANT FAILURE THEORY
FOR COMPOSITES**

ARIEF YUDHANTO

NATIONAL UNIVERSITY OF SINGAPORE

2005

**EFFECTS OF MICROMECHANICAL FACTORS IN
THE STRAIN INVARIANT FAILURE THEORY
FOR COMPOSITES**

ARIEF YUDHANTO

(B.Eng, BANDUNG INSTITUTE OF TECHNOLOGY)

**A THESIS SUBMITTED FOR THE DEGREE OF
MASTER OF ENGINEERING
DEPARTMENT OF MECHANICAL ENGINEERING
NATIONAL UNIVERSITY OF SINGAPORE**

2005

To my wife, Tuti, and my parents, Goenawan and Annie

Acknowledgement

The author would like to sincerely thank his supervisor **Associate Professor Tay Tong Earn** for his guidance, advice, encouragement and support throughout his research.

The author would also like to thank **Dr Tan Beng Chye, Vincent** for his advice and guidance on various theoretical aspects of the research.

The author would like to extend his special thanks to Solid Mechanics Lab students **Dr Serena Tan** and **Mr Liu Guangyan** for their invaluable help which has contributed greatly to the completion of this work. Thanks to my best friends **Mr Mohammad Zahid Hossain** and **Dr Zhang Bing** for their sincerity in great friendship.

Special thanks are also addressed to **JICA/AUNSEED-Net** for financial support during his studies and research at National University of Singapore. Thanks to **Dr Ichsan Setya Putra, Dr Bambang K Hadi, Dr Dwiwahju Sasongko, Dr Hari Muhammad, Professor Djoko Suharto** (Bandung Institute of Technology), **Ms Meena Thamchaipenet** (AUNSEED-Net, Thailand) and **Mrs Corrina Chin** (JICA, Singapore) for their support during my undergraduate and postgraduate studies.

Finally, the author would like to thank his beloved wife, **Tuti**, for her encouragement during his studies, research and stay in Singapore. Thanks to **Yunni & Fauzi** for providing an ‘emergency room’ with nice ambience.

Table of Contents

Acknowledgement.....	i
Table of Contents.....	ii
List of Articles by the Author.....	iv
Summary.....	v
List of Figures.....	vi
List of Tables.....	x
List of Symbols.....	xi
List of Abbreviations.....	xiv
1. Introduction.....	1
1.1 Background.....	1
1.2 Problem Statement.....	2
1.3 Research Objectives.....	3
1.4 Overview of the Thesis.....	3
2. Literature Review of Micromechanics-Based Failure Theory.....	5
2.1 Micromechanics.....	5
2.2 Failure at Micro-Level.....	7
2.3 Literature Review of Micromechanics-Based Failure Theory.....	8
3. Strain Invariant Failure Theory (SIFT).....	11
3.1 Theory Background.....	11
3.2 Critical Strain Invariants.....	14
3.3 Concept of Strain Amplification Factor.....	16
3.4 Methodology of Extracting Strain Amplification Factors.....	18
3.5 Micromechanical Modification.....	25

4. Strain Amplification Factors	27
4.1 Elastic Properties of Fiber and Matrix	27
4.2 Single Cell and Multi Cell Models	28
4.3 Square, Hexagonal and Diamond RVEs	33
4.4 Effect of Fiber Volume Fraction.....	40
4.5 Effect of Fiber Moduli, Matrix Modulus and Fiber Materials	45
4.6 Maximum Strain Amplification Factors.....	50
5. Damage Progression in Open-Hole Tension Specimen	53
5.1 Element Failure Method	53
5.2 EFM and SIFT to Predict Damage Progression.....	55
5.3 Open-Hole Tension Specimen	56
5.4 Damage Progression in Open-Hole Tension Specimen	57
5.5 Effect of Fiber Volume Fraction	59
6. Conclusions and Recommendations	63
6.1 Conclusions	63
6.1 Recommendations	65
References	66
Appendix A: Mechanical and thermo-mechanical strain amplification factors for $V_f = 50\%$	70
Appendix B: Mechanical and thermo-mechanical strain amplification factors for $V_f = 60\%$	80
Appendix C: Mechanical and thermo-mechanical strain amplification factors for $V_f = 70\%$	90

List of articles by the author

1. Yudhanto A, Tay T E and V B C Tan (2005). Micromechanical Characterization Parameters for A New Failure Criterion for Composite Structures, *International Conference on Fracture and Strength of Solids, FEOFS 2005*, Bali Island, Indonesia, 4-6 April 2005.
2. Yudhanto A, Tay T E and V B C Tan (2006). Micromechanical Characterization Parameters for A New Failure Criterion for Composite Structures. *Key Engineering Materials*, Vol. 306 – 308, pp. 781 - 786, Trans Tech Publications Inc. (*in publisher preparation*)
3. Tay T E, Liu G, Yudhanto A and V B C Tan (2005). A Multi-Scale Approach to Modeling Progressive Damage in Composite Structures, submitted to *Journal of Damage Mechanics*.

Summary

As a newly-developed failure theory for composite structures, many features in Strain Invariant Failure Theory (SIFT) must be explored to give better insight. One important feature in SIFT is micromechanical enhancement, whereby the strains in composite structures are “amplified” through factors so-called strain amplification factors. Strain amplification factors can be obtained by finite element method and it is used to include micromechanics effect as a result of fiber and matrix interaction due to mechanical and thermal loadings. However, the data of strain amplification factors is not available in the literature. In this thesis, strain amplification factors are obtained by three-dimensional finite element method. Strain amplification factors are obtained for a particular composite system, i.e. carbon/epoxy, and for a certain fiber volume fraction V_f (in this case, as reference, $V_f = 60\%$). Parametric studies have also been performed to obtain strain amplification factors for $V_f = 50\%$ and $V_f = 70\%$. Other composite systems such as glass/epoxy and boron/epoxy are also discussed in terms of strain amplification factors. Open-hole tension specimen is chosen to perform the growth of damage in composite plate. Finite element analysis incorporating Element-Failure Method (EFM) and SIFT within an in-house finite element code was performed to track the damage propagation in the open-hole tension specimen. The effect of fiber volume fraction can be captured by observing the damage propagation.

List of Figures

Figure 2-1	Photomicrograph of typical unidirectional composite: random fiber arrangement [<i>Herakovich, 1998</i>]6
Figure 2-2	Representative volume elements for micromechanics analysis (a) square array (b) hexagonal array.6
Figure 3-1	Failure envelope for polymer..... 11
Figure 3-2	Representative micromechanical blocks with (a) square, (b) hexagonal and (c) diamond packing arrays..... 18
Figure 3-3	Finite element models of square array with fiber volume fraction V_f of 60% (a) single cell model and (b) multi cell model consist of 27 single cells 19
Figure 3-4	Finite element models of hexagonal and diamond array in the multi cell arrangement ($V_f = 60\%$) (a) hexagonal and (b) diamond.....20
Figure 3-5	Micromechanical block is loaded with prescribed displacement ($\Delta L = 1$) to perform normal deformation 1, 2 or 3 and shear 12, 23 and 13 deformations. Deformed shape of three normal directions can be seen in (a) 1-direction, (b) 2-direction and (c) 3-direction and three shear displacements can be seen in (d) 12-direction, (e) 23-direction and (f) 13-direction.....21
Figure 3-6	Application of temperature difference $\Delta T = -248.56^\circ\text{C}$ into finite element model is done after all sides of micromechanical block being constrained.....23
Figure 3-7	Local strains are extracted in the single cell within multi cell in order to obtain strain amplification factors: (a) single cell is taken in the middle cut of multi cell model, (b) local strains are extracted in various positions within

	fiber and matrix phase. There are total 20 points in the matrix, fiber and interface.....	24
Figure 3-8	Location of selection points in (a) hexagonal single cell and (b) diamond single cell.....	25
Figure 4-1	Mechanical strain amplification factors of single cell and multi cell square array loaded in direction-2 (M_{22}) at the 20 selected points described in the square model.	29
Figure 4-2	Strain contour of multi cell model of square array when it is subjected to transverse loading (direction-2)	30
Figure 4-3	Mechanical amplification factors of single cell and multi cell square array loaded in 12-direction	31
Figure 4-4	Thermo-mechanical amplification factors in 2-direction of single cell and multi cell of square models.....	33
Figure 4-5	Mechanical amplification factors of square, hexagonal and diamond array loaded in 2-direction (a) mechanical amplification factors in direction-2 (b) fiber packing arrangement of square, hexagonal and diamond array.....	34
Figure 4-6	Strain contours of single cell within multi cell model of square array. Multi cell is subjected to loading in direction-2. Location of maximum strain is indicated	35
Figure 4-7	Strain contours of single cell within multi cell model of (a) hexagonal and (b) diamond arrays. Multi cells are subjected to loading in direction-2. Location of maximum strain is indicated.....	36
Figure 4-8	Comparison of strain amplification factors of direction-2 and direction-3 cases	37
Figure 4-9	Strain contour of hexagonal array subjected to direction-3 loading	38

Figure 4-10	Thermo-mechanical amplification factors of square, hexagonal and diamond array in 3-direction (selected points in micromechanics models can be seen in Figure 4-5b).....	39
Figure 4-11	Strain of square, hexagonal and diamond in direction-3	40
Figure 4-12	Mechanical amplification factors of square array with volume fraction of 50%, 60% and 70% loaded in direction-2.....	41
Figure 4-13	Mechanical amplification factors of square array with volume fraction of 50%, 60% and 70% loaded in direction-13	42
Figure 4-14	Thermo-mechanical amplification factors of square array with volume fraction of 50%, 60% and 70% in 2-direction.....	43
Figure 4-15	Effect of changing fiber longitudinal modulus (E_{11f}) on amplification factors M_{22}	46
Figure 4-16	Effect of changing fiber transverse modulus (E_{22f}) on amplification factors M_{22}	47
Figure 4-17	Effect of changing transverse modulus (G_{23f}) on amplification factors of M_{23}	48
Figure 4-18	Effect of changing matrix modulus (E_m)	49
Figure 4-19	Effect of changing fiber materials on amplification factors M_{22} . Fibers are graphite, glass and boron	50
Figure 5-1	(a) FE of undamaged composite with internal nodal forces, (b) FE of composite with matrix cracks. Components of internal nodal forces transverse to the fiber direction are modified, and (c) Completely failed element. All nett internal nodal forces of adjacent elements are zeroed	54

Figure 5-2	Schematic of the open hole tension specimen	56
Figure 5-3	Damage progression of ply-1 and ply-2 of laminated composite [45/0/-45/90]s (Vf = 60%)	57
Figure 5-4	Damage progression of ply-3 and ply-4 of laminated composite [45/0/-45/90]s (Vf = 60%)	58
Figure 5-5	Damage pattern of open-hole tension specimen CFRP [45/0/-45/90]s: comparison between experiment and schematic damage map (FEM result).....	58
Figure 5-6	Damage progression of ply-1 and ply-2 of laminated composite [45/0/-45/90]s (Vf = 50%)	59
Figure 5-7	Damage progression of ply-3 and ply-4 of laminated composite [45/0/-45/90]s (Vf = 50%)	60
Figure 5-8	Damage progression of ply-1 and ply-2 of laminated composite [45/0/-45/90]s (Vf = 70%)	60
Figure 5-9	Damage progression of ply-3 and ply-4 of laminated composite [45/0/-45/90]s (Vf = 70%)	61
Figure 5-10	Superimposed damage patterns of CFRP [45/0/-45/90]s for Vf = 50%, Vf = 60% and Vf = 70%.	62

List of Tables

Table 2-1	Type of failure in composite at micro-level and corresponding mechanism8
Table 3-1	Critical strain invariant values and corresponding laminated lay-up used to obtain the value [<i>Gosse et al, 2002</i>].....15
Table 3-2	Definition of boundary conditions BC1 to BC6 used in the extraction of mechanical strain amplification factors.22
Table 4-1	Mechanical and thermal properties of fiber (graphite—IM7) and matrix (epoxy) used in micromechanics model of composite [<i>Ha, 2002</i>].....27
Table 4-2	Mechanical amplification factors of single cell and multi cell square array loaded in direction-1232
Table 4-3	Effect of fiber volume fraction V_f on amplification factors in square array model (figures in bold are maximum values; figures in italic for next highest value).....44
Table 4-4	Elastic properties of glass and boron [<i>Gibson, 1994</i>]49
Table 4-5	Maximum mechanical amplification factors51
Table 4-6	Maximum thermo-mechanical amplification factors52

List of Symbols

Subscripts 1,2,3	Directions of material coordinate system where 1 refers to longitudinal direction of the fiber, 2 and 3 refer to transverse direction
Subscripts x, y, z	Directions of global coordinate system
Subscripts m	Matrix phase
Subscripts f	Fiber phase
V_f	Fiber volume fraction
J_1, J_2, J_3	First, second and third invariant of strain
$\epsilon_{xx}, \epsilon_{yy}, \epsilon_{zz}$	Strains in x, y and z direction
$\epsilon_{xy}, \epsilon_{xz}, \epsilon_{yz}$	Strains in xy, xz and yz direction
J_{1-Crit}	Volumetric strain invariant at matrix phase
α	Coefficients of thermal expansion
ΔT	Temperature difference
$\epsilon_{xx}^{mech}, \epsilon_{yy}^{mech}, \epsilon_{zz}^{mech}$	Mechanical strains in x, y and z directions
$\bar{\epsilon}$	Mean strain
$\epsilon'_{xx}, \epsilon'_{yy}, \epsilon'_{zz}$	Deviatoric strains in x, y and z directions

J'_1, J'_2, J'_3	Strain deviatoric tensors in 1, 2 and 3 directions
\mathcal{E}_{vm}	von Mises strain ($=\sqrt{3J'_2}$)
$\mathcal{E}_1, \mathcal{E}_2, \mathcal{E}_3$	Principal strains
$\mathcal{E}_{1y}, \mathcal{E}_{2y}, \mathcal{E}_{3y}$	Yield strains along 1-, 2- and 3-directions
J_1^m	First strain invariant at matrix phase
J_{1-Crit}^m	Critical first strain invariant at matrix phase
\mathcal{E}_{vm}^m	von Mises strain at matrix phase
$\mathcal{E}_{vm-Crit}^m$	Critical von Mises strain at matrix phase
$\mathcal{E}_{vm-Crit}^f$	Critical von Mises strain at fiber phase
$E_{11f}, E_{22f}, E_{33f}$	Young's moduli of the fiber defined using material axes
$G_{12f}, G_{13f}, G_{23f}$	Shear modulus defined using material axes
$\nu_{12f}, \nu_{13f}, \nu_{23f}$	Poisson's ratios of the fiber phase defined using material axes
$\alpha_{11f}, \alpha_{22f}, \alpha_{33f}$	Coefficient of thermal expansion of fiber in 1, 2 and 3 directions
E_m	Matrix Young's modulus
G_m	Matrix shear modulus

ν_m	Matrix Poisson's ratio
α_m	Coefficient of thermal expansion of matrix
α_i	Coefficient of thermal expansion ($i = 1, 2, 3$)
u_1, u_2, u_3	Displacements in 1-, 2- and 3-direction
$\{\mathcal{E}\}$	Total strain tensor of each phase after being amplified
$\{\mathcal{E}\}_{mech}$	Homogenized mechanical strain tensor of FE solutions
$\{\mathcal{E}\}_{thermal}$	Homogenized thermo-mechanical strain tensor of FE solutions
$[A_{ij}]$	Matrix containing mechanical amplification factors of each phase
$[T_{ij}]$	Matrix containing thermal amplification factors of each phase

List of Abbreviations

SIFT	Strain invariant failure theory
RVE	Representative volume element
EFM	Element-Failure method
FEM	Finite element method
IF1, IF2	Inter-fiber positions 1 and 2
IS	Interstitial position
M	Matrix position
F	Fiber position
ASTM	American society for testing and materials
CLT	Classical laminate theory
MCT	Multicontinuum theory
CTE	Coefficient of thermal expansion
CFRP	Carbon fiber reinforced plastics

CHAPTER 1

INTRODUCTION

1.1 Background

Composite structures have been widely applied to numerous applications for the last 40 years. The maiden application of composite structures was aircraft component where high specific stiffness, high specific strength and good fatigue resistance were required. Nowadays, composites are also strong candidates for automotive, medical, marine, sport and military structural applications. Rapid development of composite application has a significant impact on the theoretical analysis of this material, especially on the failure analysis.

Failure analysis which characterizes the strength and the modes of failure in composite has been an important subject for years. Failure criteria have been proposed to capture the onset of failure, constituent's failure, damage initiation, progression and final failure of composites. Failure criteria in composites have been assessed [*Hinton & Soden, 1998; Soden et al, 1998a; Soden et al, 1998b; Kaddour et al, 2004*], and recommendation on utilization of failure theories can be reviewed in [*Soden, Kaddour and Hinton, 2004*]. Three-dimensional failure criteria which were not included in aforementioned publications were discussed by Christensen [*Christensen, 2001*]. The clarification on practical and also newly-developed failure theories are discussed by Rousseau [*Rousseau, 2001*]. Strain Invariant Failure Theory (SIFT) is one of 3-D failure theories for composites [*Gosse & Christensen, 2001; Gosse, Christensen, Hart-Smith & Wollschlager, 2002*]. For the last three years, several authors have applied

SIFT for the analysis of damage initiation and delamination [*Li et al, 2002; Li et al, 2003; Tay et al, 2005*].

1.2 Problem Statement

As a newly-developed failure theory for composite structures, many features in Strain Invariant Failure Theory (SIFT) must be explored to give better insight on its generality. One important feature in SIFT is micromechanical enhancement whereby macro-strain of composite is “amplified” through a factor so-called strain amplification factor. Strain amplification factor can be obtained by finite element method and it is used to include micromechanics effect as a result of fiber and matrix interaction due to mechanical and thermal loadings. Gosse *et al* [2001] have provided a methodology to obtain strain amplification factors using micromechanics representative volume elements. However, the data of strain amplification factors is not available in the literatures.

Strain amplification factors can be obtained numerically from a particular composite system, e.g. carbon/epoxy composite. Altering the fiber material may cause the change in strain amplification factor. The effect of altering the fiber material with respect to strain amplification factors have not been discussed in any literature.

In the past three years, SIFT has been applied to predict composite failure by means of finite element simulation for various cases. Damage progression in three-point bend specimen, open-hole tension and stiffener were predicted by using SIFT. None has studied the effect of fiber volume fraction with respect to damage pattern in composite.

1.3 Research Objectives

The main objective of the present research is to obtain strain amplification factors from representative volume elements analyzed by the finite element method. Strain amplification factors are obtained for a particular composite system, i.e. carbon/epoxy, and for a certain fiber volume fraction V_f (in this case, as reference, $V_f = 60\%$). Parametric studies have also been performed to obtain strain amplification factors for $V_f = 50\%$ and $V_f = 70\%$. Another composite system such as glass/epoxy will also be discussed in terms of strain amplification factors.

It is important to verify present strain amplification factors with one representative case. Open-hole tension specimen is chosen to perform the growth of damage in composite plate. Finite element analysis incorporating Element-Failure Method (EFM) and SIFT within an in-house finite element code was performed to track the damage propagation in the open-hole tension specimen. The effect of fiber volume fraction can be captured by observing the damage propagation.

1.4 Overview of the Thesis

The thesis is divided into six chapters. Chapter 1 consists of background, problem statement, research objectives and overview of the thesis. Chapter 2 discusses micromechanics-based failure theories for composite structures, and damage progression in composite is briefly described. Chapter 3 deals with the Strain Invariant Failure Theory (SIFT), where the theoretical background, implementation of SIFT and strain amplification factors are discussed. Strain amplification factors are discussed in chapter 4 to give complete results of the investigation on SIFT in terms of micromechanics models, influence of fiber volume fraction and fiber and matrix elastic

properties. Chapter 5 deals with the implementation of strain amplification factors obtained from finite element simulation. Damage progression of open-hole tension specimen is simulated using EFM and SIFT. Chapter 6 is Conclusions and Recommendations.

CHAPTER 2

LITERATURE REVIEW OF MICROMECHANICS- BASED FAILURE THEORY

2.1 Micromechanics

“Micromechanics” deals with the study of composite at constituents’ level, i.e. fiber and matrix. In much of composite literature, micromechanics generally discusses about the analysis of effective composite properties, i.e. the extensional moduli, the shear moduli, Poisson’s ratios, etc., in terms of fiber and matrix properties [Hill, 1963; Budiansky, 1983; Christensen, 1990; Christensen, 1998]. In the analysis, fiber and matrix are modeled explicitly and mathematical formulations are derived based on the model. The explicit model of fiber and matrix is called *representative volume element* (RVE) and mathematical formulations can be based on mechanics of materials or elasticity theory [Sun & Vaidya, 1996].

Since fibers in unidirectional composites are normally random in nature (Figure 2-1), there is a need to idealize the fiber arrangement in the simplest form. RVE corresponds to a periodic fiber packing sequence which idealizes the randomness of fiber arrangement. RVE is also a domain of modeling whereby micromechanical data, i.e. stress, strain, displacement, can be obtained.

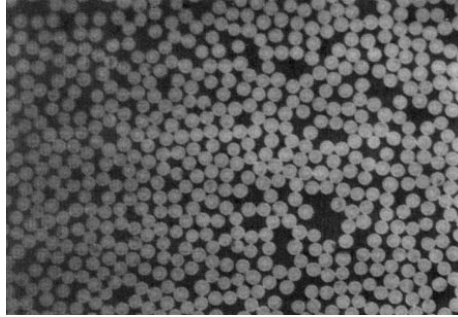


Figure 2-1 Photomicrograph of typical unidirectional composite: random fiber arrangement of composite [Herakovich, 1998]

In a very simple and ideal form, RVE consists of one fiber (usually circular) bonded by matrix material forming a generic composite block (single cell). Single cell is therefore defined as a unit block of composite describing the basic fiber arrangement within matrix phase. RVE can be in the form of square, hexagonal, diamond and random array. Figure 2-2 shows the square array and hexagonal array. RVE may also be formed by repeating several single cells to build multi cell. Multi cell can be useful to study the interaction between fibers. Concept of multi cell was proposed by Aboudi [1988] to analyze composite elastic properties.

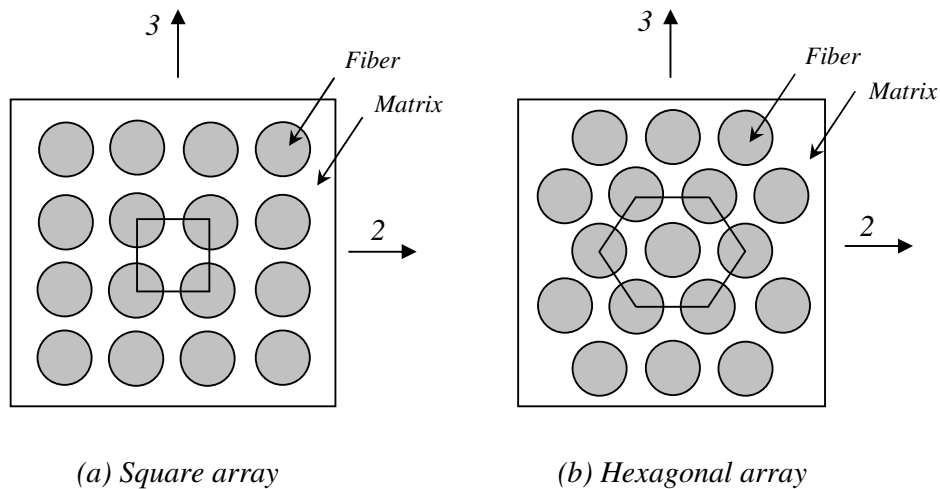


Figure 2-2 Representative volume elements for micromechanics analysis

One of key elements in micromechanics is fiber volume fraction V_f . Fiber volume fraction describes the density of fibers within matrix of composite materials. Continuous fiber composite has V_f roughly between 50% - 80%, and V_f is much lower for short fiber composite. Magnitude of effective properties of composite is closely related to V_f . Maximum V_f for square array is 0.785, while maximum V_f for hexagonal array is 0.907 [Gibson, 1994].

In micromechanics analysis, properties of composite constituents must be experimentally obtained before the mathematical or numerical analysis is carried out. Tensile strength and Young's modulus of fiber is determined by static longitudinal loading which is described in ASTM D 3379-75 [Gibson, 1994]. Fiber specimen is adhesively bonded to a backing strip which has a central longitudinal slot of fixed gage length. Once the specimen is clamped in the grips of the tensile testing machine, the strip is cut away so that only the filaments of the fiber transmit the applied tensile load. The fiber is pulled to failure, the load and elongation are recorded, and the tensile strength and modulus are calculated. Transverse modulus can be directly measured by compression tests machine [Kawabata *et al.*, 2002]. Tensile yield strength and modulus of elasticity of the matrix can be determined by ASTM D 638-90 method for tensile properties of plastics. Compressive yield strength can be measured by ASTM D 695-90 test method, and to avoid out-of-plane buckling failure a very short specimen and a support jig on each side can be used.

2.2 Failure at Micro-Level

At micro-level failure mechanisms can be in the form of fiber fracture, fiber buckling, fiber splitting, fiber pull out, fiber/matrix debonding, matrix cracking and

radial cracks. At macro-level, these failure mechanisms may form transverse cracks in planes parallel to the fibers, fiber-dominated failures in planes perpendicular to the fibers and delaminations between layers of the laminate. Defects in fiber and matrix can be introduced by severe loading conditions, environmental attacks and defect within fiber and matrix. Table 2-1 gives the type of failure and corresponding mechanism.

Table 2-1 Type of failure in composite at micro-level and corresponding mechanism

Type of failure	Mechanism
Fiber fracture	Fiber fracture usually occurs when the composite is subjected to tensile load. Maximum allowable axial tensile stress (or strain) of the fiber is exceeded.
Fiber pull out	Fiber fracture accompanied by fiber/matrix debonding
Matrix cracking	Strength of matrix is exceeded
Fiber buckling	Axial compressive stress causes fiber to buckle
Fiber splitting and radial interface crack	Transverse or hoop stresses in the fiber or interphase region between the fiber and the matrix reaches its ultimate value

2.3 Literature Review of Micromechanics-Based Failure Theory

Huang [2001, 2004a, 2004b] developed a micromechanics-based failure theory so-called “the bridging model”. The bridging model can predict the overall instantaneous compliance matrix of the lamina made from various constituent fiber and resin materials at each incremental load level and give the internal stresses of

the constituents upon the overall applied load. The lamina failure is assumed whenever one of the constituent materials attains its ultimate stress state. Using classical laminate theory (CLT), the overall instantaneous stiffness matrix of the laminate is obtained and the stress components applied to each lamina is determined. If any ply in the laminate fails, its contribution to the remaining instantaneous stiffness matrix of the laminate will no longer occur. In this way, the progressive failure process in the laminate can be identified and the laminate total strength is determined accordingly.

Multicontinuum theory (MCT) is numerical algorithm for extracting the stress and strain fields for a composites' constituent during a routine finite element analysis [Mayes and Hansen, 2004a, 2004b]. The theory assumes: (1) linear elastic behavior of the fibers and nonlinear elastic behavior of the matrix, (2) perfect bonding between fibers and matrix, (3) stress concentrations at fiber boundaries are accounted for only as a contribution to the volume average stress, (4) the effect of fiber distribution on the composite stiffness and strength is accounted for in the finite element modeling of a representative volume of microstructure, and (5) ability to fail one constituent while leaving the other intact results in a piecewise continuous composite stress-strain curve. In MCT failure theory, failure criterion is separated between fiber and matrix failure and it is expressed in terms of stresses within composite constituent.

Gosse [Gosse and Christensen, 2001; Gosse, 1999] developed micromechanics failure theory which is based on the determination of fiber and matrix failure by using critical strain invariants. The theory is called strain invariant failure theory,

abbreviated as SIFT. Failure of composite constituent is associated with one invariant of the fiber, and two invariants for the matrix. Failure is deemed to occur when one of those three invariants exceeds a critical value. For the past three years, SIFT has been tested to predict damage initiation in three-point bend specimen [Tay *et al*, 2005] and matrix dominated failure in I-beams, curved beams and T-cleats [Li *et al*, 2002; Li *et al*, 2003].

CHAPTER 3

STRAIN INVARIANT FAILURE THEORY (SIFT)

3.1 Theory Background

Deformation in solids can be decoupled into purely volumetric and purely deviatoric (distortional) portions [Gosse & Christensen, 1999]. Gosse and Christensen's finding was based on Asp *et al* [Asp, Berglund and Talreja, 1996] experimental evidence that polymer do not exhibit ellipse bi-axial failure envelope. There is a truncation in the first quadrant of bi-axial envelopes which is probably initiated by a critical dilatational deformation (Figure 3-1). Physically, this truncation suggested that microcavitation or crazing occurs in polymer. Gosse *et al* numerically derived the failure envelope for the thermoplastic polymer, and their result was similar to Asp *et al* [1996] result. Therefore, they proposed the use of a volumetric strain invariant (first invariant of strain) to assess critical dilatational behavior.

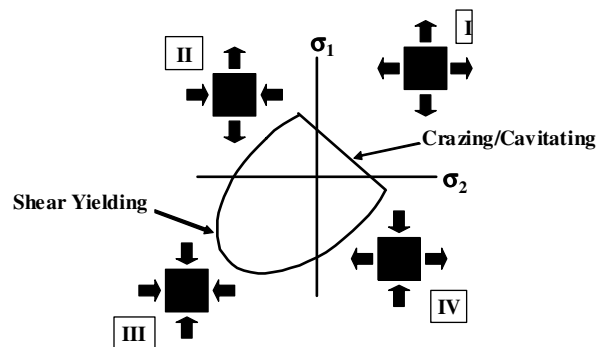


Figure 3-1 Failure envelope for polymer.

The strain invariants can be determined from the cubic characteristic equation determined from the strain tensor. They are defined by following equation [Ford & Anderson, 1977]:

$$\varepsilon^3 - J_1\varepsilon^2 + J_2\varepsilon - J_3 = 0 \quad (3-1)$$

where the first, second and the third of the strain invariants are defined by

$$J_1 = \varepsilon_{xx} + \varepsilon_{yy} + \varepsilon_{zz} \quad (3-2)$$

$$J_2 = \varepsilon_{xx}\varepsilon_{yy} + \varepsilon_{yy}\varepsilon_{zz} + \varepsilon_{zz}\varepsilon_{xx} - \frac{1}{4}(\varepsilon_{xy}^2 + \varepsilon_{yz}^2 + \varepsilon_{zx}^2) \quad (3-3)$$

$$J_3 = \varepsilon_{xx}\varepsilon_{yy}\varepsilon_{zz} + \frac{1}{4}(\varepsilon_{xy}\varepsilon_{yz}\varepsilon_{xy} - \varepsilon_{xx}\varepsilon_{yz}^2 - \varepsilon_{yy}\varepsilon_{zx}^2 - \varepsilon_{zz}\varepsilon_{xy}^2) \quad (3-4)$$

J_1 (Eq. 3-2) criterion (volumetric strain) is most appropriate for interlaminar failure dominated by volume increase of the matrix phase. However, since material would not yield under compression (except perhaps at extreme value) [Richards, Jr, 2001], consequently, J_1 is only applicable for tension specimen undergoing volume increases [Li et al, 2002]. The Gosse and Christensen [2001] suggested that when the first strain invariant exceeds a critical value (J_{1-crit}), damage will initiate.

Strain components ε_{xx} , ε_{yy} , ε_{zz} , ε_{xy} , ε_{yz} and ε_{zx} are the six components of the strain vector in general Cartesian coordinates. Effect of temperature can be incorporated by substituting free expansion term ($\alpha\Delta T$) into the strain components.

α is coefficient of thermal expansion and ΔT is temperature difference. Hence, the strain components comprise strains due to mechanical loading (superscript *mech* stands for ‘mechanical’) and free expansion terms (strain due to temperature difference). Strain components in orthogonal directions are given as follow:

$$\varepsilon_{xx} = \varepsilon_{xx}^{mech} - \alpha\Delta T; \quad \varepsilon_{yy} = \varepsilon_{yy}^{mech} - \alpha\Delta T; \quad \varepsilon_{zz} = \varepsilon_{zz}^{mech} - \alpha\Delta T \quad (3-5)$$

Deviatoric strain is defined as the deviation of absolute (normal or principal) strain from the mean strain ($\bar{\varepsilon}$). Deviatoric strain can be substituted into the cubic characteristic equation of strain and give us the following expression

$$\varepsilon'^3 + J_2'\varepsilon' - J_3' = 0 \quad (3-6)$$

where

$$J_2' = \frac{1}{6} \left[(\varepsilon_{xx} - \varepsilon_{yy})^2 + (\varepsilon_{yy} - \varepsilon_{zz})^2 + (\varepsilon_{zz} - \varepsilon_{xx})^2 \right] - \frac{1}{4} (\varepsilon_{xy}^2 + \varepsilon_{yz}^2 + \varepsilon_{zx}^2) \quad (3-7)$$

$$J_3' = \varepsilon_{xx}'\varepsilon_{yy}'\varepsilon_{zz}' + \frac{1}{4} (\varepsilon_{xy}\varepsilon_{yz}\varepsilon_{xy}' - \varepsilon_{xx}'\varepsilon_{yz}^2 - \varepsilon_{yy}'\varepsilon_{zx}^2 - \varepsilon_{zz}'\varepsilon_{xy}^2) \quad (3-8)$$

and the deviatoric strains are defined as $\varepsilon_{xx}' = \varepsilon_{xx} - \bar{\varepsilon}$, $\varepsilon_{yy}' = \varepsilon_{yy} - \bar{\varepsilon}$ and $\varepsilon_{zz}' = \varepsilon_{zz} - \bar{\varepsilon}$, where ε_{xx} , ε_{yy} and ε_{zz} are the normal strains and $\bar{\varepsilon}$ is mean strain. In the formulation, Gosse and Christensen employed strain deviatoric tensor J_2' in the

von Mises (or equivalent; described by subscript vm) strain by the following expression

$$\epsilon_{vm} = \sqrt{3J_2'} \quad (3-9)$$

Using the principal strains only, Eq. (3-9) can be rewritten as

$$\epsilon_{vm} = \sqrt{\frac{1}{2}[(\epsilon_1 - \epsilon_2)^2 + (\epsilon_1 - \epsilon_3)^2 + (\epsilon_2 - \epsilon_3)^2]} \quad (3-10)$$

where ϵ_1 , ϵ_2 and ϵ_3 are the principal strains. Since von Mises strain (ϵ_{vm}) represents the part of strain caused by change of shape, not change by volume, the thermal expansion effect is not considered. It is important to note that the stress-strain relation for this case is infinitesimal stress-strain relations. Therefore, small strains are considered.

3.2 Critical Strain Invariants

Strain invariant failure theory (SIFT) is based on first strain invariant (J_1) to accommodate the change of volume and von Mises strain (ϵ_{vm}) to accommodate the change of shape. In practice, failure in composite will occur at either the fiber or the matrix phases if any of the invariants (J_1 or ϵ_{vm}) reaches the critical value. The failure criterion in SIFT is therefore examined for matrix and fiber.

Matrix phase

Failure in the matrix will occur if :

$$J_1^m \geq J_{1-Crit}^m \tag{3-11}$$

or

$$\epsilon_{vm}^m \geq \epsilon_{vm-Crit}^m \tag{3-12}$$

Fiber phase

Failure in fiber will occur if:

$$\epsilon_{vm}^f \geq \epsilon_{vm-Crit}^f \tag{3-13}$$

where superscripts *m* and *f* refer to matrix and fiber, respectively. Subscript *Crit* refers to “critical”. SIFT states that damage in composite will initiate when *one* of the three critical strain invariant values (i.e. J_{1-Crit}^m , $\epsilon_{vm-Crit}^m$ and $\epsilon_{vm-Crit}^f$) is exceeded. Critical strain invariant values are determined from coupon tests of laminated composites with various lay-ups. Table 3-1 provides critical strain invariant values and corresponding laminated composite lay-up used to obtain the value.

Table 3-1 Critical strain invariant values and corresponding laminated composite lay-up used to obtain the value [Gosse et al, 2002]

Critical invariant	Value	Laminated composite lay-up
J_{1-Crit}^m	0.0274	[90] _n
$\epsilon_{vm-Crit}^m$	0.103	[10/-10] _{ns}
$\epsilon_{vm-Crit}^f$	0.0182	[0] _n

Originally, von Mises Criterion of Eq. 3-10 is most widely used for predicting the onset of yielding in isotropic metals [Gibson, 1994]. Since matrix is assumed to be isotropic in this case, hence Eq. 3-12 can be applied to predict matrix failure. Regarding the utilization of Eq. (3-13), similar to matrix, we also assume that the fiber is isotropic, and therefore Eq. 3-13 can also be applied to predict fiber failure. However, Hill (1948) suggested that the von Mises Criterion can be modified to include the effects of induced anisotropic behavior. Hill criterion in principal strains $\epsilon_1, \epsilon_2, \epsilon_3$ space is described by the equation:

$$A(\epsilon_1 - \epsilon_2)^2 + B(\epsilon_1 - \epsilon_3)^2 + C(\epsilon_2 - \epsilon_3)^2 = 1 \quad (3-14)$$

where A, B and C are determined from yield strains in uniaxial loading. By using Eq. (3-14), failure is predicted if the left-hand side is ≥ 1 . Constants A, B and C are given as follow:

$$2A = \frac{1}{\epsilon_{1y}^2} + \frac{1}{\epsilon_{2y}^2} - \frac{1}{\epsilon_{3y}^2}; \quad 2B = \frac{1}{\epsilon_{1y}^2} + \frac{1}{\epsilon_{3y}^2} - \frac{1}{\epsilon_{2y}^2}; \quad 2C = \frac{1}{\epsilon_{2y}^2} + \frac{1}{\epsilon_{3y}^2} - \frac{1}{\epsilon_{1y}^2} \quad (3-15)$$

where $\epsilon_{1y}, \epsilon_{2y}$ and ϵ_{3y} are yield strains along 1-, 2- and 3-directions.

3.3 Concept of Strain Amplification Factor

Strain distributions due to mechanical loading and temperature difference in composite at micro-level, i.e. fiber and matrix phases, are considerably complex. One way to observe the strain distribution in composite at micro-level is to model

fiber and matrix individually or micromechanical modeling. While the existing laminate theory does not account for either mechanical amplification of strain between fiber and matrix or the presence of thermal strains in matrix phase, micromechanical modeling is considered impractical. Therefore, the modification of homogenized lamina solution by using micromechanical factors is needed. Homogenized lamina solution provides an average state of strain representing both the fiber and matrix phase at the same point in space. Micromechanical factor aims to modify the average state of strain of both fiber and matrix [Gosse *et al*, 2002].

SIFT involves strain modification within homogenized lamina solution. In order to modify the strain, micromechanical factor so-called strain amplification factor is introduced. Based on the loading condition, there are two amplification factors, namely mechanical strain amplification factor (A_{ij}) and thermo-mechanical strain amplification factor (T_{ij}). Strain amplification factors can be obtained by finite element method.

Mechanical strain amplification factor (A_{ij}) is a normalized strain obtained from following equation:

$$A_{ij} = \frac{\varepsilon_{ij}}{(\Delta L_{ij} / L_o)} \quad (3-16)$$

where ε_{ij} local strain is obtained from a selected point in single cell for every loading direction, ΔL_{ij} is prescribed unit displacement and L_o is initial length of RVE which is parallel with loading direction.

Thermo-mechanical strain amplification factor (T_{ij}) is obtained by following formula:

$$T_{ij} = \varepsilon_{ij} - \alpha_i \Delta T \quad (3-17)$$

where α_i is coefficient of thermal expansion and ΔT is temperature difference given to the finite element model.

3.4 Methodology of Extracting Strain Amplification Factors

Finite element method was used extensively to build representative micromechanical blocks, whereby fiber and matrix are modeled three-dimensionally. Hexahedron element with 20 nodes was used. *MSC.Patran* was used to build the finite element models, while processing and post-processing steps were done using *Abaqus*. Three fiber packing arrays are considered, namely square, hexagonal and diamond (Figure 3-2). The diamond arrangement is in fact the same as square, but rotated through a 45° angle.

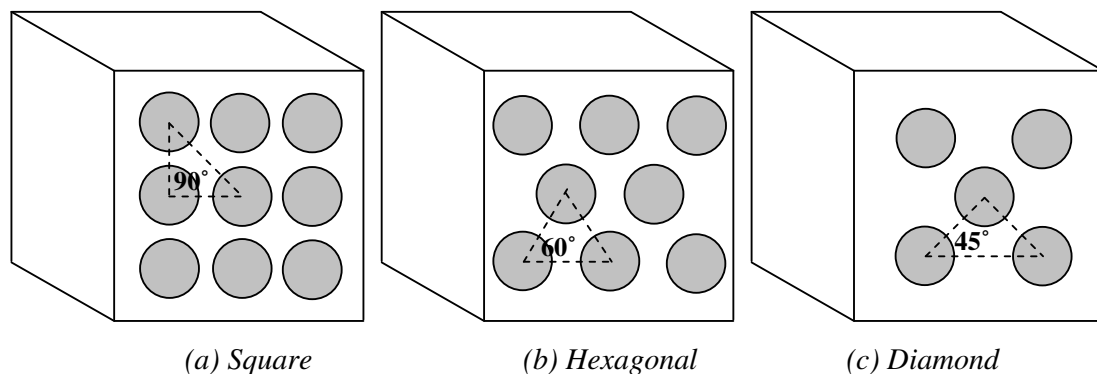


Figure 3-2. Representative micromechanical blocks

Square packing array was modeled using single cell and multi cell (Figure 3-3). Single cell is used due to its advantage to be the simplest representation of the infinite periodic arrangement of inhomogeneous material. Multi cell is a repetitive form of several single cells. Analysis using multi cell is conducted to address the interaction between fibers in the micromechanical system. Gosse et al [2001] built finite element model using single cell, and Ha [2002] built finite element model using multi cell. In their analysis as well as present analysis, the results were extracted from the single cell within multi cell.

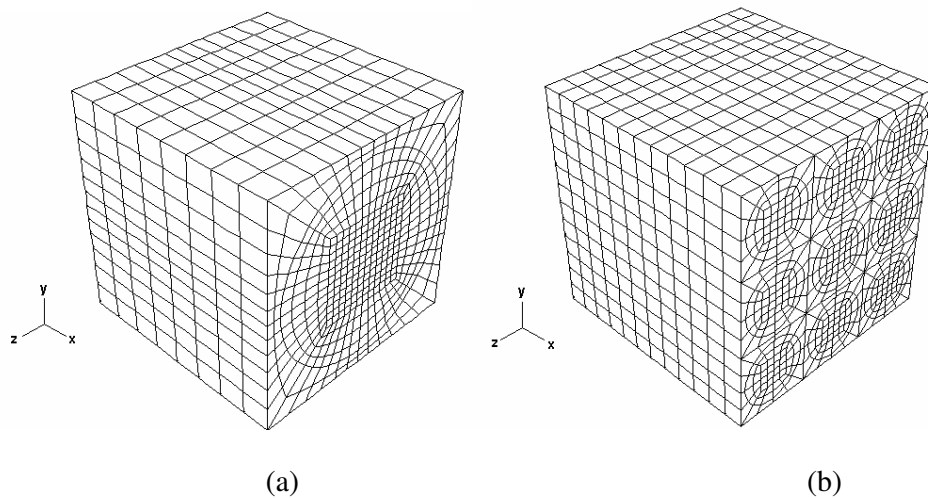


Figure 3-3. Finite element models of square array with fiber volume fraction V_f of 60% (a) single cell model, and (b) multi cell model consists of 27 single cells.

Single cell of square array in Figure (3-3) was arranged by 3456 elements, whilst the multi cell was arranged by 6912 elements. Since the multi cell is a repetitive form of 27 single cells, the elements of multi cell should be 27 times of that single cell. However, due to computer limitation, multi cell of square packing array was only arranged by 6912 elements.

Finite element models for hexagonal and diamond packing arrays can be seen in Figure (3-4). The hexagonal model consists of 6336 elements. The diamond model consists of 6144 elements. Finite element models of square, hexagonal and diamond packing arrays have fiber volume fraction V_f of 60%. These models are used as references for finite element models with $V_f = 50%$ and $V_f = 70%$. Fiber volume fraction was found to be a critical variable in the amplification factors extraction [Gosse & Christensen, 1999], and the effect of fiber volume factor with respect to the amplification factors will be discussed in Chapter 4.

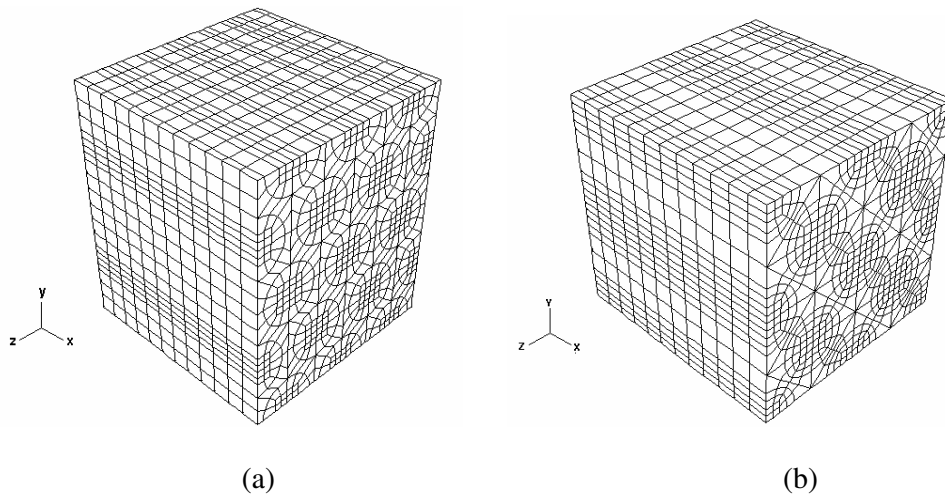


Figure 3-4. Finite element models of hexagonal and diamond array in the multi cell arrangement ($V_f = 60%$) (a) hexagonal and (b) diamond.

Three finite element models of square, hexagonal and diamond arrays are subjected to mechanical and thermo-mechanical loadings in order to obtain strain amplification factors. For mechanical loading, each finite element model is given prescribed unit displacements in three cases of normal and three cases of shear deformations. As an illustration, in order to obtain strain amplification factors for prescribed displacement in the fiber (or l -) direction for one of the faces, the

model is constrained in the other five faces. The procedure is repeated each time in order to obtain strain amplification factors for displacements in the other two orthogonal (2- and 3-) directions. Figure 3-5 shows the deformed shape of three normal displacements. The local coordinate system used as a reference describing boundary conditions can be seen in Figure 3-5 (a) – (c). Similarly, for shear deformations, the prescribed shear strain is applied in each of the three directions. Figure 3-5 (d) – (f) shows the displaced shape of three shear deformations. Figure 3-5 illustrates the deformation of FE model. Hexagonal and diamond arrays are also subjected to similar loadings as in square arrays.

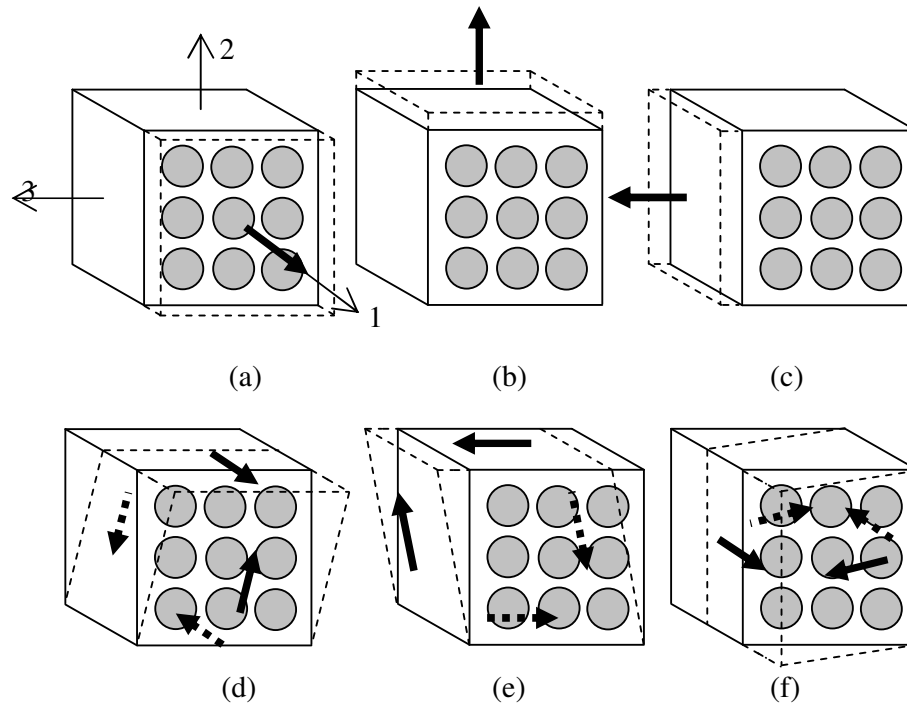


Figure 3-5. Micromechanical block is loaded with prescribed displacement ($\Delta L = 1$) to perform normal deformation 1, 2 or 3 and shear 12, 23 and 13 deformations. Deformed shape of three normal directions can be seen in (a) 1-direction, (b) 2-direction and (c) 3-direction and three shear displacements can be seen in (d) 12-direction, (e) 23-direction and (f) 13-direction.

Boundary conditions for mechanical loading cases can be summarized in Table 3-2. For example, if we want to extract strains in fiber direction, we give constant displacement of one unit $\bar{\epsilon}_{11} = 1$ in front surface (see Figure 3-5 (a)), we restrain other five surfaces $\bar{\epsilon}_{22} = \bar{\epsilon}_{33} = \bar{\gamma}_{12} = \bar{\gamma}_{13} = \bar{\gamma}_{23} = 0$, and impose zero degree of temperature $\Delta T = 0$. For other directions, readers may refer to Table 3-2.

Table 3-2. Definition of boundary conditions BC1 to BC6 used in the extraction of mechanical strain amplification factors.

Loading direction	Boundary conditions*
Direction-1 (fiber direction/longitudinal)	$\bar{\epsilon}_{11} = 1, \bar{\epsilon}_{22} = \bar{\epsilon}_{33} = \bar{\gamma}_{12} = \bar{\gamma}_{13} = \bar{\gamma}_{23} = 0, \Delta T = 0$
Direction-2 (transverse direction)	$\epsilon_{22} = 1, \epsilon_{11} = \epsilon_{33} = \gamma_{12} = \gamma_{13} = \gamma_{23} = 0, \Delta T = 0$
Direction-3 (transverse direction)	$\epsilon_{33} = 1, \epsilon_{11} = \epsilon_{22} = \gamma_{12} = \gamma_{13} = \gamma_{23} = 0, \Delta T = 0$
Direction-12 (in-plane shear)	$\gamma_{12} = 1, \epsilon_{11} = \epsilon_{22} = \epsilon_{33} = \gamma_{13} = \gamma_{23} = 0, \Delta T = 0$
Direction-23 (out of plane shear)	$\gamma_{23} = 1, \epsilon_{11} = \epsilon_{22} = \epsilon_{33} = \gamma_{12} = \gamma_{13} = 0, \Delta T = 0$
Direction-13 (in-plane shear)	$\gamma_{13} = 1, \epsilon_{11} = \epsilon_{22} = \epsilon_{33} = \gamma_{12} = \gamma_{23} = 0, \Delta T = 0$

** direction is following convention in Figure 3-5 (a)*

In addition to the mechanical amplification factors above, thermo-mechanical amplification factors may be obtained by constraining all the faces from expansion ($u_1 = u_2 = u_3 = 0$ for all faces) and performing a thermo-mechanical analysis by prescribing a unit temperature differential ΔT above the stress-free

temperature (Figure 3-6). It is important to note that this thermo-mechanical analysis is conducted separately from mechanical analysis.

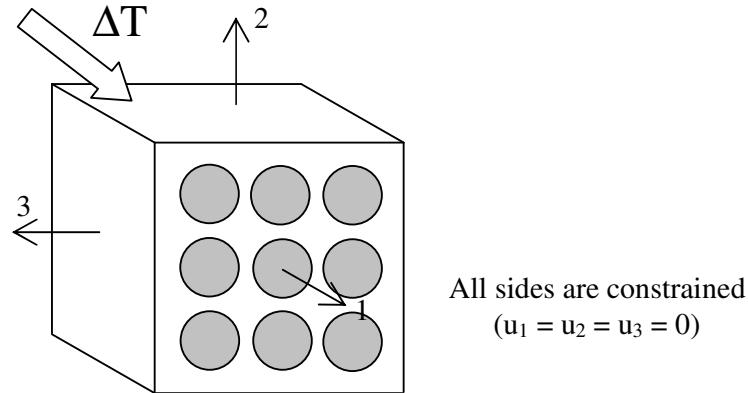


Figure 3-6. Application of temperature difference $\Delta T = -248.56^{\circ}\text{C}$ into finite element model is done after all sides of micromechanical block being constrained.

Mechanical and thermal loadings described previously are imposed to the finite element model in order to obtain local mechanical strains in the selected points. The local strains are extracted from various positions within one single cell inside multi cell and normalized with respect to the prescribed strain. The single cell is taken in the middle of the multi cell model (Figure 3-7a). Twenty points in the single cell are then chosen for the extraction of local strain values (Figure 3-7b); the points F1 - F8 are located at the fiber in the fiber-matrix interface, F9 is located at the center of the (assumed circular) fiber, M1 - M8 are located at the matrix in the fiber-matrix interface, IF1 and IF2 are inter-fiber positions, and IS corresponds to the interstitial position. Inter-fiber is defined as a point where fibers are closest to each other, and interstitial is a point where the fibers are farthest from each other.

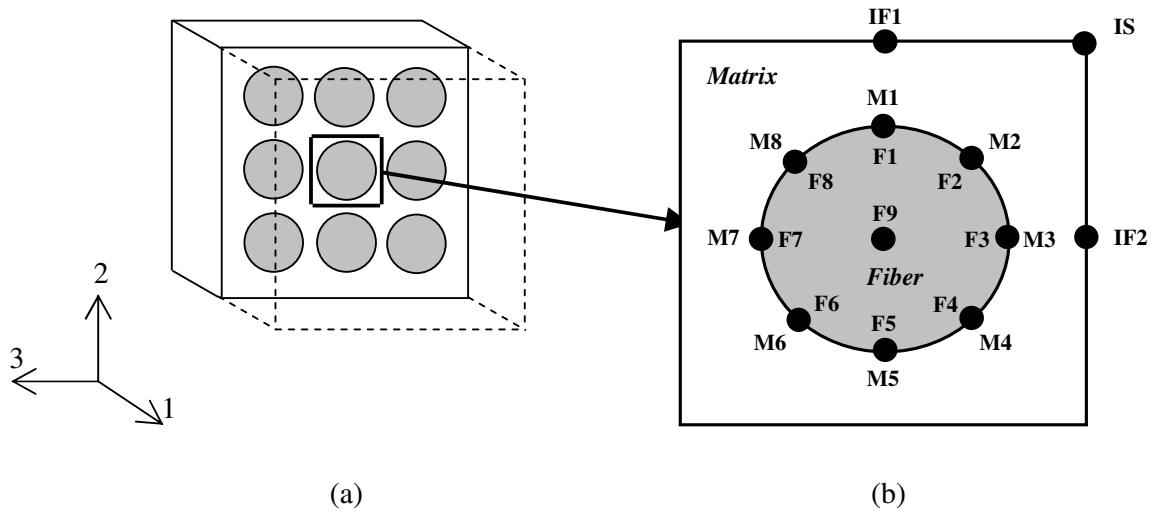


Figure 3-7. Local strains are extracted in the single cell within multi cell in order to obtain strain amplification factors: (a) single cell is taken in the middle cut of multi cell model, (b) local strains are extracted in various positions within fiber and matrix phase. There are total 20 points in the matrix, fiber and interface.

Figure 3-7 shows the extraction points in square array, while Figure 3-8a and 3-8b shows the extraction points in hexagonal and diamond arrays, respectively. There are 6 mechanical and 6 thermo-mechanical strain amplification factors for each position; since there are 20 positions and 3 fiber arrangements, the total number of amplification factors is 720 (i.e. $12 \times 20 \times 3$). It should be noted that for a given matrix and fiber material system, the suite of micromechanical block analyses need only be performed once; the resulting amplification factors are stored in a look-up table or subroutine. The output of strains from a macro-finite element analysis is efficiently amplified through this look-up subroutine before the strain invariant values are calculated and compared with the corresponding critical values.

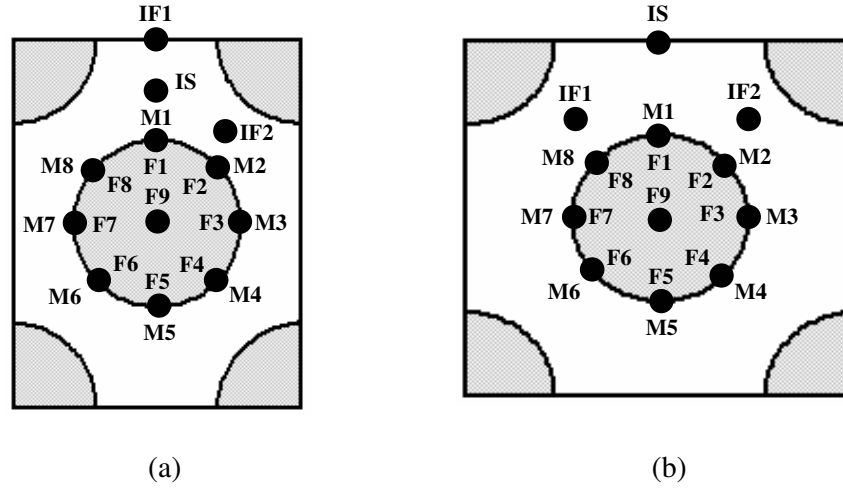


Figure 3-8. Location of selection points in (a) hexagonal single cell and (b) diamond single cell

3.5 Micromechanical Modification

After amplification factors have been extracted, the micromechanical modification can be carried out. In the homogenized finite element model of composite, for example, each strain tensor component due to the application of mechanical and thermal loadings are transformed into local coordinate system. The transformed strain tensor component is micromechanically modified using mechanical and thermal amplification factors, and transformed back into global coordinate system. Once this final transformation is completed the modified mechanical and thermal solutions are superimposed for each tensor component for each node in the body. The micromechanical modification using amplification factors can be described using following equation:

$$\{\boldsymbol{\varepsilon}\}_{total} = [A_{ij}] \{\boldsymbol{\varepsilon}\}_{mech} + [A_{ij}] \{\boldsymbol{\varepsilon}\}_{thermal} + [T_{ij}] \Delta T \quad (3-18)$$

where

$\{\boldsymbol{\varepsilon}\}_{total}$ is the total strain tensor of each phase after being amplified

$\{\boldsymbol{\varepsilon}\}_{mech}$ is the homogenized mechanical strain tensor of FE solutions

$\{\boldsymbol{\varepsilon}\}_{thermal}$ is the homogenized thermo-mechanical strain tensor of FE solutions

$[A_{ij}]$ is matrix containing mechanical amplification factors of each phase

$[T_{ij}]$ is matrix containing thermal amplification factors of each phase

ΔT is the temperature difference applied to the model

It is generally believed that J_1 -driven failure is dominated by volume changes in the matrix phase [Tay et al, 2005]. Therefore, the first strain invariant J_1 (Eq. 3-2) is calculated with strains amplified only at the IF1, IF2 and IS positions within the matrix phase in the micromechanical block. On the other hand, the von Mises strain (Eq. 3-10) may be amplified with factors not only within matrix region (IF1, IF2 and IS) or fiber-matrix interface in matrix region (M1 – M8), but also the center of fiber (F9) and fiber-matrix interface (F1 – F8). We designate the superscript m for the former case to denote “matrix” (i.e. $\boldsymbol{\varepsilon}_{vm}^m$), and the superscript f for the latter case to denote “fiber” (i.e. $\boldsymbol{\varepsilon}_{vm}^f$).

CHAPTER 4

STRAIN AMPLIFICATION FACTORS

4.1 Elastic Properties of Fiber and Matrix

Before conducting micromechanical finite element analysis, fiber and matrix properties must be defined. In present analysis, the fiber is assumed to be transversely isotropic and the matrix is isotropic. Fiber is made of graphite (IM7) and matrix is epoxy. The mechanical and thermal properties of fiber and matrix can be seen in Table 4-1. The subscripts m and f refer to matrix and fiber respectively; the subscript 1 indicates the axial fiber direction, the subscripts 2 and 3 the transverse directions. Elastic properties of fiber and matrix were obtained from Ha [2002].

Table 4-1. Mechanical and thermal properties fiber (graphite—IM7) and matrix (epoxy) used in micromechanics model of composite [Ha, 2002]

Fiber (Graphite: IM7)	Magnitude
Axial modulus E_{11f} , in GPa	303
Transverse modulus $E_{22f} (= E_{33f})$, in GPa	15.2
Shear modulus $G_{12f} (= G_{13f})$, in GPa	9.65
Shear modulus G_{23f} , in GPa	6.32
Poisson's ratio $\nu_{12f} (= \nu_{13f} = \nu_{23f})$	0.2
Coefficient of thermal expansion α_{1f} , in /deg C	0.0
Coefficient of thermal expansion $\alpha_{22f} (= \alpha_{33f})$, in $\mu\epsilon/\text{deg C}$	8.28
Matrix (Epoxy)	
Young's modulus E_m , in GPa	3.31
Shear modulus G_m , in GPa	1.23
Poisson's ratio ν_m	0.35
Coefficient of thermal expansion α_m , in $\mu\epsilon/\text{deg C}$	57.6

4.2 Single Cell and Multi Cell Models

Single cell and multi cell of square array are modeled and mechanical and thermal analyses are performed (FE models of single cell and multi cell can be reviewed in Figure 3-3). As mentioned in section 3.3, mechanical strain amplification factors are obtained from a model subjected to a prescribed loading. There are six loadings: three normal deformations (direction-1, direction-2, direction-3) and three shear deformations (direction-12, direction-13, direction-23).

Strain amplification factors for models subjected to direction-1 loadings (M_{11}) are all 1.0 at any selected points in the fiber and matrix suggesting that there is no strain magnification for loading in fiber direction (longitudinal direction). However, there are amplification of strains in fiber and matrix when the models are subjected to transverse loadings and shear loadings. For instance, Figure (4-1) shows the mechanical amplification factors resulted from single cell and multi cell models of square array subjected to transverse loading (direction-2), namely M_{22} . Due to rotational symmetry, the strain amplification factors for direction-3 (M_{33}) yields the same results as direction-2, however, the positions are rotated 90 degree counter-clockwise. In Figure 4-1, the horizontal-axis refers to selection points in micromechanics model. We can see that the strains are amplified in matrix region, i.e. interfiber (IF1) and fiber-matrix interface (M1, M2, M4, M5, M6, M8).

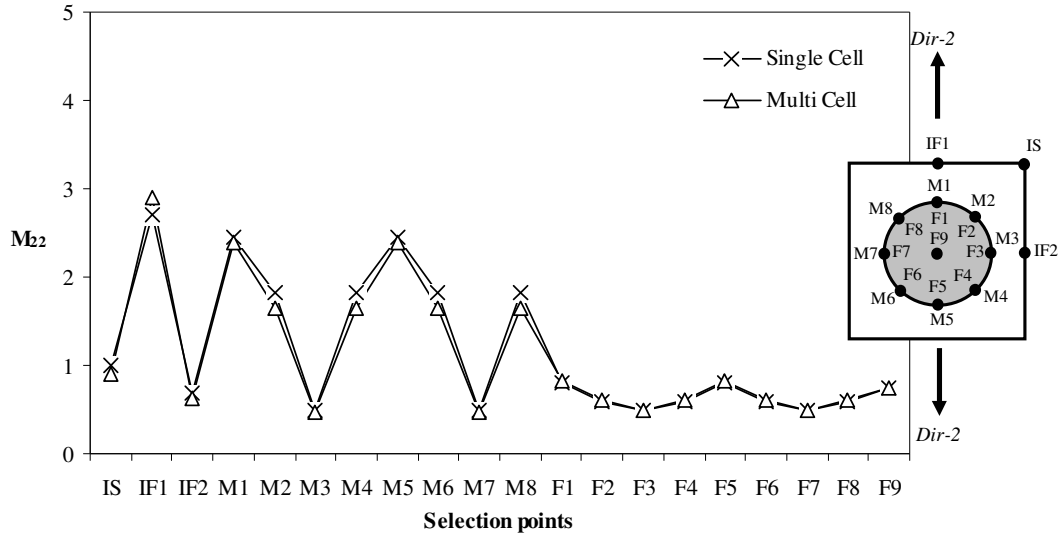


Figure 4-1. Mechanical strain amplification factors of single cell and multi cell square array loaded in direction-2 (M_{22}) at the 20 selected points described in the square model.

Strain amplification factors of several matrix points, i.e. IF1, M1, M2, M4, M5, M6, M8, have relatively higher value compared to those of fiber points (F1 – F9). This is due to the fact that graphite fiber is stiffer than epoxy matrix in longitudinal and transverse directions. It should be noted that mechanical strain amplification factors correspond to the local strains of the micromechanics model. Strain amplification factors at IF1, M1 and M5 have considerably higher value than other points in the matrix and fiber. The strains are relatively larger in the area where the fibers are near to each other, i.e. interfiber and fiber-matrix interface close to interfiber. Figure 4-2 shows the strain contour of multi cell square model subjected to transverse loading (direction-2) obtained from finite element analysis. Location of maximum strain suggests the possible damage initiation locus. It means that for particular loading condition damage will likely to occur at the position where the maximum amplification factors are located.

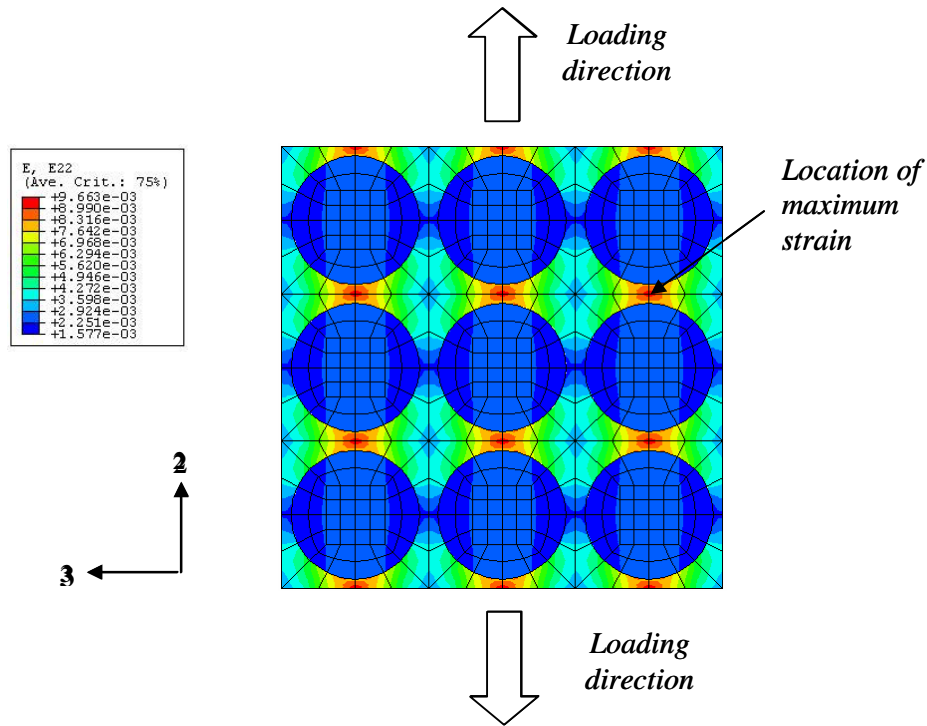


Figure 4-2 Strain contour of multi cell model of square array when it is subjected to transverse loading (direction-2)

Among six loading directions, the highest amplification factor is obtained when both models are subjected to in-plane deformation (i.e. 12- and 13-direction), and it occurs in matrix region of fiber-matrix interface (M1 and M5). Figure (4-3) shows mechanical amplification factors of single cell and multi cell square array loaded in 12-direction.

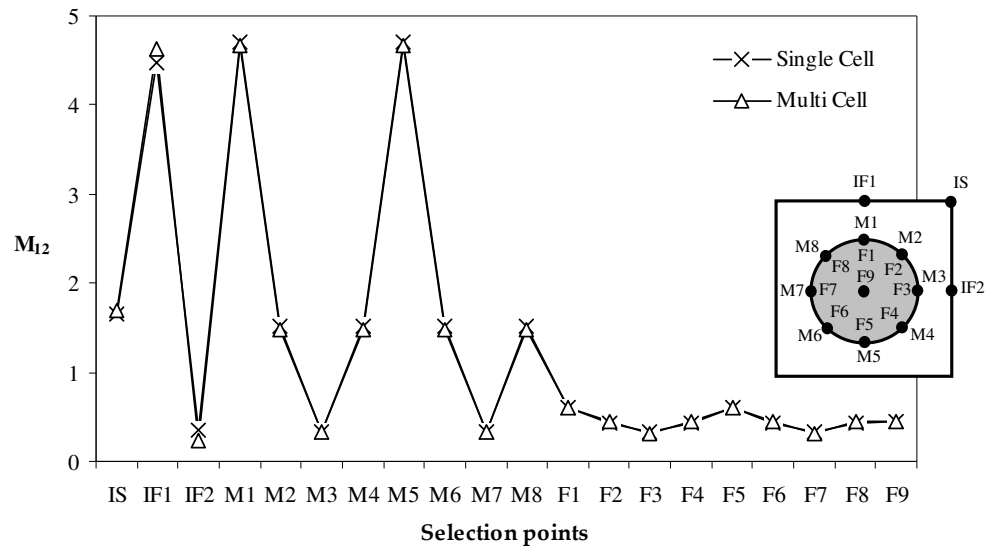


Figure 4-3. Mechanical amplification factors of single cell and multi cell square array loaded in 12-direction

From Table 4-2, for fiber phase the difference of amplification factors between single cell and multi cell is less than 9%. For matrix phase the difference of amplification factors between single cell and multi cell results is less than 13%, except in the interfiber points of IF1 and IF2 (the difference is almost 34%). In-plane shear loadings (i.e. direction-12 and direction-13) introduce higher strain in matrix phase, particularly in the interfiber, compared to other loadings. For direction-12 loading, the maximum strain amplification factor is located in M1 and M5, while for direction-13 loading, the maximum value is located in M3 and M7 since the model is rotationally symmetry. In Table 4-2, the highest values of amplification factors are shown in bold fonts, while the next highest values are shown in italic font.

Table 4-2 Mechanical amplification factors of single cell and multi cell square array loaded in 12-direction

Position	Matrix region		Position	Fiber region	
	Single Cell	Multi Cell		Single Cell	Multi Cell
IS	1.663180	1.685385	F1	0.600404	0.604593
IF1	4.471800	4.638720	F2	0.427618	0.438783
IF2	0.350679	0.235793	F3	0.326480	0.315483
M1	4.704650	4.661880	F4	0.427618	0.438777
M2	1.512710	1.477155	F5	0.600404	0.604590
M3	0.326725	0.322482	F6	0.427618	0.438768
M4	1.512710	1.477140	F7	0.326480	0.315486
M5	4.704650	4.661640	F8	0.427618	0.438768
M6	1.512710	1.477110	F9	0.441038	0.440373
M7	0.326725	0.322491			
M8	1.512720	1.477122			

For single cell and multi cell of square array with $V_f = 60\%$, the strain amplification factors due to thermal difference (thermo-mechanical amplification factor) is very small compared to mechanical loadings. The strains are extracted for six directions, i.e. ϵ_{11} , ϵ_{22} , ϵ_{33} , ϵ_{12} , ϵ_{13} and ϵ_{23} . The maximum thermo-mechanical amplification factor is obtained for direction-2, which is 0.0215 (Figure 4-4), and this value is located in IF2 of matrix phase. However, later it will be shown in section 4.4 that effect of temperature becomes more profound when the volume fraction is increased.

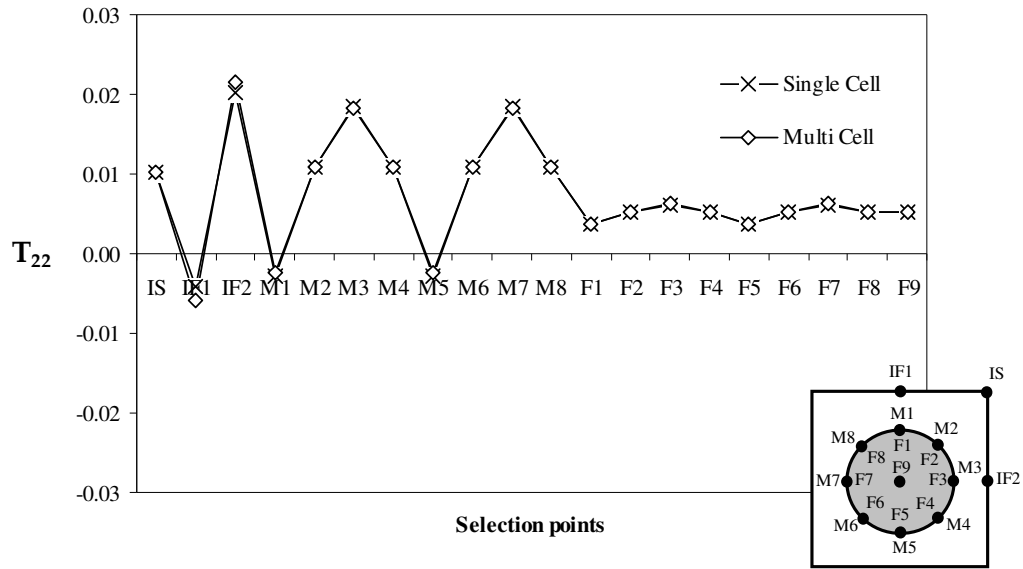


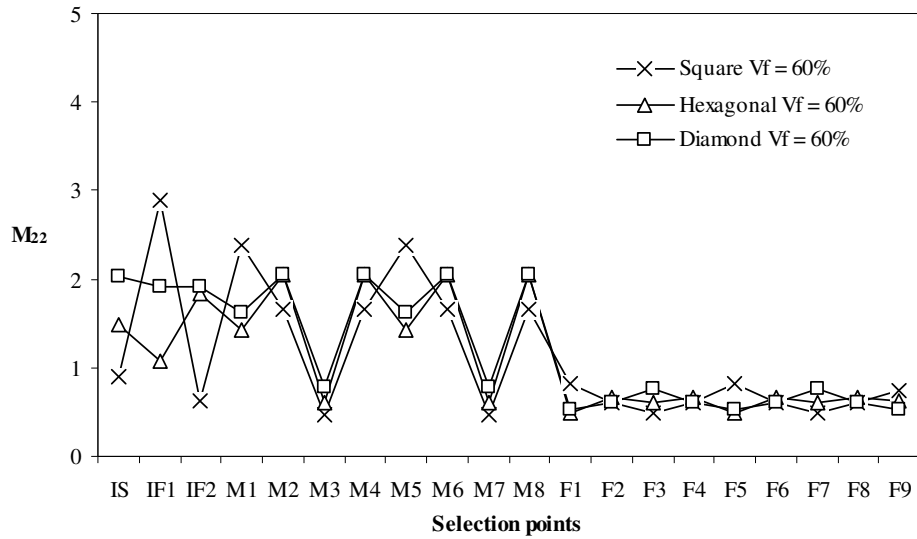
Figure 4-4. Thermo-mechanical amplification factors in 2-direction of single cell and multi cell of square array

4.3 Square, Hexagonal and Diamond RVEs

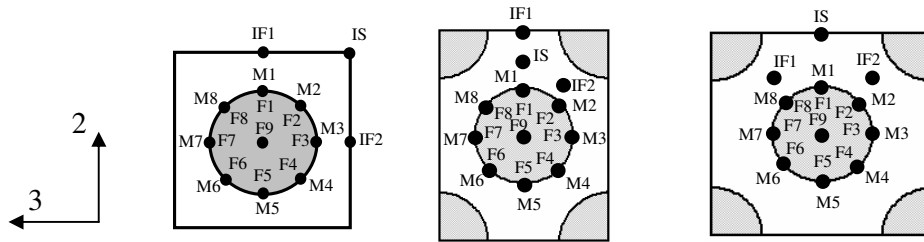
Similar to square array, strains of hexagonal and diamond array are also extracted. Three models have fiber volume fraction of 60%. Figure (4-5) shows mechanical amplification factors obtained when the three models are subjected to transverse direction loading (direction-2).

Generally, it is seen that the variation of amplification factors of square, hexagonal and diamond array occurs in the matrix phase rather than in fiber phase, especially in the interfiber and interstitial. The variation of amplification factors in the interfiber and interstitial is due to (1) the difference of defining the locations of both interstitial and interfiber for square, hexagonal and diamond, (2) the distance

between two closest fibers, which give rise to different strain magnitude. The amplification factors of hexagonal and diamond are similar at any points in fiber and matrix except in interfiber (IF1) and interstitial (IS). The similarity is due to the fact that the packing arrangement between diamond and hexagonal is similar. However, in interfiber and interstitial there is difference of amplification factors. This is because of different definition of interfiber positions (IF1 and IF2) and the different strain magnitude in interstitial point.



(a) Mechanical amplification factors in direction-2



(b) fiber packing arrangement of square, hexagonal and diamond.

Figure 4-5. Mechanical amplification factors of square, hexagonal and diamond array loaded in 2-direction

Amplification factors of square array are deviating from diamond and hexagonal in IS, IF1, IF2, M1 and M5. The amplification factor in interstitial position (IS) for square array is lower than those of diamond and hexagonal array. This is because the distance between fiber and interstitial point is smaller for square compared to diamond and hexagonal, which in turn will lower the strain at the interstitial point. At the interfiber of IF1, the amplification factor of square array is higher than that of hexagonal and diamond, while at the IF2, the result is contrary to that of IF1. At IF2, the amplification factors of diamond and hexagonal are similar and higher than that of square array. Due to loading in transverse direction (direction-2), large amount of strain occur in the interfiber and fiber-matrix interface. For square array, strain will reach the maximum at IF1, while for diamond and hexagonal, the strain will reach maximum at M2, M4, M6 and M8 (fiber-matrix interface). The strain contours for square, hexagonal and diamond are given in Figure 4-6; locations of maximum strain are marked.

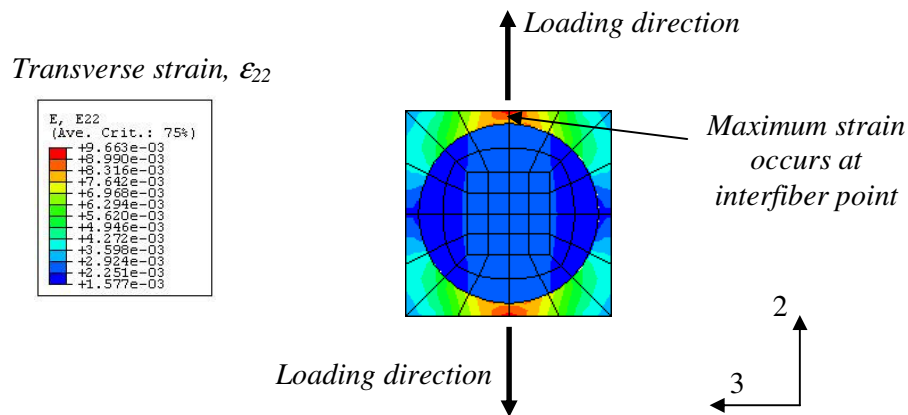


Figure 4-6 Strain contours of single cell within multi cell model of square array. Multi cell is subjected to loading in direction-2. Location of maximum strain is indicated.

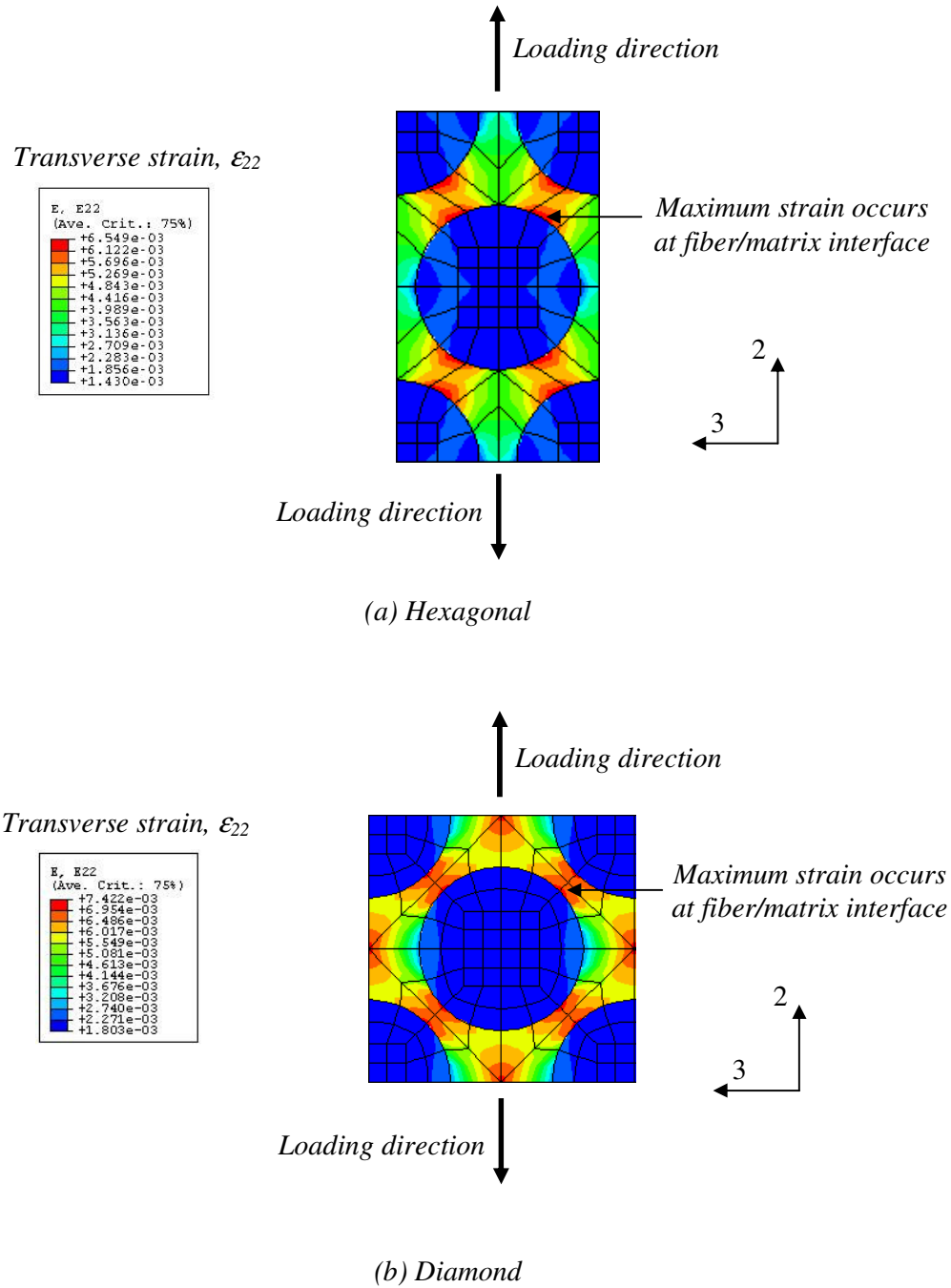


Figure 4-7 Strain contours of single cell within multi cell model of (a) hexagonal and (b) diamond array. Multi cell is subjected to loading in direction-2. Location of maximum strain is indicated.

It is important to note that in square and diamond arrays the magnitude of strain amplification factors between cases of direction-2 and direction-3 are identical since the arrays are similar viewed from direction-2 and direction-3. In square and diamond arrays, direction-2 is a 90 degree rotation of direction-3. However, it is not the case for the hexagonal array. Results of maximum strain amplification factors for hexagonal arrays loaded in direction-2 and direction-3 are different, particularly at selection points in matrix region. Figure 4-8 shows the comparison of amplification factors between direction-2 and direction-3 cases. Figure 4-9 shows hexagonal array subjected to direction-3 loading. High strain is located at interfiber position (i.e. IF1) indicated by red contour. If we compare Figure 4-9 with Figure 4-7 (a) the location of maximum strain is obviously different since the fiber arrangements of hexagonal array viewed from direction-2 and direction-3 are also different.

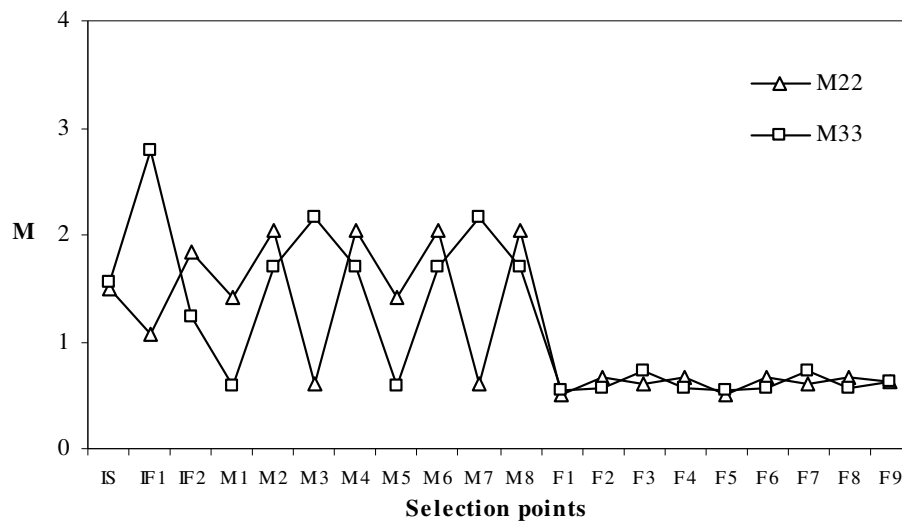


Figure 4-8 Comparison of strain amplification factors of direction-2 and direction-3 cases.

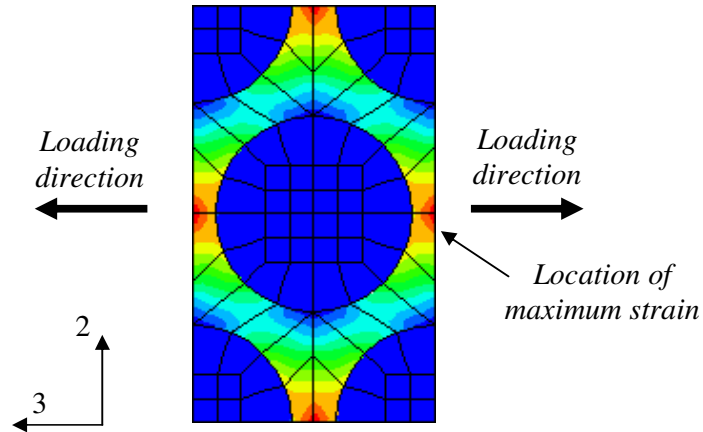


Figure 4-9 Strain contour of hexagonal array subjected to direction-3 loading.

The maximum value of amplification factors occurs when the model is subjected to in-plane shear deformation (13-direction and 12-direction), and it occurs in square array. The location of maximum amplification factors is interfiber (IF1) and fiber-matrix interface (M1 and M5).

In thermal analysis, difference of coefficient of thermal expansion between fiber and matrix produces strains in the matrix phase for square and in both fiber and matrix for hexagonal and diamond. Zero strains are found in the fiber phase of square array in direction-1. Zero strains are also found in most of fiber and matrix phases of square, hexagonal and diamond in direction-12, direction-13 and direction-23.

Among three models, maximum thermo-mechanical amplification factors occur in the fiber-matrix interface of hexagonal array. Maximum values are obtained when the strains are extracted for transverse direction (direction-3). Figure (4-10) shows the thermo-mechanical amplification factors obtained from square, hexagonal and diamond arrays for direction-3. Again, differences of thermo-mechanical

amplification factors are found in interfiber (IF1 and IF2) and fiber-matrix interface (M3 and M7) of square, hexagonal and diamond. This is due to the different strain magnitudes correspond to the distance between fibers and different mechanism of strain transfers. Strain contours for square, hexagonal and diamond can be seen in Figure (4-11).

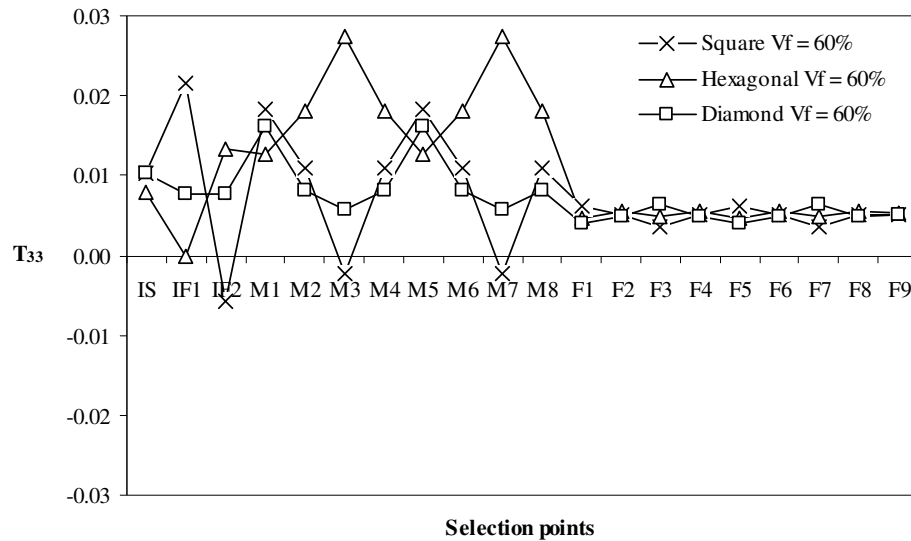


Figure 4-10 Thermo-mechanical amplification factors of square, hexagonal and diamond array in 3-direction (selected points in micromechanics models can be seen in Figure 4-5b)

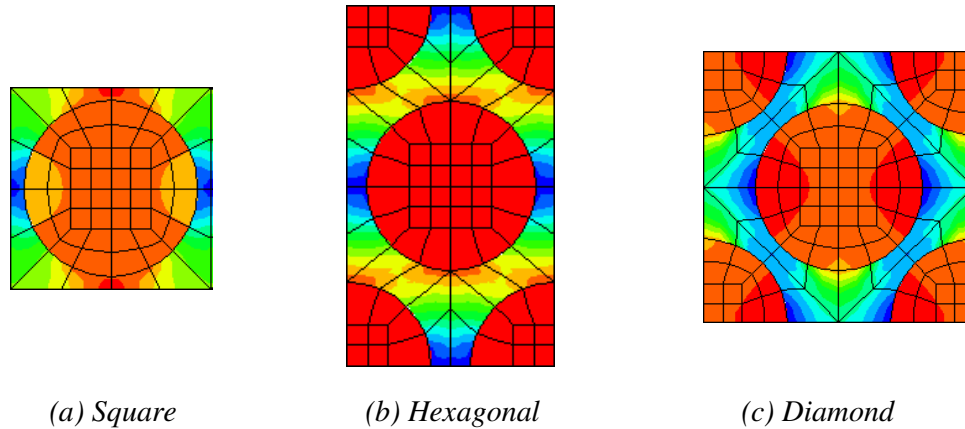


Figure 4-11 Strain of square, hexagonal and diamond in direction-3

4.4 Effect of Fiber Volume Fraction

Evaluation on fiber volume fraction (V_f) is performed in terms of amplification factors. The effect of fiber volume fraction with respect to the amplification factors is examined for square array only. The finite element models are built for three volume fractions of 50%, 60% and 70%.

Fiber volume fraction has no effect when square model is subjected to direction-1 loading. The magnitude of amplification factors remain 1.0 at any points in the fiber and matrix for direction-1 loading. The results imply that the amplification factors are not affected by geometry of the fiber, i.e. radius of the fiber.

For transverse loading (i.e. direction-2), considerable difference of amplification factors occurs at the interfiber points of IF1 and IF2 and fiber-matrix interface of M1 and M5 (Figure 4-12). From Figure 4-12, it can be seen that increasing fiber volume fraction will increase the amplification factors in IF1, M1 and M5. In IF1, increasing volume fraction by 10% will give 8.9% – 14% difference of amplification factors,

while at M1 and M5, increasing volume fraction by 10% will give 15.6% - 16.3% difference.

The opposite situation happens in IF2: increasing fiber volume fraction will reduce amplification factors. In IF2, increasing fiber volume fraction by 10% will reduce amplification factors by 45.8% - 48.4%. Strain magnitude in IF2 is reduced as larger amount of strains occur in IF1 due to distance reduction between fibers.

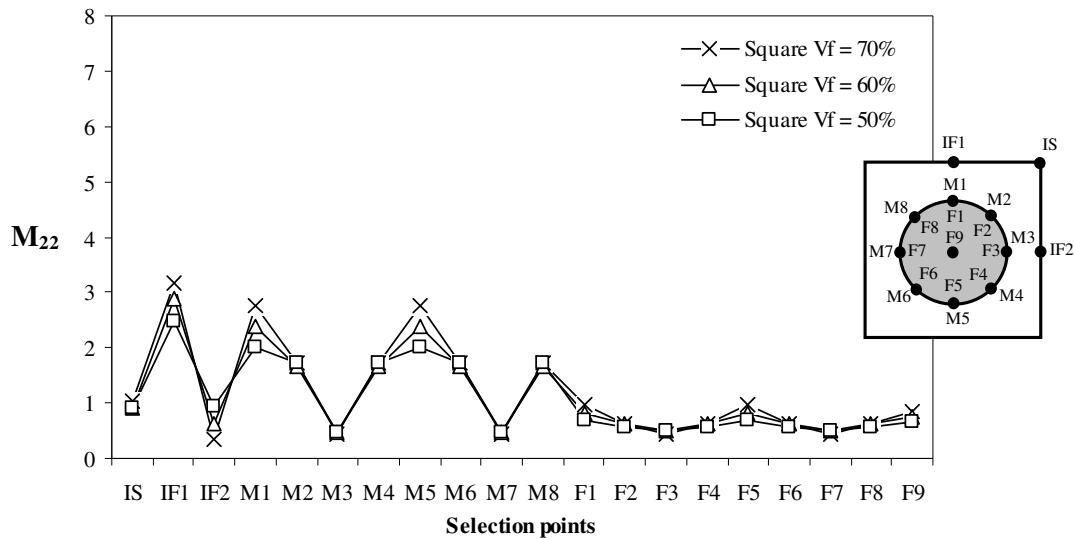


Figure 4-12 Mechanical amplification factors of square array with volume fraction of 50%, 60% and 70% loaded in direction-2.

Under in-plane shear deformation-13, the increasing of amplification factors occurs profoundly in the interfiber of IF2 and fiber-matrix interface of M3 and M7. Increasing fiber volume fraction by 10% will increase amplification factors of 30.3% (from $V_f = 50\%$ to $V_f = 60\%$) and 73.5% (from $V_f = 60\%$ to $V_f = 70\%$).

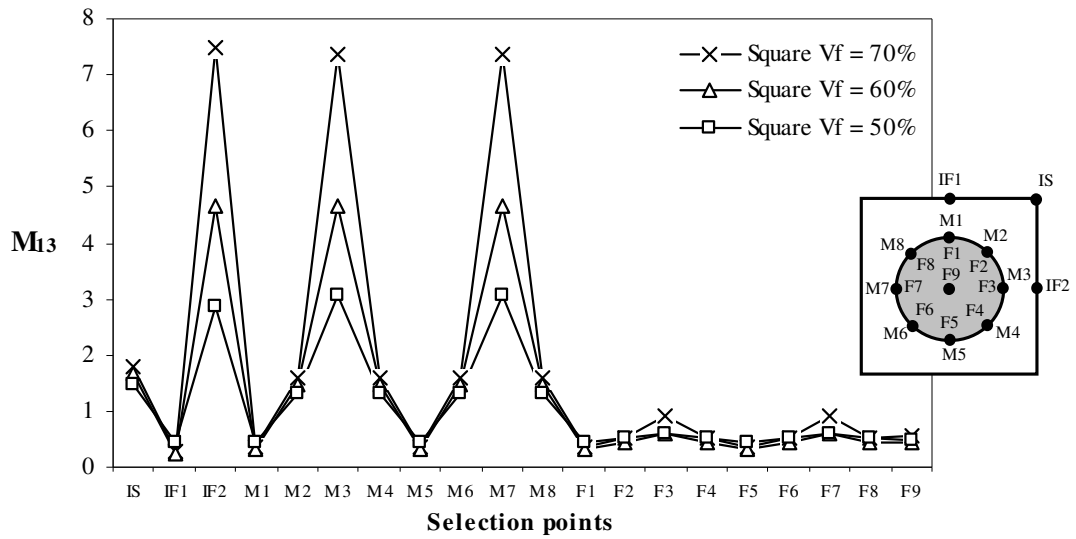


Figure 4-13. Mechanical amplification factors of square array with volume fraction of 50%, 60% and 70% loaded in direction-13

Increasing fiber volume fraction gives less effect to the thermo-mechanical amplification factors. We can see in Figure (4-14) that in interfiber IF1 and fiber-matrix interface of M1 and M5 increasing fiber volume fraction will actually decrease the amplification factor. In fiber points, increase of fiber volume fraction will slightly decrease the amplification factor.

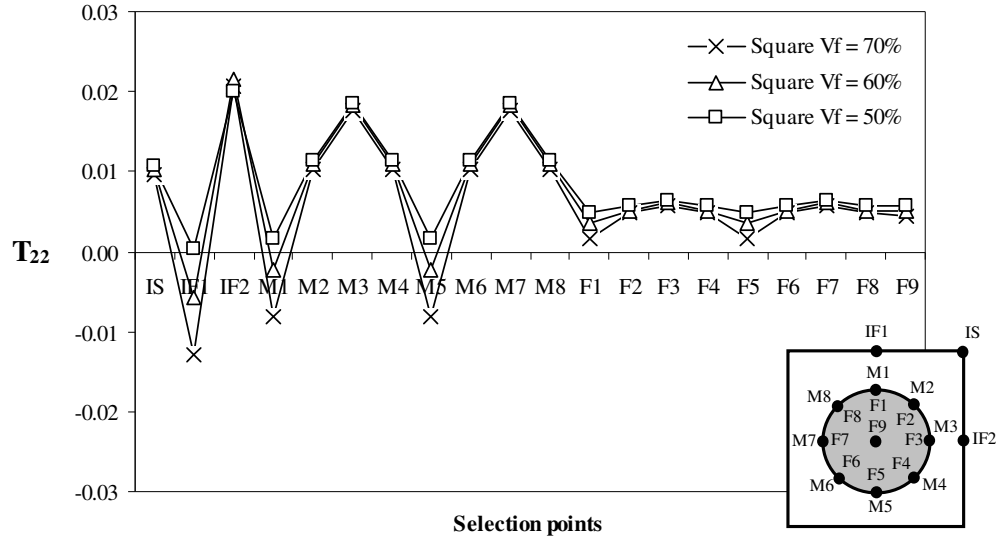


Figure 4-14. Thermo-mechanical amplification factors of square array with volume fraction of 50%, 60% and 70% in 2-direction

Table 4-3 shows the effect of fiber volume fraction on maximum amplification factors in square array. In summary, for loading in transverse directions (direction-2 and direction-3), the maximum amplification factors appear in the interfiber regions (IF1 and IF2) suggesting the possible failure in the matrix material, although the next highest values occur at the fiber-matrix interface (M1, M5, M3, M7). For shear cases in the direction-12 and direction-13, amplification factors for the highest and next highest values are extremely close, especially for the fiber volume $V_f = 60\%$ case. This suggests that failure in the case of pure shear is almost equally likely to occur in the matrix (IF1 and IF2) as in the fiber-matrix interface (M1, M5, M3 and M7). For the case of shear across the fibers in direction-23, failure in the matrix is more likely to be in the interstitial position (IS) although failure in the fiber-matrix interface may still occur. At $V_f = 70\%$, the preferred failure site appears to switch to

the fiber-matrix interface from the interstitial position. In this regard, increasing fiber volume fraction will increase maximum amplification factors. However, with lower magnitude of maximum amplification factors, it does not mean that resin-rich composites (for example composite with $V_f = 50\%$) are more resistant to damage, because the elastic properties of composite will also change with the fiber volume fraction.

Table 4-3 Effect of fiber volume fraction V_f on amplification factors in square array model (figures in bold are maximum values; figures in italic for next highest values)

Fiber volume fraction		Dir-1	Dir-2	Dir-3	Dir-12	Dir-13	Dir-23
Vf = 50%	Maximum amplification factor	1	2.494 <i>2.012</i>	2.494 <i>2.012</i>	3.308 <i>3.049</i>	3.308 <i>3.049</i>	2.280 <i>2.041</i>
	Position	All points	IF1 <i>M1, M5</i>	IF2 <i>M3, M7</i>	IF1 <i>M1, M5</i>	IF2 <i>M3, M7</i>	IS <i>M1, M3, M5, M7</i>
Vf = 60%	Maximum amplification factor	1	2.897 <i>2.383</i>	2.897 <i>2.383</i>	4.662 <i>4.639</i>	4.662 <i>4.639</i>	2.623 <i>2.575</i>
	Position	All points	IF1 <i>M1, M5</i>	IF2 <i>M3, M7</i>	M1, M5 <i>IF1</i>	M3, M7 <i>IF2</i>	IS <i>M1, M3, M5, M7</i>
Vf = 70%	Maximum amplification factor	1	3.156 <i>2.771</i>	3.156 <i>2.771</i>	7.502 <i>7.347</i>	7.502 <i>7.347</i>	3.904 <i>3.747</i>
	Position	All points	IF1 <i>M1, M5</i>	IF2 <i>M3, M7</i>	IF1 <i>M1, M5</i>	IF2 <i>M3, M7</i>	M1, M3, M5, M7 <i>IF1, IF2</i>

4.5 Effect of Fiber Moduli, Matrix Modulus and Fiber Material

Effect of fiber moduli, matrix modulus and fiber material on amplification factors is discussed. Elastic properties of the fiber, i.e. E_{11f} (fiber longitudinal modulus), E_{22f} (fiber transverse modulus) and G_{23f} (out-of-plane shear modulus), and elastic property of matrix (E_m) are changed by 20%. Notation with star (*) represents the altered property. For example, if the longitudinal fiber modulus is increased by 20%, the notation becomes $E_{11f}^*/E_{11f} = 1.2$, or if the fiber modulus is decreased by 20% the notation becomes $E_{11f}^*/E_{11f} = 0.8$. The meaning of notation (*) applies to the designation of other moduli. Since changing fiber and matrix moduli, and also matrix modulus, has no effect on amplification factors of M_{11} , the analysis is conducted for M_{22} instead.

In this section, there are five cases to be discussed in terms of strain amplification factors:

1. Effect of longitudinal modulus E_{11f}
2. Effect of transverse modulus E_{22f}
3. Effect of out-of-plane shear modulus G_{23f}
4. Effect of matrix modulus E_m
5. Effect of fiber materials (carbon, glass and boron fibers)

Effect of fiber longitudinal modulus E_{11f}

Figure (4-14) shows that increasing fiber longitudinal modulus (E_{11f}) by 20% will have no effect on the amplification factors of transverse direction (M_{22}) in matrix region as well as in fiber region. However, reducing E_{11f} by 20% will decrease the amplification factors in fiber points of F3, F4, F7 and F8, and increase the amplification factors in fiber points of F1, F2, F5 and F6.

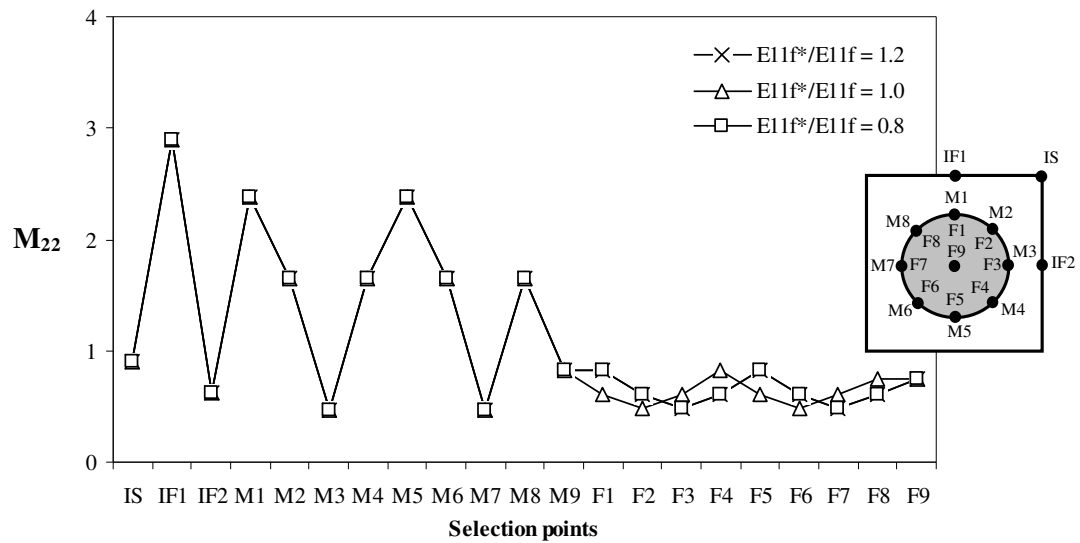


Figure 4-15. Effect of changing fiber longitudinal modulus (E_{11f}) on amplification factors M_{22}

Effect of fiber transverse modulus E_{22f}

Figure (4-16) shows the effect of changing the transverse modulus (E_{22f}) on amplification factors in direction-2 (M_{22}). It can be seen that increasing E_{22f} by 20% will increase amplification factors in matrix points of IF1, M1, M2, M4, M5 and M8. However, this is not the case for matrix points of IF2, M3, M7 and fiber points of F1 – F9; at those points the amplification factors will somewhat decrease. And, decreasing E_{22f} by 20% will decrease amplification factors at IF1, M1, M2, M4, M5

and M8, but it will increase the amplification factors at IF2, M3, M7 and fiber points of F1 – F9. Generally, increasing and decreasing fiber transverse modulus will have an effect to the strain amplification factors in transverse direction.

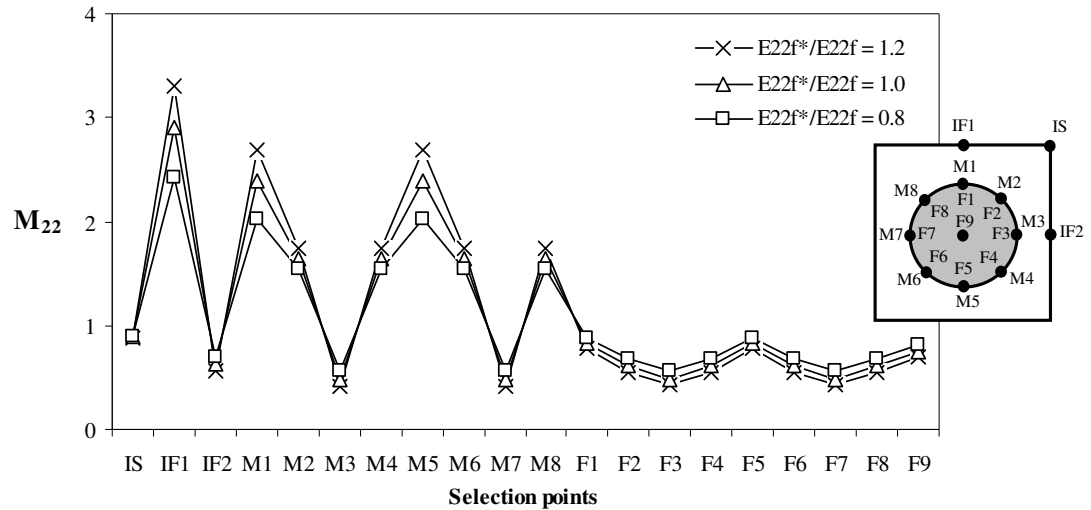


Figure 4-16. Effect of changing fiber transverse modulus (E_{22f}) on amplification factors M_{22}

Effect of fiber shear modulus G_{23f}

Increasing fiber shear modulus (G_{23f}) by 20% will increase amplification factors of shear direction-23 (M_{23}) in matrix region (Figure 4-17), i.e. IS, IF1, IF2, M1, M3, M5 and M7 (maximum difference is 8.2%). Increasing G_{23f} by 20% will instead decrease amplification factors M_{23} of fiber points F1 – F9 (maximum difference is 19%).

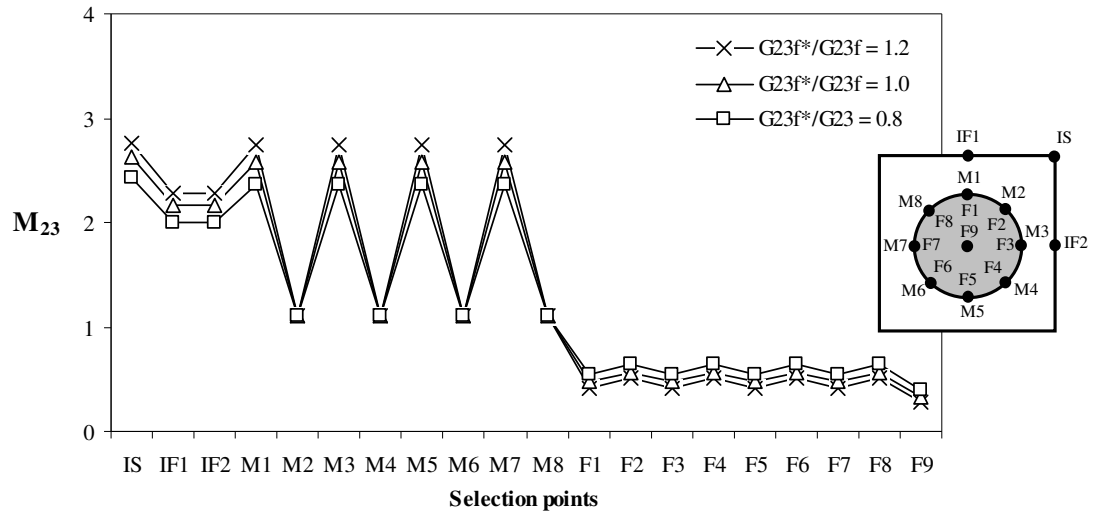


Figure 4-17. Effect of changing fiber transverse modulus (G_{23f}) on amplification factors M_{23}

Effect of matrix modulus E_m

Increasing matrix modulus by 20% will decrease amplification factors by maximum 18.6% in matrix points of IF1, M1, M2, M4, M5 and M8 (Figure 4-18). However, this is not the case for matrix points of IF2, M3, M7; increasing matrix modulus by 20% will also increase amplification factors M_{22} . This condition is similar with the case of changing E_{22f} . In fiber points F1 – F9, increasing matrix modulus will increase amplification factors M_{22} by average 11%.

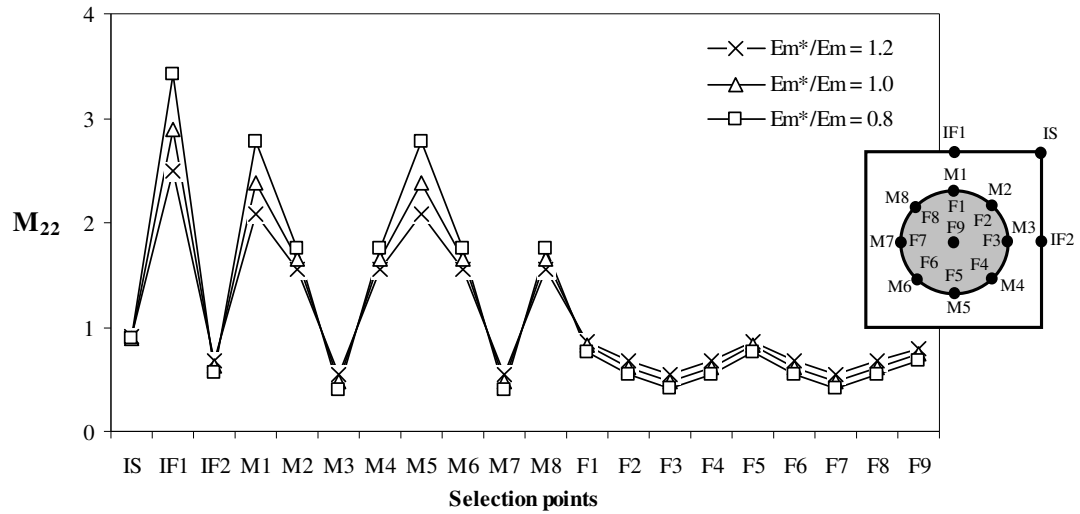


Figure 4-18. Effect of changing matrix modulus (E_m) on amplification factors M_{22}

Effect of fiber materials

Effect of changing fiber materials is discussed. Analyses have been conducted by using graphite fiber (or carbon fiber) and epoxy matrix, so-called graphite/epoxy composite system. The analysis is carried out to compare the strain amplification factors when the graphite fibers are replaced by other fiber materials like glass fibers and boron fibers. Elastic properties for graphite fibers and epoxy can be reviewed in Table 4-1. Table 4-4 describes the elastic properties of glass and boron fibers.

Table 4-4. Elastic properties of glass and boron [Gibson, 1994]

S-Glass	Magnitude
E , in GPa	85.5
G , in GPa	35.65
Poisson's ratio ν_f	0.2
Coefficient of thermal expansion α , in $\mu\epsilon/\text{deg C}$	5.04
Boron	
E , in GPa	399.90
G , in GPa	166.85
Poisson's ratio ν_f	0.2
Coefficient of thermal expansion α , in $\mu\epsilon/\text{deg C}$	5.04

The effect of changing fiber materials is examined for strain amplification factors in direction-2 (M_{22}). As can be observed in Figure 4-18, boron/epoxy and glass/epoxy composites will give higher amplification factors compared to graphite/epoxy in matrix points of IF1, M1, M5, and M8. Large difference of amplification factors occurs in IF1, M1 and M5 which are aligned with center point of fiber. However, in fiber region, boron/epoxy and glass/epoxy system will give lower amplification factors than graphite epoxy.

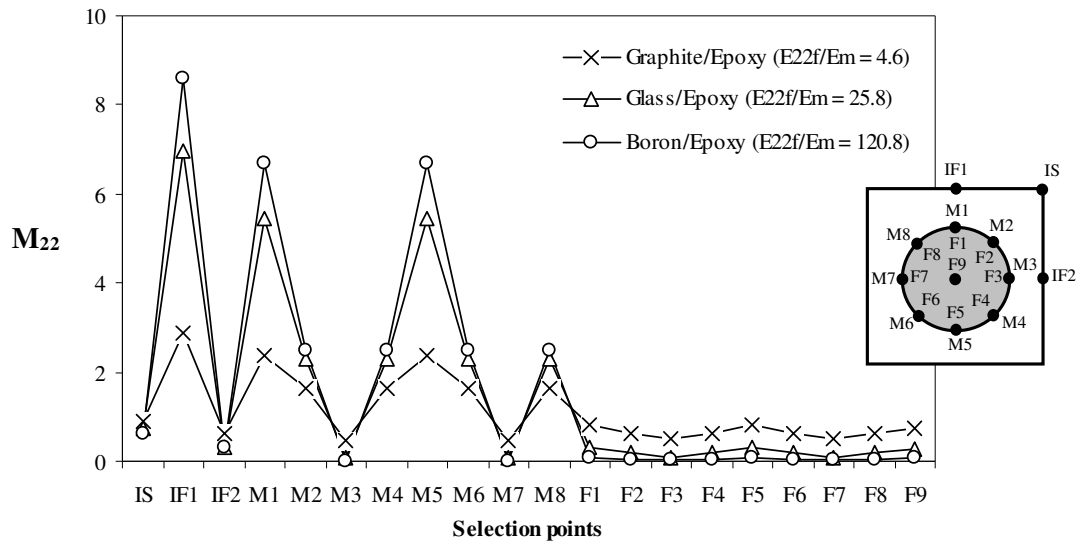


Figure 4-19. Effect of changing fiber materials on amplification factors M_{22} . Fibers are graphite, glass and boron.

4.6 Maximum Strain Amplification Factors

Table 4-5 shows the location of maximum amplification factors for square, hexagonal and diamond arrays. The fiber volume fraction is 50%, 60% and 70%. For square array, location of maximum value is at the interfiber and fiber-matrix interface. For hexagonal array, location of maximum value is at the fiber-matrix

interface. For diamond array, location of maximum value is at the interfiber and fiber-matrix interface. The location of maximum value corresponds to the locus of damage initiation in composites. It can be seen in Table 4-5 that for three fiber arrangements of square, hexagonal and diamond and also for fiber volume fraction of 50% - 70%, the damage at micro-level occurs due to in-plane shear loading (direction-12 and direction-13). The similarity of loading implies that damage will easily occur due to pure in-plane shear regardless the fiber arrangement or the fiber volume fraction. Compared to other loading conditions, deformation in matrix phase due to in-plane loading is larger at interfiber or fiber-matrix interface. This gives rise to the higher strains at those points. In this sense, interaction between shear modulus of fiber and matrix takes an important role in increasing the strains at interfiber and fiber-matrix interface.

Table 4-5. Maximum mechanical amplification factors

Fiber packing	Fiber volume fraction	Maximum amplification factor	Direction of deformation	Location
Square	50%	3.308	In-plane shear 12, 13	Interfiber (matrix)
	60%	4.662	In-plane shear 12, 13	Fiber-matrix interface (matrix)
	70%	7.502	In-plane shear 12, 13	Interfiber (matrix)
Hexagonal	50%	3.023	In-plane shear 13	Fiber-matrix interface (matrix)
	60%	3.529	In-plane shear 13	Fiber-matrix interface (matrix)
	70%	3.767	In-plane shear 13	Fiber-matrix interface (matrix)
Diamond	50%	2.502	In-plane shear 12, 13	Fiber-matrix interface (matrix)
	60%	2.425	In-plane shear 12, 13	Interfiber (matrix)
	70%	4.010	In-plane shear 12, 13	Interfiber (matrix)

Table 4-6 shows that for square and hexagonal arrays the maximum thermo-mechanical amplification factors are obtained when the residual strains are obtained from transverse direction. For diamond array, maximum thermo-mechanical strain is obtained from shear-23 deformation. The location of maximum amplification factor for square and diamond arrays is at the interfiber. For hexagonal the location of maximum thermo-mechanical amplification factors is at the interfiber and fiber-matrix interface. From thermal loading, similar to mechanical loading, it implies that the damage will likely to occur at the interfiber and fiber-matrix interface.

Table 4-6. Maximum thermo-mechanical amplification factors

Fiber packing	Fiber volume fraction	Maximum amplification factor	Direction of deformation	Location
Square	50%	0.020	Transverse 2, 3	Interfiber (matrix)
	60%	0.022	Transverse 2, 3	Interfiber (matrix)
	70%	0.021	Transverse 2, 3	Interfiber (matrix)
Hexagonal	50%	0.018	Transverse 2	Fiber-matrix interface (matrix)
	60%	0.027	Transverse 3	Interfiber (matrix)
	70%	5.476	Transverse 3	Interfiber (matrix)
Diamond	50%	0.019	Out-of-plane shear 23	Interfiber (matrix)
	60%	0.027	Out-of-plane shear 23	Interfiber (matrix)
	70%	0.034	Out-of-plane shear 23	Interfiber (matrix)

CHAPTER 5

DAMAGE PROGRESSION IN OPEN-HOLE TENSION SPECIMEN

5.1 Element-Failure Method

The element-failure concept is particularly suited for failure analysis of composite structures, where there are multiple failure modes and certain modes of failure do not completely preclude the ability of the composite material to sustain stresses. For the purpose of illustration, consider an FE of an undamaged composite material (Figure (5-1a)), experiencing a set of nodal forces. Suppose damage in the form of matrix micro-cracks are formed (which may or may not be uniformly distributed within the FE), the load-carrying capacity of the FE will be compromised, very likely in a directionally and spatially dependent manner (Figure (5-1b)). In conventional material degradation models [*Tserpes et al, 2001; Camanho and Matthews, 1999; Shokrieh and Lessard, 1998*] this reduction in load-carrying capacity is achieved by reducing or zeroing certain pertinent material stiffness properties of the damaged finite element. For example, if failure is determined to have occurred in the fiber direction (breaking of fibers in tension) the fiber-direction Young's modulus E_{11} may be set to zero. In the element-failure method, however, the reduction is effected by applying a set of external nodal forces such that the net internal nodal forces of elements adjacent to the damaged element are reduced or zeroed (the latter if complete failure or fracture is implied (Figure 5-1c)).

The decision whether to fail an element is guided by a suitable failure theory and in each step, only one element is failed. The “correct” or required set of applied nodal forces to achieve the reduction within each step is determined by successive iterations until the nett internal nodal forces (residuals) of the adjacent elements converge to the desired values. After this, the stresses within the failed element no longer have physical meaning although compatibility may be preserved. This process leaves the original (undamaged) material stiffness properties unchanged, and is thus computationally efficient as every step and iteration is simply an analysis with the updated set of loading conditions at the nodes. For this reason, it may also be called the nodal force modification method. Hence, no reformulation of the FE stiffness matrix is necessary.

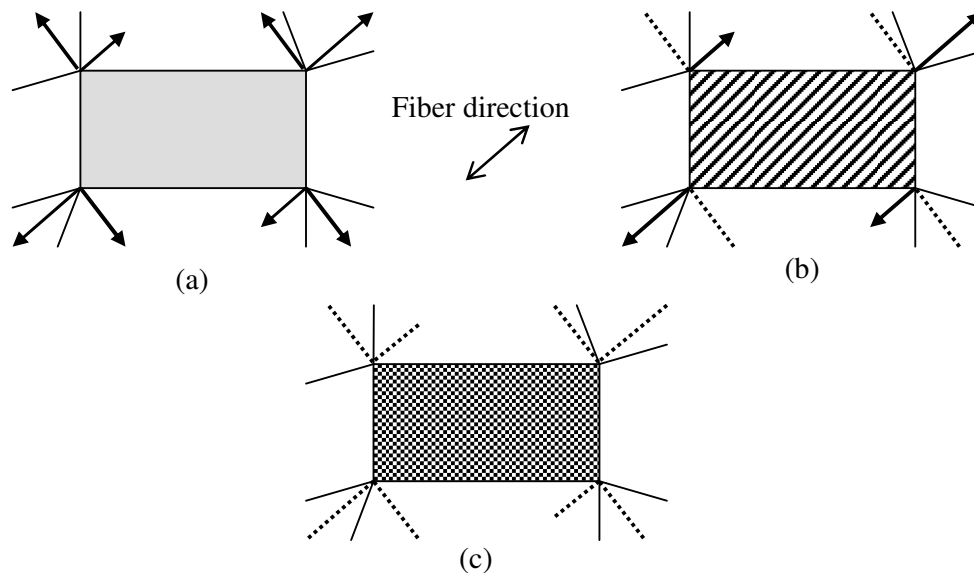


Figure 5-1 (a) FE of undamaged composite with internal nodal forces, (b) FE of composite with matrix cracks. Components of internal nodal forces transverse to the fiber direction are modified, and (c) Completely failed element. All nett internal nodal forces of adjacent elements are zeroed.

5.2 EFM and SIFT to Predict Damage Progression

The aims of current research are to predict the damage progression in composite laminates and to observe qualitatively the effect of changing the fiber volume fraction of composite with respect to the damage pattern. Damage progression in composite laminates can be predicted by using Element Failure Method and the failure criterion used is Strain Invariant Failure Theory.

In an in-house finite element code consisting EFM algorithm and SIFT, data of strain amplification factors is stored with fiber volume fraction of 50%, 60% and 70%. A subroutine of finite element analysis is made to transform strain tensors from global coordinate to local coordinate system. After being transformed, strain tensors are modified using stored strain amplification factors with certain fiber volume fraction, e.g. $V_f = 60\%$, following Eq. (3-18). The modified strain tensors are then transformed back into global coordinate system. If a modified strain in global coordinate systems reaches critical strain invariant quantity (see Eq. (3-11) – Eq. (3-13)), damage will initiate and then propagate. Critical strain invariant quantity is obtained from experiments.

As reference, the specified fiber volume fraction is 60%. Fiber volume fraction is then altered into 50% and 70% to observe the effect of increasing or decreasing fiber volume fraction by 10% with respect to damage progression.

5.3 Open-Hole Tension (OHT) Specimen

The case of composite quasi-isotropic plate with notch is built and damage was expected to initiate at the edge of the hole. One half of the open-hole tension specimen is symmetrically built. Plate has dimensions of 76.2 mm x 76.2 mm. Total thickness of the plate is 1.28 mm. Diameter of the hole is 12.7 mm.

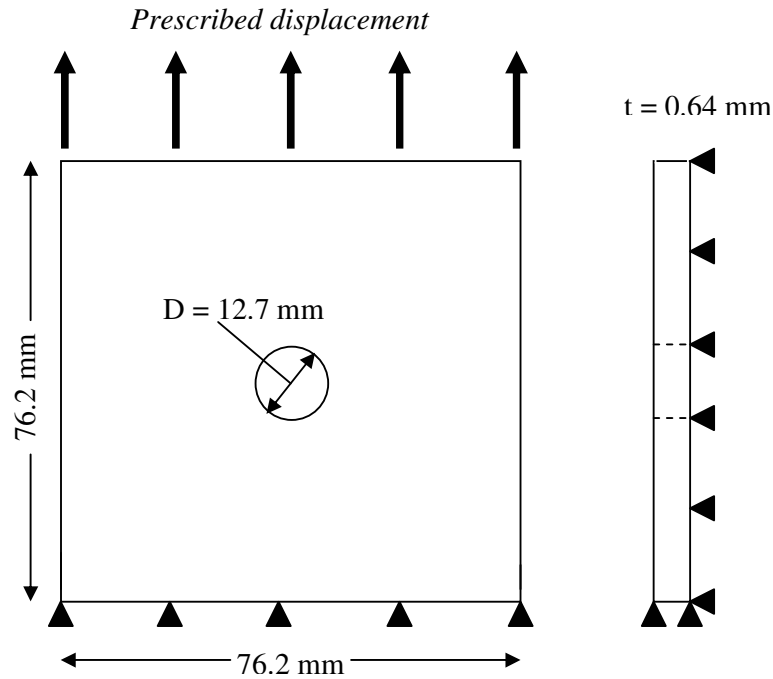


Figure 5-2. Schematic of the open hole tension specimen

Schematic of open-hole tension specimen is shown in Figure (5-2). In the symmetry through-the-thickness, surface of symmetry is restrained so that it will not move laterally (out of plane). Unit displacement is prescribed as loading condition on the top of the plate. At the bottom, plate is restrained.

5.4 Damage Progression in Open-Hole Tension Specimen

Figure (5-3) and (5-4) illustrate the predicted damage progression of each ply of laminated composite $[45/0/-45/90]_s$, when 250 elements are failed. It is important to note that the amplification factors used in this analysis are obtained for fiber volume fraction of 60%. Generally, the damage initiates at the right and left of area close to the central hole. Ply-2 (0 degree) has large amount of failed elements which are dominantly failed by ϵ_{vm}^m . Small amount of damage is indicated in ply-1 (45 deg) and ply-3 (-45 deg). Ply-4 (90 deg) shows the damage which propagate in horizontal direction. All of elements in ply-4 are failed by J_1 .

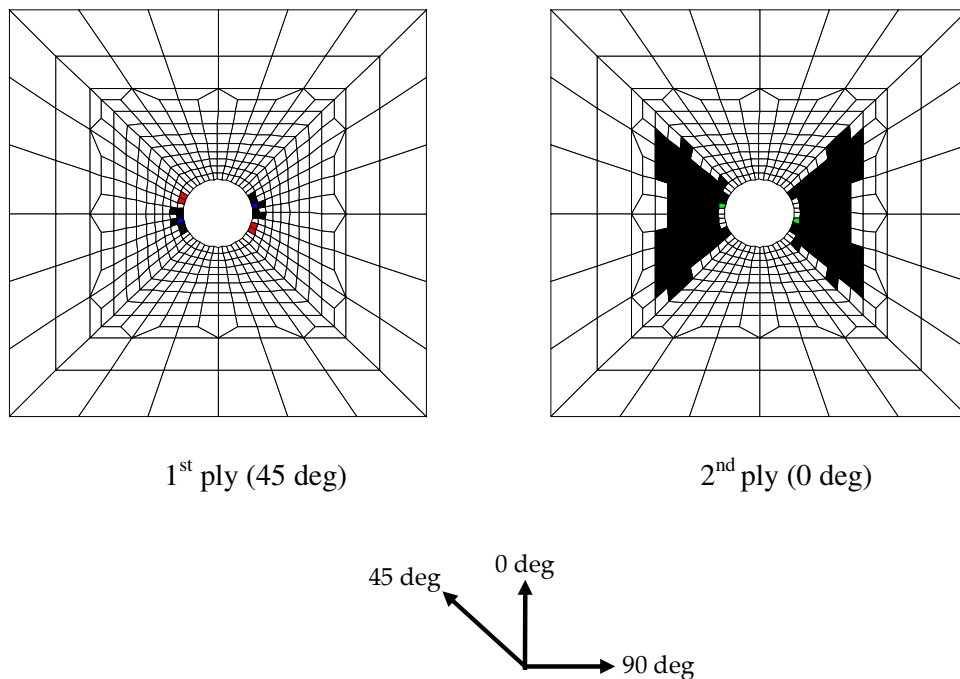


Figure 5-3. Damage progression of ply-1 and ply-2 of laminated composite $[45/0/-45/90]_s$ ($V_f = 60\%$)

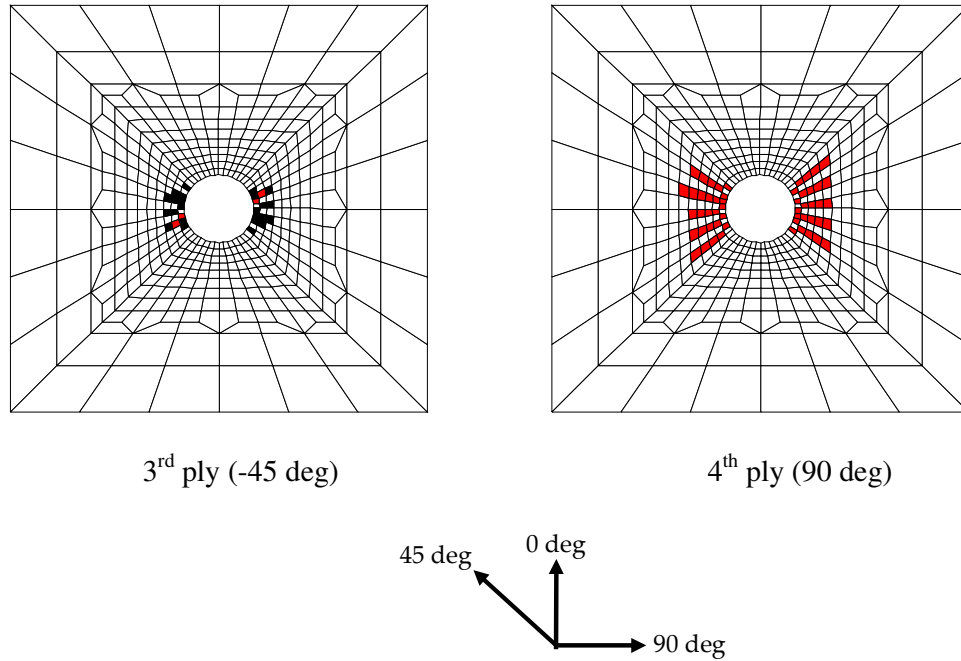


Figure 5-4. Damage progression of ply-3 and ply-4 of laminated composite $[45/0/-45/90]_s$ ($V_f = 60\%$)

Damage pattern resulted from finite element simulation (redrawn as schematic figure) is in a good agreement with the experimental result (Figure (5-5)).

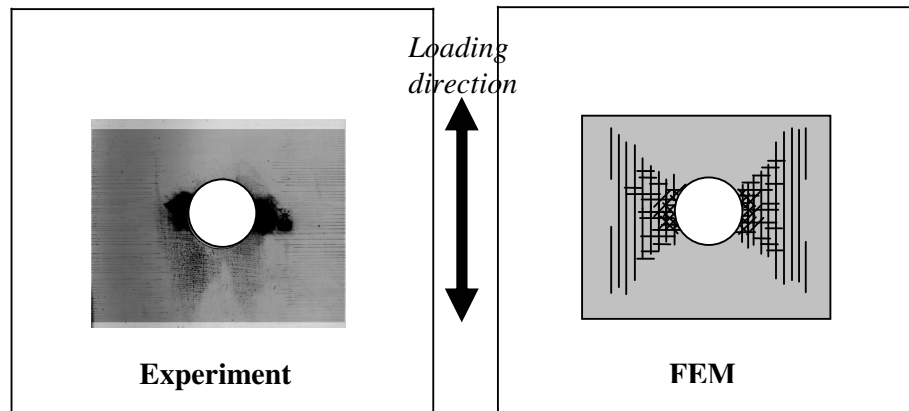


Figure 5-5. Damage pattern of open-hole tension specimen CFRP $[45/0/-45/90]_s$: comparison between experiment and schematic damage map (FEM result)

5.5 Effect of Fiber Volume Fraction

Effect of fiber volume fraction with respect to the damage progression in open-hole tension is investigated. Strain amplification factors in EFM-SIFT in-house code were modified. Two cases were conducted: **Case 1**, where the strain amplification factors were modified from $V_f = 60\%$ to $V_f = 50\%$, and **Case 2**, where the strain amplification factors were modified from $V_f = 60\%$ to $V_f = 70\%$.

Case 1: $V_f = 50\%$

Figure (5-6) and (5-7) show the damage progression of four plies of CFRP [45/0-45/90]_s. Ply-1, Ply-3 and Ply-4 were all failed by J_1 matrix. Damage in ply-1 (45 deg) tends to propagate towards 45 degree, while ply-2 (0 deg) shows no damage. Large amount of damage can be observed in Ply-4 (90 deg).

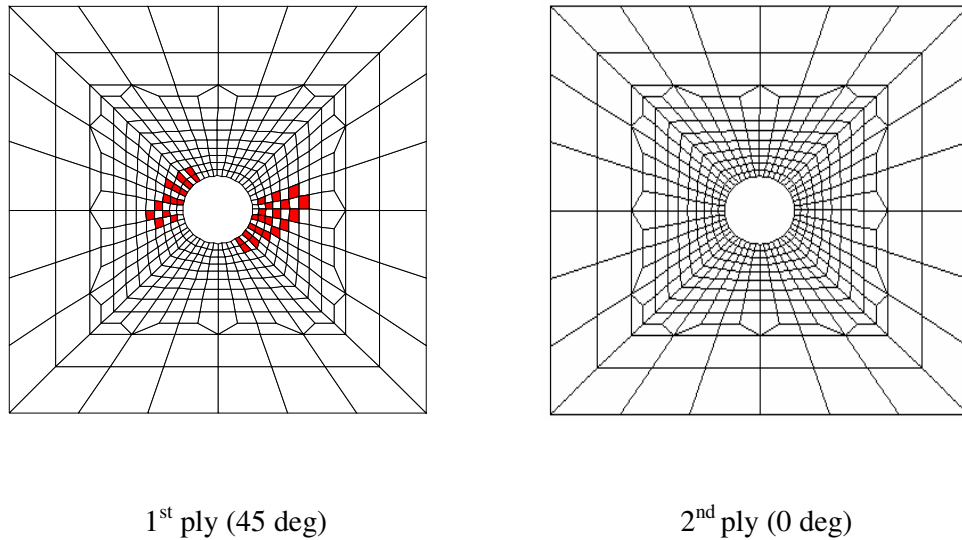


Figure 5-6. Damage progression of ply-1 and ply-2 of laminated composite [45/0-45/90]_s ($V_f = 50\%$)

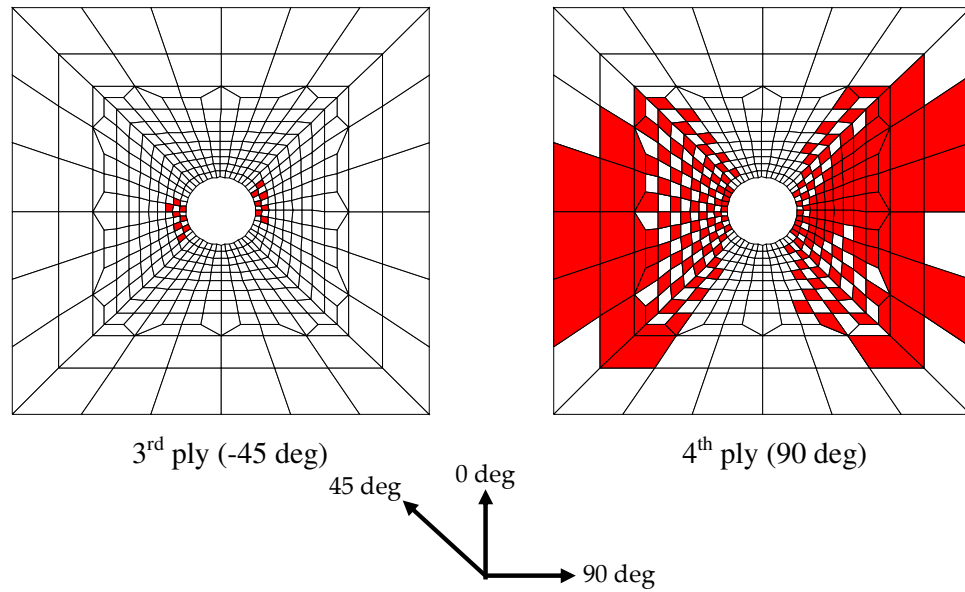


Figure 5-7. Damage progression of ply-3 and ply-4 of laminated composite $[45/0/-45/90]_s$ ($V_f = 50\%$)

Case 2: $V_f = 70\%$

Figure (5-8) and (5-9) show the damage progression of CFRP $[45/0-45/90]_s$ with $V_f = 70\%$. Compared to $V_f = 60\%$, the damage in four plies of $V_f = 70\%$ show the change in direction. All plies failed by J_I matrix.

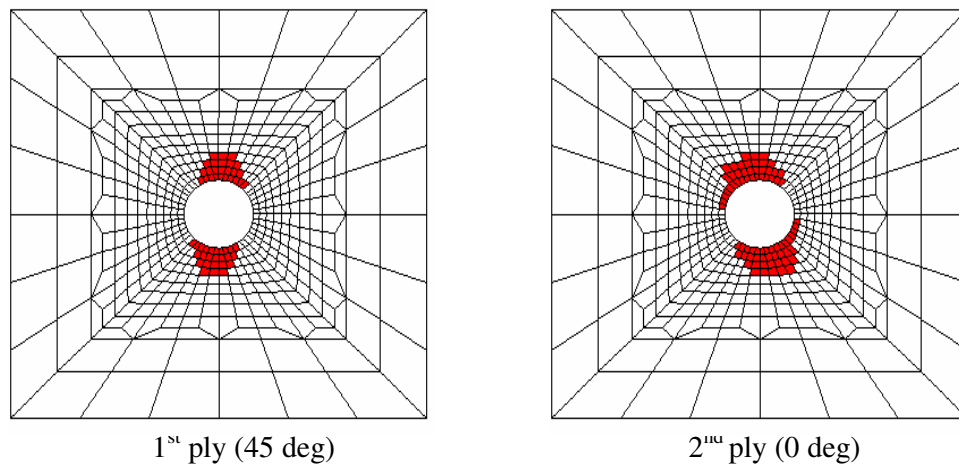


Figure 5-8. Damage progression of ply-1 and ply-2 of laminated composite $[45/0/-45/90]_s$ ($V_f = 70\%$)

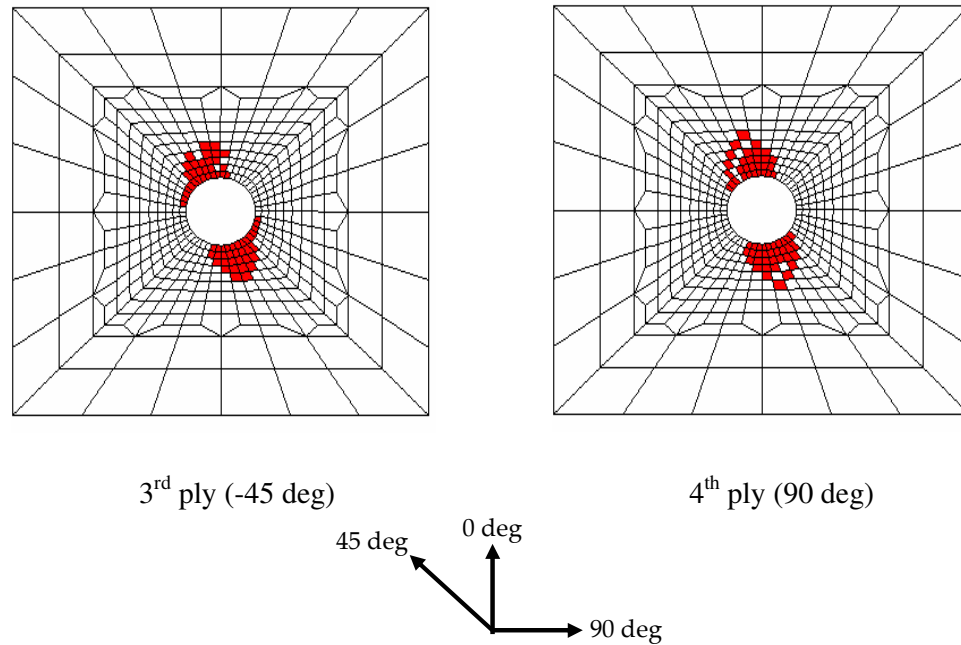
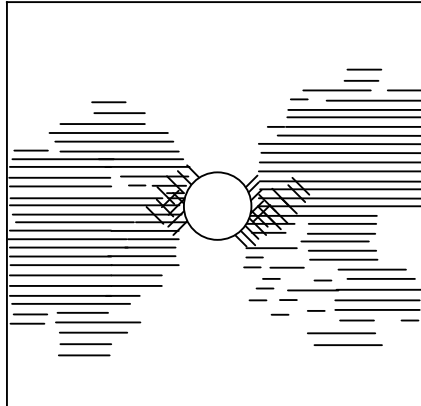


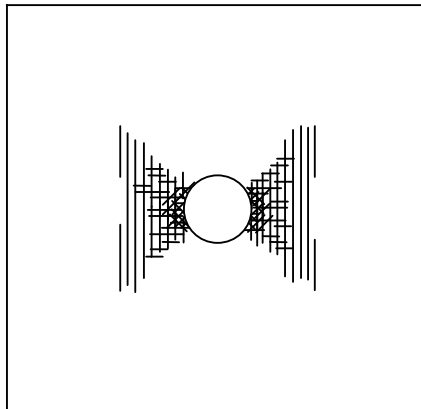
Figure 5-9. Damage progression of ply-3 and ply-4 of laminated composite $[45/0/-45/90]_s$ ($V_f = 70\%$)

Critical strain invariant were set to be constant (valid for $V_f = 60\%$) and only strain amplification factors were changed. The qualitative comparison is made in terms of the damage pattern. Damage pattern for three cases can be seen in Figure (5-10). It shows that damage pattern of Case 1 ($V_f = 50\%$) shows the largest damage, while Case 2 ($V_f = 70\%$) and Case Reference ($V_f = 60\%$) show smaller damage. This qualitative comparison shows that the damage progression in composites is function of volume fraction. Increasing fiber volume fraction from 60% to 70% will change the location of damage progression.

$V_f = 50\%$



$V_f = 60\%$



$V_f = 70\%$

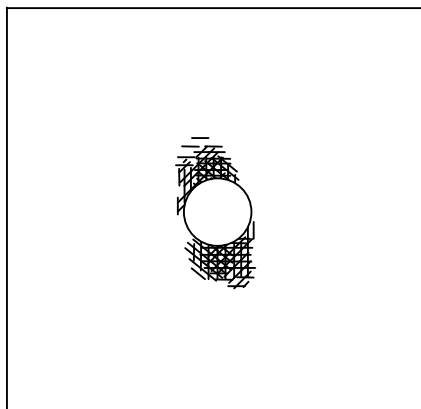


Figure 5-10. Superimposed damage patterns of CFRP [45/0/-45/90]_s for $V_f = 50\%$, $V_f = 60\%$ and $V_f = 70\%$.

CHAPTER 6

CONCLUSIONS AND RECOMMENDATIONS

6.1 Conclusions

The central goals of this research have been to obtain strain amplification factors that can be used to implement strain invariant failure theory in analyzing failure in composite structures. Three representative volume elements, namely square, hexagonal and diamond arrays were built and analyzed using three-dimensional finite element method. The research was carried out to investigate the effect of fiber volume fraction and fiber material properties with respect to the strain amplification factors. The strain amplification factors obtained were also implemented to study the damage propagation of open-hole tension specimen. Conclusions are described as follow:

1. Strain amplification factors are obtained from representative volume elements of square, hexagonal and diamond arrays with fiber volume fraction of 50%, 60% and 70%, and stored as a subroutine in the appendix.
2. Single cell and multi cell of square array produce similar results of strain amplification factors, and the highest values of amplification factors are 4.705 (single cell) and 4.662 (multi cell). These highest values occur in the fiber-matrix interface of M1 and M5. The highest amplification factors suggest that the failure of composite will likely to occur at M1 and M5.
3. Three fiber packing arrays of square, hexagonal and diamond have shown variation in terms of mechanical and thermo-mechanical amplification

factors. The variation is due to (1) the difference of defining the locations of both interstitial and interfiber for square, hexagonal and diamond, (2) the distance between two closest fibers, which gives rise to different strain magnitude.

4. The maximum amplification factors appear in the interfiber regions (IF1 and IF2) for transverse loading (direction-2 and direction-3) and this suggests that the possible failure in the matrix material occurs at these points.
5. Failure in the case of pure shear (direction-12 and direction-13) is likely to occur in the matrix (IF1 and IF2) as in the fiber-matrix interface (M1, M5, M3 and M7).
6. For direction-23 loading, failure in the matrix is more likely to be in the interstitial position (IS) although failure in the fiber-matrix interface may still occur.
7. Generally, increasing fiber volume fraction will increase maximum amplification factors.
8. Resin-rich composites (for example composite with $V_f = 50\%$) may not be more resistant to damage compared to composites with $V_f = 60\%$ and $V_f = 70\%$, because the elastic properties of composite will also change with the fiber volume fraction.
9. Changing fiber and matrix material can cause change in amplification factors especially at IF1, M1 and M5 in the matrix phase.
10. For three RVEs of square, hexagonal and diamond and also for fiber volume fraction of 50% - 70%, the damage at micro-level occurs due to in-plane shear loading (direction-12 and direction-13)

11. Damage will easily occur due to pure in-plane shear regardless the fiber arrangement or the fiber volume fraction.
12. Damage progression is predicted by element-failure method and SIFT. Specimen with $V_f = 60\%$ is used as a reference. Reducing fiber volume fraction from 60% to 50% will make the damage emanates from the notch and spread out to the entire plate. Increasing fiber volume fraction from 60% to 70% will make the damage change its shape and emanates from the top and bottom of the notch.

6.2 Recommendations

The recommendations for the future research are summarized as follow:

1. Damage progression analysis of open-hole tension specimen by using EFM-SIFT was using critical strain invariants of carbon/epoxy composites ($V_f = 60\%$) obtained from published paper. Critical strain invariant can also be obtained experimentally for the case of $V_f = 50\%$ and 70% .
2. Analysis of damage progression can be extended to study different composite system such as glass/epoxy. Again, the critical strain invariants can also be obtained for glass/epoxy.

REFERENCES

- [1] Hinton M. J. & Soden P. D. Predicting Failure in Composite Laminates: The Background to the Exercise, *Composite Science & Tech.*, Vol. 58, pp. 1001 – 1010, 1998.
- [2] Soden P. D., Hinton M. J. & Kaddour A. S. Lamina Properties, Lay-Up Configurations and Loading Conditions for A Range of Fibre-Reinforced Composite Laminates, *Composite Science & Tech.*, Vol. 58, pp. 1011 – 1022, 1998.
- [3] Soden P. D., Hinton M. J. & Kaddour A. S. A Comparison of the Predictive Capabilities of Current Failure Theories for Composite Laminates, *Composite Science & Tech.*, Vol. 58, pp. 1225 – 1254, 1998.
- [4] Kaddour A. S., Hinton M. J. & Soden P. D. A Comparison of the Predictive Capabilities of Current Failure Theories for Composite Laminates: Additional Contributions, *Composite Science & Tech.*, Vol. 64, pp. 449 – 476, 2004.
- [5] Soden P. D, Kaddour A. S. & Hinton M. J. Recommendations for Designers and Researchers Resulting from the World-Wide Failure Exercise, *Composite Science & Tech.*, Vol. 64, pp. 589 – 604, 2004.
- [6] Christensen R. M. A Survey of and Evaluation Methodology for Fiber Composite Material Failure Theories. Proc. of 20th ICTAM, Kluwer Academic Publisher, Netherlands, 2001.
- [7] Rousseau, C. Q. A Range of Practical Failure Criteria for Laminated Composites, *Composite Structures: Theory and Practices*, Peter Grant and Carl. Q. Rousseau, editors. West Conshohocken, PA: ASTM, 2001.

- [8] Gosse J. H., Christensen S. Strain Invariant Failure Criteria for Polymers in Composite Materials, *AIAA-2001-1184*, 2001.
- [9] Gosse J. H., Christensen S., Hart-Smith J., Wollschlager J. A. Strain Invariant Failure Theory. Part 1: Damage Initiation in Composite Materials, 6th Composite Durability Workshop (CDW-6), Tokyo, Japan, November 14-15, 2002.
- [10] Tay T. E., Tan S. H. N., Tan V. B. C. and Gosse J. H. Damage Progression by the Element-Failure Method (EFM) and Strain Invariant Failure Theory (SIFT), *Composite Science and Technology*, vol. 65, pp. 935-944, 2005.
- [11] Tay T. E., Liu G., Yudhanto A. and Tan V. B. C. A Multi-Scale Approach to Modeling Progressive Damage in Composite Structures. (*Submitted to Journal of Damage Mechanics, 2005*)
- [12] Li R., Kelly D., Crosky A. An Evaluation of Failure Criteria for Matrix Induced Failure in Composite Materials, *Composite Structures*, Vol. 57, pp. 385 – 391, 2002.
- [13] Li R., Kelly D., Ness R. Application of a First Invariant Strain Criterion for Matrix Failure in Composite Materials, *Journal of Composite Materials*, Vol. 37, No. 22, pp. 1977 – 1998, 2003.
- [14] Hill R. Elastic Properties of Reinforced Solids: Some Theoretical Principles. *J. Mech. Phys. Solids*, Vol. 11, pp. 357 – 372, 1963.
- [15] Budiansky B. Micromechanics. *Computers & Structures*, Vol. 16, No. 1 – 4, pp. 3 – 12, 1983.
- [16] Christensen R M. A Critical Evaluation for A Class of Micromechanics Models. *J. Mech. Phys. Solids*, Vol. 38, No. 3, pp. 379 – 404, 1990.

- [17] Christensen R. M. Two Theoretical Elasticity Micromechanics Models. *J. Elasticity*, Vol. 50, pp. 15 – 25, 1998.
- [18] Sun C. T. and Vaidya R. S. Prediction of Composite Properties from a Representative Volume Element, *Composites Science and Tech.*, Vol. 56, pp. 171 – 179, 1996.
- [19] Gibson R. F. Principles of Composite Material Mechanics, McGraw-Hill Int'l Ed., 1994.
- [20] Kawabata S., Niwa M. and Yamashita Y. Recent Developments in the Evaluation Technology of Fiber and Textiles: Toward the Engineered Design of Textile Performance. *J. Applied Polymer Science*, Vol. 83, pp. 687 – 702, 2002.
- [21] Huang Z. M. Micromechanical Prediction of Ultimate Strength of Transversely Isotropic Fibrous Composites. *Int. J. Solids and Structures*, Vol. 38, pp. 4147 – 4172, 2001.
- [22] Huang Z. M. A Bridging Model Prediction of the Ultimate Strength of Composite Laminates Subjected to Biaxial Loads. *Composite Sci. Tech.*, Vol. 64, pp. 395 – 448, 2004a.
- [23] Huang Z. M. Correlation of the Bridging Model Predictions of the Biaxial Failure Strength of Fibrous Laminates with Experiments, *Composite Sci. Tech.*, Vol. 64, pp. 529 – 548, 2004b.
- [24] Mayes J. S. and Hansen A. C. Composite Laminate Failure Analysis using Multicontinuum Theory. *Composites Sci. Tech.*, Vol. 64, pp. 379 – 394, 2004.
- [25] Mayes J. S. and Hansen A. C. A Comparison of Multicontinuum Theory Based Failure Simulation with Experimental Results. *Composites Sci. Tech.*, Vol. 64, pp. 517 – 527, 2004.

- [26] Asp L. E., Berglund L. A. and Talreja R. A Criterion for Crack Initiation in Glassy Polymers Subjected to A Composite-Like Stress State, *Composite Sci. & Tech.*, Vol. 56, pp. 1089 – 1097, 1996.
- [27] Ha, S. K. Micromechanics in the Analysis of Composite Structures, 6th Composite Durability Workshop (CDW-6), Tokyo, Japan, November 14 – 15, 2002.
- [28] Aboudi J. Micromechanical Analysis of the Strength of Unidirectional Fiber Composites, *Composite Science & Tech.*, Vol. 33, pp. 79 – 96, 1988.
- [29] Ford H. and Anderson J. Advance Mechanics of Materials. 2nd Edition, Ellis Horwood Ltd., 1977.
- [30] Tserpes K. I., Papanikos P. and Kermanidis T., "A Three Dimensional Progressive Damage Model for Bolted Joints in Composite Laminates", *Fatigue Fracture Engineering Materials Structures*, Vol. 24, pp. 663 – 675, 2001.
- [31] Camanho P. P. and Matthews F. L., "A Progressive Damage Model for Mechanically Fastened Joints in Composite Laminates", *Journal of Composite Materials*, Vol. 33, No. 24, pp. 2248 – 2279, 1999.
- [32] Shokrieh M. M. and Lessard L. B., "Progressive Fatigue Damage Modeling of Composite Materials, Part I: Modeling", *Journal of Composite Materials*, Vol. 34, No. 13, pp. 1056 – 1079, 2000.

APPENDIX A

Mechanical and Thermo-Mechanical Strain Amplification Factors for $V_f = 50\%$

Strain Amplification Factors at Matrix Phase

```
! square array, IS
  mfact(1,1) = 1
  mfact(1,2) = 0.899
  mfact(1,3) = 0.899
  mfact(1,4) = 1.578
  mfact(1,5) = 2.280
  mfact(1,6) = 1.465
  tfact(1,1) = temperaturefactor * 0.014317
  tfact(1,2) = temperaturefactor * 0.010302
  tfact(1,3) = temperaturefactor * 0.010302
  tfact(1,4) = temperaturefactor * 0
  tfact(1,5) = temperaturefactor * 0
  tfact(1,6) = temperaturefactor * 0

! square array, IF1
  mfact(2,1) = 1
  mfact(2,2) = 2.494
  mfact(2,3) = 0.928
  mfact(2,4) = 3.308
  mfact(2,5) = 1.560
  mfact(2,6) = 0.450
  tfact(2,1) = temperaturefactor * 0.014317
  tfact(2,2) = temperaturefactor * (-0.005781)
  tfact(2,3) = temperaturefactor * 0.021477
  tfact(2,4) = temperaturefactor * 0
  tfact(2,5) = temperaturefactor * 0
  tfact(2,6) = temperaturefactor * 0

! square array, IF2
  mfact(3,1) = 1
  mfact(3,2) = 0.928
  mfact(3,3) = 2.494
  mfact(3,4) = 0.316
  mfact(3,5) = 1.506
  mfact(3,6) = 2.854
  tfact(3,1) = temperaturefactor * 0.014317
  tfact(3,2) = temperaturefactor * 0.021477
  tfact(3,3) = temperaturefactor * (-0.005781)
  tfact(3,4) = temperaturefactor * 0
  tfact(3,5) = temperaturefactor * 0
  tfact(3,6) = temperaturefactor * 0
```

```
! hexagonal array, IS
  mfact(4,1) = 1
  mfact(4,2) = 1.341
  mfact(4,3) = 1.371
  mfact(4,4) = 1.583
  mfact(4,5) = 1.356
  mfact(4,6) = 1.631
  tfact(4,1) = temperaturefactor * 0.01431704
  tfact(4,2) = temperaturefactor * 0.01006270
  tfact(4,3) = temperaturefactor * 0.007904
  tfact(4,4) = temperaturefactor * (-0.00000003)
  tfact(4,5) = temperaturefactor * 0.00000001
  tfact(4,6) = temperaturefactor * 0

! hexagonal array, IF1
  mfact(5,1) = 1
  mfact(5,2) = 1.261
  mfact(5,3) = 2.346
  mfact(5,4) = 0.508
  mfact(5,5) = 1.151
  mfact(5,6) = 2.710
  tfact(5,1) = temperaturefactor * 0.01431706
  tfact(5,2) = temperaturefactor * 0.01867971
  tfact(5,3) = temperaturefactor * (-0.000025)
  tfact(5,4) = temperaturefactor * (-0.00000002)
  tfact(5,5) = temperaturefactor * 0
  tfact(5,6) = temperaturefactor * 0

! hexagonal array, IF2
  mfact(6,1) = 1
  mfact(6,2) = 1.696
  mfact(6,3) = 1.141
  mfact(6,4) = 2.061
  mfact(6,5) = 1.948
  mfact(6,6) = 1.138
  tfact(6,1) = temperaturefactor * 0.01431705
  tfact(6,2) = temperaturefactor * 0.00508236
  tfact(6,3) = temperaturefactor * 0.013298
  tfact(6,4) = temperaturefactor * 0
  tfact(6,5) = temperaturefactor * 0.01333343
  tfact(6,6) = temperaturefactor * 0

! diamond array, IS
  mfact(7,1) = 1
  mfact(7,2) = 1.818
  mfact(7,3) = 1.818
  mfact(7,4) = 1.676
  mfact(7,5) = 0.462
  mfact(7,6) = 1.555
  tfact(7,1) = temperaturefactor * 0.014317
  tfact(7,2) = temperaturefactor * 0.008204
  tfact(7,3) = temperaturefactor * 0.008204
  tfact(7,4) = temperaturefactor * 0
  tfact(7,5) = temperaturefactor * 0.024843
  tfact(7,6) = temperaturefactor * 0
```



```
! diamond array, IF1
  mfact(8,1) = 1
  mfact(8,2) = 1.445
  mfact(8,3) = 1.445
  mfact(8,4) = 1.934
  mfact(8,5) = 2.046
  mfact(8,6) = 1.762
  tfact(8,1) = temperaturefactor * 0.014317
  tfact(8,2) = temperaturefactor * 0.009799
  tfact(8,3) = temperaturefactor * 0.009799
  tfact(8,4) = temperaturefactor * 0
  tfact(8,5) = temperaturefactor * 0.024843
  tfact(8,6) = temperaturefactor * 0

! diamond array, IF2
  mfact(9,1) = 1
  mfact(9,2) = 1.445
  mfact(9,3) = 1.445
  mfact(9,4) = 1.934
  mfact(9,5) = 2.046
  mfact(9,6) = 1.762
  tfact(9,1) = temperaturefactor * 0.014317
  tfact(9,2) = temperaturefactor * 0.008204
  tfact(9,3) = temperaturefactor * 0.008204
  tfact(9,4) = temperaturefactor * 0
  tfact(9,5) = temperaturefactor * (-0.024843)
  tfact(9,6) = temperaturefactor * 0
```

Strain Amplification Factors at Fiber Phase

```
! diamond array

!F1
  mfact(10,1) = 1
  mfact(10,2) = 0.492
  mfact(10,3) = 0.622
  mfact(10,4) = 0.327
  mfact(10,5) = 0.464
  mfact(10,6) = 0.599
  tfact(10,1) = temperaturefactor * 0
  tfact(10,2) = temperaturefactor * 0.006586
  tfact(10,3) = temperaturefactor * 0.003849
  tfact(10,4) = temperaturefactor * 0
  tfact(10,5) = temperaturefactor * 0
  tfact(10,6) = temperaturefactor * 0

!F2
  mfact(11,1) = 1
  mfact(11,2) = 0.524
  mfact(11,3) = 0.524
  mfact(11,4) = 0.413
  mfact(11,5) = 0.546
  mfact(11,6) = 0.525
  tfact(11,1) = temperaturefactor * 0
  tfact(11,2) = temperaturefactor * 0.004928
  tfact(11,3) = temperaturefactor * 0.004928
  tfact(11,4) = temperaturefactor * 0.003260
  tfact(11,5) = temperaturefactor * 0
  tfact(11,6) = temperaturefactor * 0
```

!F3

mfact (12,1) = 1
mfact (12,2) = 0.622
mfact (12,3) = 0.492
mfact (12,4) = 0.485
mfact (12,5) = 0.464
mfact (12,6) = 0.442
tfact (12,1) = temperaturefactor * 0
tfact (12,2) = temperaturefactor * 0.003849
tfact (12,3) = temperaturefactor * 0.006586
tfact (12,4) = temperaturefactor * 0
tfact (12,5) = temperaturefactor * 0
tfact (12,6) = temperaturefactor * 0

!F4

mfact (13,1) = 1
mfact (13,2) = 0.524
mfact (13,3) = 0.524
mfact (13,4) = 0.413
mfact (13,5) = 0.546
mfact (13,6) = 0.525
tfact (13,1) = temperaturefactor * 0
tfact (13,2) = temperaturefactor * 0.004928
tfact (13,3) = temperaturefactor * 0.004928
tfact (13,4) = temperaturefactor * (-0.003260)
tfact (13,5) = temperaturefactor * 0
tfact (13,6) = temperaturefactor * 0

!F5

mfact (14,1) = 1
mfact (14,2) = 0.492
mfact (14,3) = 0.622
mfact (14,4) = 0.327
mfact (14,5) = 0.464
mfact (14,6) = 0.599
tfact (14,1) = temperaturefactor * 0
tfact (14,2) = temperaturefactor * 0.006586
tfact (14,3) = temperaturefactor * 0.003849
tfact (14,4) = temperaturefactor * 0
tfact (14,5) = temperaturefactor * 0
tfact (14,6) = temperaturefactor * 0

!F6

mfact (15,1) = 1
mfact (15,2) = 0.524
mfact (15,3) = 0.524
mfact (15,4) = 0.413
mfact (15,5) = 0.546
mfact (15,6) = 0.525
tfact (15,1) = temperaturefactor * 0
tfact (15,2) = temperaturefactor * 0.004928
tfact (15,3) = temperaturefactor * 0.004928
tfact (15,4) = temperaturefactor * 0.003260
tfact (15,5) = temperaturefactor * 0
tfact (15,6) = temperaturefactor * 0

```
!F7
mfact (16,1) = 1
mfact (16,2) = 0.622
mfact (16,3) = 0.492
mfact (16,4) = 0.485
mfact (16,5) = 0.464
mfact (16,6) = 0.442
tfact (16,1) = temperaturefactor * 0
tfact (16,2) = temperaturefactor * 0.003849
tfact (16,3) = temperaturefactor * 0.006586
tfact (16,4) = temperaturefactor * 0
tfact (16,5) = temperaturefactor * 0
tfact (16,6) = temperaturefactor * 0

!F8
mfact (17,1) = 1
mfact (17,2) = 0.524
mfact (17,3) = 0.524
mfact (17,4) = 0.413
mfact (17,5) = 0.546
mfact (17,6) = 0.525
tfact (17,1) = temperaturefactor * 0
tfact (17,2) = temperaturefactor * 0.004928
tfact (17,3) = temperaturefactor * 0.004928
tfact (17,4) = temperaturefactor * (-0.003260)
tfact (17,5) = temperaturefactor * 0
tfact (17,6) = temperaturefactor * 0

!F9
mfact (18,1) = 1
mfact (18,2) = 0.489
mfact (18,3) = 0.489
mfact (18,4) = 0.390
mfact (18,5) = 0.658
mfact (18,6) = 0.537
tfact (18,1) = temperaturefactor * 0
tfact (18,2) = temperaturefactor * 0.005079
tfact (18,3) = temperaturefactor * 0.005079
tfact (18,4) = temperaturefactor * 0
tfact (18,5) = temperaturefactor * 0
tfact (18,6) = temperaturefactor * 0

! square array

!F1
mfact (19,1) = 1
mfact (19,2) = 0.699
mfact (19,3) = 0.508
mfact (19,4) = 0.458
mfact (19,5) = 0.380
mfact (19,6) = 0.421
tfact (19,1) = temperaturefactor * 0
tfact (19,2) = temperaturefactor * 0.003657
tfact (19,3) = temperaturefactor * 0.006273
tfact (19,4) = temperaturefactor * 0
tfact (19,5) = temperaturefactor * 0
tfact (19,6) = temperaturefactor * 0
```

```
!F2
mfact (20,1) = 1
mfact (20,2) = 0.566
mfact (20,3) = 0.566
mfact (20,4) = 0.368
mfact (20,5) = 0.452
mfact (20,6) = 0.505
tfact (20,1) = temperaturefactor * 0
tfact (20,2) = temperaturefactor * 0.005193
tfact (20,3) = temperaturefactor * 0.005193
tfact (20,4) = temperaturefactor * 0
tfact (20,5) = temperaturefactor * 0.002376
tfact (20,6) = temperaturefactor * 0

!F3
mfact (21,1) = 1
mfact (21,2) = 0.508
mfact (21,3) = 0.699
mfact (21,4) = 0.281
mfact (21,5) = 0.380
mfact (21,6) = 0.597
tfact (21,1) = temperaturefactor * 0
tfact (21,2) = temperaturefactor * 0.006273
tfact (21,3) = temperaturefactor * 0.003657
tfact (21,4) = temperaturefactor * 0
tfact (21,5) = temperaturefactor * 0
tfact (21,6) = temperaturefactor * 0

!F4
mfact (22,1) = 1
mfact (20,2) = 0.566
mfact (20,3) = 0.566
mfact (20,4) = 0.368
mfact (20,5) = 0.452
mfact (20,6) = 0.505
tfact (22,1) = temperaturefactor * 0
tfact (22,2) = temperaturefactor * 0.005193
tfact (22,3) = temperaturefactor * 0.005193
tfact (22,4) = temperaturefactor * 0
tfact (22,5) = temperaturefactor * (-0.002377)
tfact (22,6) = temperaturefactor * 0

!F5
mfact (23,1) = 1
mfact (23,2) = 0.699
mfact (23,3) = 0.508
mfact (23,4) = 0.458
mfact (23,5) = 0.380
mfact (23,6) = 0.421
tfact (23,1) = temperaturefactor * 0
tfact (23,2) = temperaturefactor * 0.003657
tfact (23,3) = temperaturefactor * 0.006273
tfact (23,4) = temperaturefactor * 0
tfact (23,5) = temperaturefactor * 0
tfact (23,6) = temperaturefactor * 0
```

```
!F6
mfact (24,1) = 1
mfact (20,2) = 0.566
mfact (20,3) = 0.566
mfact (20,4) = 0.368
mfact (20,5) = 0.452
mfact (20,6) = 0.505
tfact (24,1) = temperaturefactor * 0
tfact (24,2) = temperaturefactor * 0.005193
tfact (24,3) = temperaturefactor * 0.005193
tfact (24,4) = temperaturefactor * 0
tfact (24,5) = temperaturefactor * 0.002378
tfact (24,6) = temperaturefactor * 0

!F7
mfact (25,1) = 1
mfact (25,2) = 0.508
mfact (25,3) = 0.699
mfact (25,4) = 0.281
mfact (25,5) = 0.380
mfact (25,6) = 0.597
tfact (25,1) = temperaturefactor * 0
tfact (25,2) = temperaturefactor * 0.006273
tfact (25,3) = temperaturefactor * 0.003657
tfact (25,4) = temperaturefactor * 0
tfact (25,5) = temperaturefactor * 0
tfact (25,6) = temperaturefactor * 0

!F8
mfact (26,1) = 1
mfact (20,2) = 0.566
mfact (20,3) = 0.566
mfact (20,4) = 0.368
mfact (20,5) = 0.452
mfact (20,6) = 0.505
tfact (26,1) = temperaturefactor * 0
tfact (26,2) = temperaturefactor * 0.005193
tfact (26,3) = temperaturefactor * 0.005193
tfact (26,4) = temperaturefactor * 0
tfact (26,5) = temperaturefactor * (-0.002377)
tfact (26,6) = temperaturefactor * 0

!F9
mfact (27,1) = 1
mfact (27,2) = 0.658
mfact (27,3) = 0.658
mfact (27,4) = 0.382
mfact (27,5) = 0.313
mfact (27,6) = 0.489
tfact (27,1) = temperaturefactor * 0
tfact (27,2) = temperaturefactor * 0.005141
tfact (27,3) = temperaturefactor * 0.005141
tfact (27,4) = temperaturefactor * 0
tfact (27,5) = temperaturefactor * 0
tfact (27,6) = temperaturefactor * 0
```

```
! hexagonal array
!F1
  mfact (28,1) = 1
  mfact (28,2) = 0.477
  mfact (28,3) = 0.506
  mfact (28,4) = 0.348
  mfact (28,5) = 0.564
  mfact (28,6) = 0.394
  tfact (28,1) = temperaturefactor * 0
  tfact (28,2) = temperaturefactor * 0.0055846
  tfact (28,3) = temperaturefactor * 0.004587
  tfact (28,4) = temperaturefactor * (-0.00000004)
  tfact (28,5) = temperaturefactor * 0
  tfact (28,6) = temperaturefactor * 0
!F2
  mfact (29,1) = 1
  mfact (29,2) = 0.579
  mfact (29,3) = 0.531
  mfact (29,4) = 0.396
  mfact (29,5) = 0.462
  mfact (29,6) = 0.343
  tfact (29,1) = temperaturefactor * 0
  tfact (29,2) = temperaturefactor * 0.00479629
  tfact (29,3) = temperaturefactor * 0.005510
  tfact (29,4) = temperaturefactor * (-0.00028540)
  tfact (29,5) = temperaturefactor * 0
  tfact (29,6) = temperaturefactor * 0
!F3
  mfact (30,1) = 1
  mfact (30,2) = 0.580
  mfact (30,3) = 0.638
  mfact (30,4) = 0.344
  mfact (30,5) = 0.332
  mfact (30,6) = 0.391
  tfact (30,1) = temperaturefactor * 0
  tfact (30,2) = temperaturefactor * 0.00560928
  tfact (30,3) = temperaturefactor * 0.004844
  tfact (30,4) = temperaturefactor * 0
  tfact (30,5) = temperaturefactor * 0
  tfact (30,6) = temperaturefactor * 0
!F4
  mfact (31,1) = 1
  mfact (29,2) = 0.579
  mfact (29,3) = 0.531
  mfact (29,4) = 0.396
  mfact (29,5) = 0.462
  mfact (29,6) = 0.343
  tfact (31,1) = temperaturefactor * 0
  tfact (31,2) = temperaturefactor * 0.00479629
  tfact (31,3) = temperaturefactor * 0.005510
  tfact (31,4) = temperaturefactor * 0.00028541
  tfact (31,5) = temperaturefactor * 0
  tfact (31,6) = temperaturefactor * 0
```

```
!F5
mfact (32,1) = 1
mfact (28,2) = 0.477
mfact (28,3) = 0.506
mfact (28,4) = 0.348
mfact (28,5) = 0.564
mfact (28,6) = 0.394
tfact (32,1) = temperaturefactor * 0
tfact (32,2) = temperaturefactor * 0.00558460
tfact (32,3) = temperaturefactor * 0.004587
tfact (32,4) = temperaturefactor * 0.00000004
tfact (32,5) = temperaturefactor * 0
tfact (32,6) = temperaturefactor * 0

!F6
mfact (33,1) = 1
mfact (29,2) = 0.579
mfact (29,3) = 0.531
mfact (29,4) = 0.396
mfact (29,5) = 0.462
mfact (29,6) = 0.343
tfact (33,1) = temperaturefactor * 0
tfact (33,2) = temperaturefactor * 0.00479631
tfact (33,3) = temperaturefactor * 0.005510
tfact (33,4) = temperaturefactor * (-0.00028508)
tfact (33,5) = temperaturefactor * 0
tfact (33,6) = temperaturefactor * 0

!F7
mfact (34,1) = 1
mfact (34,2) = 0.568
mfact (34,3) = 0.638
mfact (34,4) = 0.344
mfact (34,5) = 0.332
mfact (34,6) = 0.391
tfact (34,1) = temperaturefactor * 0
tfact (34,2) = temperaturefactor * 0.00560930
tfact (34,3) = temperaturefactor * 0.004844
tfact (34,4) = temperaturefactor * 0
tfact (34,5) = temperaturefactor * 0
tfact (34,6) = temperaturefactor * 0

!F8
mfact (35,1) = 1
mfact (29,2) = 0.579
mfact (29,3) = 0.531
mfact (29,4) = 0.396
mfact (29,5) = 0.462
mfact (29,6) = 0.343
tfact (35,1) = temperaturefactor * 0
tfact (35,2) = temperaturefactor * 0.00479631
tfact (35,3) = temperaturefactor * 0.005510
tfact (35,4) = temperaturefactor * 0.00028507
tfact (35,5) = temperaturefactor * 0
tfact (35,6) = temperaturefactor * 0
```

!F9

```
mfact(36,1) = 1
mfact(36,2) = 0.565
mfact(36,3) = 0.563
mfact(36,4) = 0.369
mfact(36,5) = 0.468
mfact(36,6) = 0.368
tfact(36,1) = temperaturefactor * 0
tfact(36,2) = temperaturefactor * 0.00519100
tfact(36,3) = temperaturefactor * 0.005229
tfact(36,4) = temperaturefactor * 0
tfact(36,5) = temperaturefactor * 0
tfact(36,6) = temperaturefactor * 0
```


APPENDIX B

Mechanical and Thermo-Mechanical Strain Amplification Factors for $V_f = 60\%$

Strain Amplification Factors at Matrix Phase

```
! square array, IS
  mfact(1,1) = 1
  mfact(1,2) = 0.897
  mfact(1,3) = 0.897
  mfact(1,4) = 1.685
  mfact(1,5) = 2.623
  mfact(1,6) = 1.685
  tfact(1,1) = temperaturefactor * 0.014317
  tfact(1,2) = temperaturefactor * 0.010302
  tfact(1,3) = temperaturefactor * 0.010302
  tfact(1,4) = temperaturefactor * 0
  tfact(1,5) = temperaturefactor * 0
  tfact(1,6) = temperaturefactor * 0

! square array, IF1
  mfact(2,1) = 1
  mfact(2,2) = 2.897
  mfact(2,3) = 0.625
  mfact(2,4) = 4.639
  mfact(2,5) = 2.160
  mfact(2,6) = 0.236
  tfact(2,1) = temperaturefactor * 0.014317
  tfact(2,2) = temperaturefactor * (-0.005781)
  tfact(2,3) = temperaturefactor * 0.021477
  tfact(2,4) = temperaturefactor * 0
  tfact(2,5) = temperaturefactor * 0
  tfact(2,6) = temperaturefactor * 0

! square array, IF2
  mfact(3,1) = 1
  mfact(3,2) = 0.625
  mfact(3,3) = 2.897
  mfact(3,4) = 0.236
  mfact(3,5) = 2.160
  mfact(3,6) = 4.639
  tfact(3,1) = temperaturefactor * 0.014317
  tfact(3,2) = temperaturefactor * 0.021477
  tfact(3,3) = temperaturefactor * (-0.005781)
  tfact(3,4) = temperaturefactor * 0
  tfact(3,5) = temperaturefactor * 0
  tfact(3,6) = temperaturefactor * 0
```

```
! hexagonal array, IS
  mfact(4,1) = 1
  mfact(4,2) = 1.488
  mfact(4,3) = 1.564
  mfact(4,4) = 1.464
  mfact(4,5) = 1.564
  mfact(4,6) = 1.908
  tfact(4,1) = temperaturefactor * 0.01431704
  tfact(4,2) = temperaturefactor * 0.01006270
  tfact(4,3) = temperaturefactor * 0.007904
  tfact(4,4) = temperaturefactor * (-0.00000003)
  tfact(4,5) = temperaturefactor * 0.00000001
  tfact(4,6) = temperaturefactor * 0

! hexagonal array, IF1
  mfact(5,1) = 1
  mfact(5,2) = 1.079
  mfact(5,3) = 2.786
  mfact(5,4) = 0.293
  mfact(5,5) = 1.580
  mfact(5,6) = 3.524
  tfact(5,1) = temperaturefactor * 0.01431706
  tfact(5,2) = temperaturefactor * 0.01867971
  tfact(5,3) = temperaturefactor * (-0.000025)
  tfact(5,4) = temperaturefactor * (-0.00000002)
  tfact(5,5) = temperaturefactor * 0
  tfact(5,6) = temperaturefactor * 0

! hexagonal array, IF2
  mfact(6,1) = 1
  mfact(6,2) = 1.833
  mfact(6,3) = 1.242
  mfact(6,4) = 2.428
  mfact(6,5) = 1.242
  mfact(6,6) = 1.239
  tfact(6,1) = temperaturefactor * 0.01431705
  tfact(6,2) = temperaturefactor * 0.00508236
  tfact(6,3) = temperaturefactor * 0.013298
  tfact(6,4) = temperaturefactor * 0
  tfact(6,5) = temperaturefactor * 0.01333343
  tfact(6,6) = temperaturefactor * 0

! diamond array, IS
  mfact(7,1) = 1
  mfact(7,2) = 2.026
  mfact(7,3) = 2.026
  mfact(7,4) = 1.706
  mfact(7,5) = 0.416
  mfact(7,6) = 1.643
  tfact(7,1) = temperaturefactor * 0.014317
  tfact(7,2) = temperaturefactor * 0.010265
  tfact(7,3) = temperaturefactor * 0.010279
  tfact(7,4) = temperaturefactor * 0
  tfact(7,5) = temperaturefactor * (-0.000001)
  tfact(7,6) = temperaturefactor * 0
```

```
! diamond array, IF1
  mfact(8,1) = 1
  mfact(8,2) = 1.905
  mfact(8,3) = 1.905
  mfact(8,4) = 2.425
  mfact(8,5) = 1.892
  mfact(8,6) = 2.234
  tfact(8,1) = temperaturefactor * 0.014317
  tfact(8,2) = temperaturefactor * 0.007683
  tfact(8,3) = temperaturefactor * 0.007687
  tfact(8,4) = temperaturefactor * 0
  tfact(8,5) = temperaturefactor * (-0.027185)
  tfact(8,6) = temperaturefactor * 0

! diamond array, IF2
  mfact(9,1) = 1
  mfact(9,2) = 1.905
  mfact(9,3) = 1.905
  mfact(9,4) = 2.425
  mfact(9,5) = 1.892
  mfact(9,6) = 2.234
  tfact(9,1) = temperaturefactor * 0.014317
  tfact(9,2) = temperaturefactor * 0.008204
  tfact(9,3) = temperaturefactor * 0.008204
  tfact(9,4) = temperaturefactor * 0
  tfact(9,5) = temperaturefactor * 0.0227168
  tfact(9,6) = temperaturefactor * 0
```

Strain Amplification Factors at Fiber Phase

```
! diamond array

!F1
  mfact(10,1) = 1
  mfact(10,2) = 0.518
  mfact(10,3) = 0.758
  mfact(10,4) = 0.321
  mfact(10,5) = 0.492
  mfact(10,6) = 0.716
  tfact(10,1) = temperaturefactor * 0
  tfact(10,2) = temperaturefactor * 0.006409
  tfact(10,3) = temperaturefactor * 0.003985
  tfact(10,4) = temperaturefactor * 0
  tfact(10,5) = temperaturefactor * (-0.000003)
  tfact(10,6) = temperaturefactor * 0

!F2
  mfact(11,1) = 1
  mfact(11,2) = 0.607
  mfact(11,3) = 0.607
  mfact(11,4) = 0.480
  mfact(11,5) = 0.579
  mfact(11,6) = 0.609
  tfact(11,1) = temperaturefactor * 0
  tfact(11,2) = temperaturefactor * 0.004924
  tfact(11,3) = temperaturefactor * 0.004929
  tfact(11,4) = temperaturefactor * 0
  tfact(11,5) = temperaturefactor * 0.002562
  tfact(11,6) = temperaturefactor * 0
```

!F3

```
mfact (12,1) = 1
mfact (12,2) = 0.758
mfact (12,3) = 0.518
mfact (12,4) = 0.578
mfact (12,5) = 0.492
mfact (12,6) = 0.451
tfact (12,1) = temperaturefactor * 0
tfact (12,2) = temperaturefactor * 0.003978
tfact (12,3) = temperaturefactor * 0.006414
tfact (12,4) = temperaturefactor * 0
tfact (12,5) = temperaturefactor * (-0.000002)
tfact (12,6) = temperaturefactor * 0
```

!F4

```
mfact (13,1) = 1
mfact (13,2) = 0.607
mfact (13,3) = 0.607
mfact (13,4) = 0.480
mfact (13,5) = 0.579
mfact (13,6) = 0.609
tfact (13,1) = temperaturefactor * 0
tfact (13,2) = temperaturefactor * 0.004920
tfact (13,3) = temperaturefactor * 0.004928
tfact (13,4) = temperaturefactor * 0
tfact (13,5) = temperaturefactor * (-0.002573)
tfact (13,6) = temperaturefactor * 0
```

!F5

```
mfact (14,1) = 1
mfact (14,2) = 0.518
mfact (14,3) = 0.758
mfact (14,4) = 0.321
mfact (14,5) = 0.492
mfact (14,6) = 0.716
tfact (14,1) = temperaturefactor * 0
tfact (14,2) = temperaturefactor * 0.006411
tfact (14,3) = temperaturefactor * 0.003980
tfact (14,4) = temperaturefactor * 0
tfact (14,5) = temperaturefactor * (-0.000009)
tfact (14,6) = temperaturefactor * 0
```

!F6

```
mfact (15,1) = 1
mfact (15,2) = 0.607
mfact (15,3) = 0.607
mfact (15,4) = 0.480
mfact (15,5) = 0.579
mfact (15,6) = 0.609
tfact (15,1) = temperaturefactor * 0
tfact (15,2) = temperaturefactor * 0.004928
tfact (15,3) = temperaturefactor * 0.004926
tfact (15,4) = temperaturefactor * 0
tfact (15,5) = temperaturefactor * 0.002558
tfact (15,6) = temperaturefactor * 0
```

```
!F7
mfact (16,1) = 1
mfact (16,2) = 0.758
mfact (16,3) = 0.518
mfact (16,4) = 0.578
mfact (16,5) = 0.492
mfact (16,6) = 0.451
tfact (16,1) = temperaturefactor * 0
tfact (16,2) = temperaturefactor * 0.003984
tfact (16,3) = temperaturefactor * 0.006410
tfact (16,4) = temperaturefactor * 0
tfact (16,5) = temperaturefactor * (-0.000004)
tfact (16,6) = temperaturefactor * 0

!F8
mfact (17,1) = 1
mfact (17,2) = 0.607
mfact (17,3) = 0.607
mfact (17,4) = 0.480
mfact (17,5) = 0.579
mfact (17,6) = 0.609
tfact (17,1) = temperaturefactor * 0
tfact (17,2) = temperaturefactor * 0.004925
tfact (17,3) = temperaturefactor * 0.004926
tfact (17,4) = temperaturefactor * 0
tfact (17,5) = temperaturefactor * (-0.002568)
tfact (17,6) = temperaturefactor * 0

!F9
mfact (18,1) = 1
mfact (18,2) = 0.529
mfact (18,3) = 0.529
mfact (18,4) = 0.428
mfact (18,5) = 0.788
mfact (18,6) = 0.615
tfact (18,1) = temperaturefactor * 0
tfact (18,2) = temperaturefactor * 0.005110
tfact (18,3) = temperaturefactor * 0.005112
tfact (18,4) = temperaturefactor * 0
tfact (18,5) = temperaturefactor * (-0.000007)
tfact (18,6) = temperaturefactor * 0

! square array

!F1
mfact (19,1) = 1
mfact (19,2) = 0.824
mfact (19,3) = 0.487
mfact (19,4) = 0.605
mfact (19,5) = 0.459
mfact (19,6) = 0.315
tfact (19,1) = temperaturefactor * 0
tfact (19,2) = temperaturefactor * 0.003657
tfact (19,3) = temperaturefactor * 0.006273
tfact (19,4) = temperaturefactor * 0
tfact (19,5) = temperaturefactor * 0
tfact (19,6) = temperaturefactor * 0
```

```
!F2
mfact (20,1) = 1
mfact (20,2) = 0.612
mfact (20,3) = 0.612
mfact (20,4) = 0.439
mfact (20,5) = 0.569
mfact (20,6) = 0.439
tfact (20,1) = temperaturefactor * 0
tfact (20,2) = temperaturefactor * 0.005193
tfact (20,3) = temperaturefactor * 0.005193
tfact (20,4) = temperaturefactor * 0
tfact (20,5) = temperaturefactor * 0.002376
tfact (20,6) = temperaturefactor * 0

!F3
mfact (21,1) = 1
mfact (21,2) = 0.487
mfact (21,3) = 0.824
mfact (21,4) = 0.316
mfact (21,5) = 0.475
mfact (21,6) = 0.605
tfact (21,1) = temperaturefactor * 0
tfact (21,2) = temperaturefactor * 0.006273
tfact (21,3) = temperaturefactor * 0.003657
tfact (21,4) = temperaturefactor * 0
tfact (21,5) = temperaturefactor * 0
tfact (21,6) = temperaturefactor * 0

!F4
mfact (22,1) = 1
mfact (22,2) = 0.613
mfact (22,3) = 0.612
mfact (22,4) = 0.439
mfact (22,5) = 0.569
mfact (22,6) = 0.439
tfact (22,1) = temperaturefactor * 0
tfact (22,2) = temperaturefactor * 0.005193
tfact (22,3) = temperaturefactor * 0.005193
tfact (22,4) = temperaturefactor * 0
tfact (22,5) = temperaturefactor * (-0.002377)
tfact (22,6) = temperaturefactor * 0

!F5
mfact (23,1) = 1
mfact (23,2) = 0.824
mfact (23,3) = 0.487
mfact (23,4) = 0.605
mfact (23,5) = 0.475
mfact (23,6) = 0.316
tfact (23,1) = temperaturefactor * 0
tfact (23,2) = temperaturefactor * 0.003657
tfact (23,3) = temperaturefactor * 0.006273
tfact (23,4) = temperaturefactor * 0
tfact (23,5) = temperaturefactor * 0
tfact (23,6) = temperaturefactor * 0
```

```
!F6
mfact (24,1) = 1
mfact (24,2) = 0.612
mfact (24,3) = 0.612
mfact (24,4) = 0.439
mfact (24,5) = 0.569
mfact (24,6) = 0.439
tfact (24,1) = temperaturefactor * 0
tfact (24,2) = temperaturefactor * 0.005193
tfact (24,3) = temperaturefactor * 0.005193
tfact (24,4) = temperaturefactor * 0
tfact (24,5) = temperaturefactor * 0.002378
tfact (24,6) = temperaturefactor * 0

!F7
mfact (25,1) = 1
mfact (25,2) = 0.487
mfact (25,3) = 0.824
mfact (25,4) = 0.316
mfact (25,5) = 0.475
mfact (25,6) = 0.605
tfact (25,1) = temperaturefactor * 0
tfact (25,2) = temperaturefactor * 0.006273
tfact (25,3) = temperaturefactor * 0.003657
tfact (25,4) = temperaturefactor * 0
tfact (25,5) = temperaturefactor * 0
tfact (25,6) = temperaturefactor * 0

!F8
mfact (26,1) = 1
mfact (26,2) = 0.612
mfact (26,3) = 0.612
mfact (26,4) = 0.569
mfact (26,5) = 0.439
mfact (26,6) = 0.439
tfact (26,1) = temperaturefactor * 0
tfact (26,2) = temperaturefactor * 0.005193
tfact (26,3) = temperaturefactor * 0.005193
tfact (26,4) = temperaturefactor * 0
tfact (26,5) = temperaturefactor * (-0.002377)
tfact (26,6) = temperaturefactor * 0

!F9
mfact (27,1) = 1
mfact (27,2) = 0.749
mfact (27,3) = 0.749
mfact (27,4) = 0.440
mfact (27,5) = 0.335
mfact (27,6) = 0.440
tfact (27,1) = temperaturefactor * 0
tfact (27,2) = temperaturefactor * 0.005141
tfact (27,3) = temperaturefactor * 0.005141
tfact (27,4) = temperaturefactor * 0
tfact (27,5) = temperaturefactor * 0
tfact (27,6) = temperaturefactor * 0
```

```
! hexagonal array

!F1
mfact (28,1) = 1
mfact (28,2) = 0.495
mfact (28,3) = 0.553
mfact (28,4) = 0.332
mfact (28,5) = 0.644
mfact (28,6) = 0.482
tfact (28,1) = temperaturefactor * 0
tfact (28,2) = temperaturefactor * 0.005585
tfact (28,3) = temperaturefactor * 0.004587
tfact (28,4) = temperaturefactor * (-0.00000004)
tfact (28,5) = temperaturefactor * 0
tfact (28,6) = temperaturefactor * 0

!F2
mfact (29,1) = 1
mfact (29,2) = 0.564
mfact (29,3) = 0.666
mfact (29,4) = 0.414
mfact (29,5) = 0.510
mfact (29,6) = 0.378
tfact (29,1) = temperaturefactor * 0
tfact (29,2) = temperaturefactor * 0.004796
tfact (29,3) = temperaturefactor * 0.005510
tfact (29,4) = temperaturefactor * (-0.000285)
tfact (29,5) = temperaturefactor * 0
tfact (29,6) = temperaturefactor * 0

!F3
mfact (30,1) = 1
mfact (30,2) = 0.607
mfact (30,3) = 0.733
mfact (30,4) = 0.327
mfact (30,5) = 0.366
mfact (30,6) = 0.467
tfact (30,1) = temperaturefactor * 0
tfact (30,2) = temperaturefactor * 0.005609
tfact (30,3) = temperaturefactor * 0.004844
tfact (30,4) = temperaturefactor * 0
tfact (30,5) = temperaturefactor * 0
tfact (30,6) = temperaturefactor * 0

!F4
mfact (31,1) = 1
mfact (31,2) = 0.623
mfact (31,3) = 0.564
mfact (31,4) = 0.414
mfact (31,5) = 0.510
mfact (31,6) = 0.378
tfact (31,1) = temperaturefactor * 0
tfact (31,2) = temperaturefactor * 0.004796
tfact (31,3) = temperaturefactor * 0.005510
tfact (31,4) = temperaturefactor * 0.000285
tfact (31,5) = temperaturefactor * 0
tfact (31,6) = temperaturefactor * 0
```



```
!F5
mfact (32,1) = 1
mfact (32,2) = 0.495
mfact (32,3) = 0.553
mfact (32,4) = 0.332
mfact (32,5) = 0.644
mfact (32,6) = 0.482
tfact (32,1) = temperaturefactor * 0
tfact (32,2) = temperaturefactor * 0.005585
tfact (32,3) = temperaturefactor * 0.004587
tfact (32,4) = temperaturefactor * 0
tfact (32,5) = temperaturefactor * 0
tfact (32,6) = temperaturefactor * 0

!F6
mfact (33,1) = 1
mfact (33,2) = 0.666
mfact (33,3) = 0.564
mfact (33,4) = 0.414
mfact (33,5) = 0.510
mfact (33,6) = 0.378
tfact (33,1) = temperaturefactor * 0
tfact (33,2) = temperaturefactor * 0.004796
tfact (33,3) = temperaturefactor * 0.005510
tfact (33,4) = temperaturefactor * (-0.000285)
tfact (33,5) = temperaturefactor * 0
tfact (33,6) = temperaturefactor * 0

!F7
mfact (34,1) = 1
mfact (34,2) = 0.607
mfact (34,3) = 0.733
mfact (34,4) = 0.327
mfact (34,5) = 0.366
mfact (34,6) = 0.467
tfact (34,1) = temperaturefactor * 0
tfact (34,2) = temperaturefactor * 0.005609
tfact (34,3) = temperaturefactor * 0.004844
tfact (34,4) = temperaturefactor * 0
tfact (34,5) = temperaturefactor * 0
tfact (34,6) = temperaturefactor * 0

!F8
mfact (35,1) = 1
mfact (35,2) = 0.666
mfact (35,3) = 0.564
mfact (35,4) = 0.414
mfact (35,5) = 0.510
mfact (35,6) = 0.379
tfact (35,1) = temperaturefactor * 0
tfact (35,2) = temperaturefactor * 0.004796
tfact (35,3) = temperaturefactor * 0.005510
tfact (35,4) = temperaturefactor * 0.000285
tfact (35,5) = temperaturefactor * 0
tfact (35,6) = temperaturefactor * 0
```

!F9

```
mfact(36,1) = 1
mfact(36,2) = 0.632
mfact(36,3) = 0.628
mfact(36,4) = 0.257
mfact(36,5) = 0.553
mfact(36,6) = 0.424
tfact(36,1) = temperaturefactor * 0
tfact(36,2) = temperaturefactor * 0.005191
tfact(36,3) = temperaturefactor * 0.005229
tfact(36,4) = temperaturefactor * 0
tfact(36,5) = temperaturefactor * 0
tfact(36,6) = temperaturefactor * 0
```

APPENDIX C

Mechanical and Thermo-Mechanical Strain Amplification Factors for $V_f = 70\%$

Strain Amplification Factors at Matrix Phase

```
! square array, IS
  mfact(1,1) = 1
  mfact(1,2) = 1.050
  mfact(1,3) = 1.050
  mfact(1,4) = 1.799
  mfact(1,5) = 2.780
  mfact(1,6) = 1.799
  tfact(1,1) = temperaturefactor * 0.014317
  tfact(1,2) = temperaturefactor * 0.009653
  tfact(1,3) = temperaturefactor * 0.009653
  tfact(1,4) = temperaturefactor * 0
  tfact(1,5) = temperaturefactor * 0
  tfact(1,6) = temperaturefactor * 0

! square array, IF1
  mfact(2,1) = 1
  mfact(2,2) = 3.156
  mfact(2,3) = 0.339
  mfact(2,4) = 7.502
  mfact(2,5) = 3.747
  mfact(2,6) = 0.266
  tfact(2,1) = temperaturefactor * 0.014317
  tfact(2,2) = temperaturefactor * (-0.012840)
  tfact(2,3) = temperaturefactor * 0.020731
  tfact(2,4) = temperaturefactor * 0
  tfact(2,5) = temperaturefactor * 0
  tfact(2,6) = temperaturefactor * 0

! square array, IF2
  mfact(3,1) = 1
  mfact(3,2) = 0.339
  mfact(3,3) = 3.165
  mfact(3,4) = 0.266
  mfact(3,5) = 3.747
  mfact(3,6) = 7.502
  tfact(3,1) = temperaturefactor * 0.014317
  tfact(3,2) = temperaturefactor * 0.020731
  tfact(3,3) = temperaturefactor * (-0.012840)
  tfact(3,4) = temperaturefactor * 0
  tfact(3,5) = temperaturefactor * 0
  tfact(3,6) = temperaturefactor * 0
```

```
! hexagonal array, IS
  mfact(4,1) = 1
  mfact(4,2) = 1.153
  mfact(4,3) = 1.823
  mfact(4,4) = 1.599
  mfact(4,5) = 1.365
  mfact(4,6) = 2.093
  tfact(4,1) = temperaturefactor * 0.01431704
  tfact(4,2) = temperaturefactor * (-0.145117)
  tfact(4,3) = temperaturefactor * 2.376578
  tfact(4,4) = temperaturefactor * (-0.000001)
  tfact(4,5) = temperaturefactor * 0
  tfact(4,6) = temperaturefactor * 0

! hexagonal array, IF1
  mfact(5,1) = 1
  mfact(5,2) = 0.746
  mfact(5,3) = 2.880
  mfact(5,4) = 3.357
  mfact(5,5) = 1.690
  mfact(5,6) = 1.357
  tfact(5,1) = temperaturefactor * 0.01431706
  tfact(5,2) = temperaturefactor * (-1.057588)
  tfact(5,3) = temperaturefactor * 5.475851
  tfact(5,4) = temperaturefactor * 0
  tfact(5,5) = temperaturefactor * 0
  tfact(5,6) = temperaturefactor * 0

! hexagonal array, IF2
  mfact(6,1) = 1
  mfact(6,2) = 2.117
  mfact(6,3) = 1.467
  mfact(6,4) = 3.357
  mfact(6,5) = 1.690
  mfact(6,6) = 1.357
  tfact(6,1) = temperaturefactor * 0.01431705
  tfact(6,2) = temperaturefactor * (-0.458891)
  tfact(6,3) = temperaturefactor * 1.217131
  tfact(6,4) = temperaturefactor * (-3.290785)
  tfact(6,5) = temperaturefactor * 0
  tfact(6,6) = temperaturefactor * 0

! diamond array, IS
  mfact(7,1) = 1
  mfact(7,2) = 2.140
  mfact(7,3) = 2.140
  mfact(7,4) = 1.958
  mfact(7,5) = 0.665
  mfact(7,6) = 1.721
  tfact(7,1) = temperaturefactor * 0.014317
  tfact(7,2) = temperaturefactor * 0.009608
  tfact(7,3) = temperaturefactor * 0.009608
  tfact(7,4) = temperaturefactor * 0
  tfact(7,5) = temperaturefactor * 0
  tfact(7,6) = temperaturefactor * 0
```

```
! diamond array, IF1
  mfact(8,1) = 1
  mfact(8,2) = 2.889
  mfact(8,3) = 2.889
  mfact(8,4) = 4.010
  mfact(8,5) = 1.504
  mfact(8,6) = 3.234
  tfact(8,1) = temperaturefactor * 0.014317
  tfact(8,2) = temperaturefactor * 0.003697
  tfact(8,3) = temperaturefactor * 0.003697
  tfact(8,4) = temperaturefactor * 0
  tfact(8,5) = temperaturefactor * (-0.033631)
  tfact(8,6) = temperaturefactor * 0

! diamond array, IF2
  mfact(9,1) = 1
  mfact(9,2) = 2.889
  mfact(9,3) = 2.889
  mfact(9,4) = 4.010
  mfact(9,5) = 1.504
  mfact(9,6) = 4.010
  tfact(9,1) = temperaturefactor * 0.014317
  tfact(9,2) = temperaturefactor * 0.003697
  tfact(9,3) = temperaturefactor * 0.003697
  tfact(9,4) = temperaturefactor * 0
  tfact(9,5) = temperaturefactor * 0.033631
  tfact(9,6) = temperaturefactor * 0
```

Strain Amplification Factors at Fiber Phase

```
! diamond array

!F1
  mfact(10,1) = 1
  mfact(10,2) = 0.548
  mfact(10,3) = 0.868
  mfact(10,4) = 0.348
  mfact(10,5) = 0.496
  mfact(10,6) = 0.842
  tfact(10,1) = temperaturefactor * 0
  tfact(10,2) = temperaturefactor * 0.006326
  tfact(10,3) = temperaturefactor * 0.003360
  tfact(10,4) = temperaturefactor * 0
  tfact(10,5) = temperaturefactor * 0
  tfact(10,6) = temperaturefactor * 0

!F2
  mfact(11,1) = 1
  mfact(11,2) = 0.783
  mfact(11,3) = 0.783
  mfact(11,4) = 0.708
  mfact(11,5) = 0.548
  mfact(11,6) = 0.765
  tfact(11,1) = temperaturefactor * 0
  tfact(11,2) = temperaturefactor * 0.003606
  tfact(11,3) = temperaturefactor * 0.003606
  tfact(11,4) = temperaturefactor * 0
  tfact(11,5) = temperaturefactor * 0.004115
  tfact(11,6) = temperaturefactor * 0
```

!F3

mfact (12,1) = 1
mfact (12,2) = 0.868
mfact (12,3) = 0.548
mfact (12,4) = 0.761
mfact (12,5) = 0.496
mfact (12,6) = 0.448
tfact (12,1) = temperaturefactor * 0
tfact (12,2) = temperaturefactor * 0.003360
tfact (12,3) = temperaturefactor * 0.006326
tfact (12,4) = temperaturefactor * 0
tfact (12,5) = temperaturefactor * 0
tfact (12,6) = temperaturefactor * 0

!F4

mfact (13,1) = 1
mfact (11,2) = 0.783
mfact (11,3) = 0.783
mfact (11,4) = 0.708
mfact (11,5) = 0.548
mfact (11,6) = 0.765
tfact (13,1) = temperaturefactor * 0
tfact (13,2) = temperaturefactor * 0.003606
tfact (13,3) = temperaturefactor * 0.003606
tfact (13,4) = temperaturefactor * 0
tfact (13,5) = temperaturefactor * (-0.004115)
tfact (13,6) = temperaturefactor * 0

!F5

mfact (14,1) = 1
mfact (10,2) = 0.548
mfact (10,3) = 0.868
mfact (10,4) = 0.348
mfact (10,5) = 0.496
mfact (10,6) = 0.842
tfact (14,1) = temperaturefactor * 0
tfact (14,2) = temperaturefactor * 0.006326
tfact (14,3) = temperaturefactor * 0.003360
tfact (14,4) = temperaturefactor * 0
tfact (14,5) = temperaturefactor * 0
tfact (14,6) = temperaturefactor * 0

!F6

mfact (15,1) = 1
mfact (11,2) = 0.783
mfact (11,3) = 0.783
mfact (11,4) = 0.708
mfact (11,5) = 0.548
mfact (11,6) = 0.765
tfact (15,1) = temperaturefactor * 0
tfact (15,2) = temperaturefactor * 0.003606
tfact (15,3) = temperaturefactor * 0.003606
tfact (15,4) = temperaturefactor * 0
tfact (15,5) = temperaturefactor * 0.004115
tfact (15,6) = temperaturefactor * 0

```
!F7
mfact (16,1) = 1
mfact (12,2) = 0.868
mfact (12,3) = 0.548
mfact (12,4) = 0.761
mfact (12,5) = 0.496
mfact (12,6) = 0.448
tfact (16,1) = temperaturefactor * 0
tfact (16,2) = temperaturefactor * 0.003360
tfact (16,3) = temperaturefactor * 0.006326
tfact (16,4) = temperaturefactor * 0
tfact (16,5) = temperaturefactor * 0
tfact (16,6) = temperaturefactor * 0

!F8
mfact (17,1) = 1
mfact (11,2) = 0.783
mfact (11,3) = 0.783
mfact (11,4) = 0.708
mfact (11,5) = 0.548
mfact (11,6) = 0.765
tfact (17,1) = temperaturefactor * 0
tfact (17,2) = temperaturefactor * 0.003606
tfact (17,3) = temperaturefactor * 0.003606
tfact (17,4) = temperaturefactor * 0
tfact (17,5) = temperaturefactor * (-0.004115)
tfact (17,6) = temperaturefactor * 0

!F9
mfact (18,1) = 1
mfact (18,2) = 0.582
mfact (18,3) = 0.582
mfact (18,4) = 0.555
mfact (18,5) = 0.930
mfact (18,6) = 0.730
tfact (18,1) = temperaturefactor * 0
tfact (18,2) = temperaturefactor * 0.004367
tfact (18,3) = temperaturefactor * 0.004367
tfact (18,4) = temperaturefactor * 0
tfact (18,5) = temperaturefactor * 0
tfact (18,6) = temperaturefactor * 0

! square array

!F1
mfact (19,1) = 1
mfact (19,2) = 0.970
mfact (19,3) = 0.435
mfact (19,4) = 0.902
mfact (19,5) = 0.692
mfact (19,6) = 0.355
tfact (19,1) = temperaturefactor * 0
tfact (19,2) = temperaturefactor * 0.001627
tfact (19,3) = temperaturefactor * 0.005777
tfact (19,4) = temperaturefactor * 0
tfact (19,5) = temperaturefactor * 0
tfact (19,6) = temperaturefactor * 0
```

```
!F2
mfact (20,1) = 1
mfact (20,2) = 0.631
mfact (20,3) = 0.631
mfact (20,4) = 0.510
mfact (20,5) = 0.678
mfact (20,6) = 0.510
tfact (20,1) = temperaturefactor * 0
tfact (20,2) = temperaturefactor * 0.004838
tfact (20,3) = temperaturefactor * 0.004838
tfact (20,4) = temperaturefactor * 0
tfact (20,5) = temperaturefactor * (-0.002818)
tfact (20,6) = temperaturefactor * 0

!F3
mfact (21,1) = 1
mfact (21,2) = 0.435
mfact (21,3) = 0.970
mfact (21,4) = 0.355
mfact (21,5) = 0.692
mfact (21,6) = 0.902
tfact (21,1) = temperaturefactor * 0
tfact (21,2) = temperaturefactor * 0.005777
tfact (21,3) = temperaturefactor * 0.001627
tfact (21,4) = temperaturefactor * 0
tfact (21,5) = temperaturefactor * 0
tfact (21,6) = temperaturefactor * 0

!F4
mfact (22,1) = 1
mfact (20,2) = 0.631
mfact (20,3) = 0.631
mfact (20,4) = 0.510
mfact (20,5) = 0.678
mfact (20,6) = 0.510
tfact (22,1) = temperaturefactor * 0
tfact (22,2) = temperaturefactor * 0.004838
tfact (22,3) = temperaturefactor * 0.004838
tfact (22,4) = temperaturefactor * 0
tfact (22,5) = temperaturefactor * 0.002817
tfact (22,6) = temperaturefactor * 0

!F5
mfact (23,1) = 1
mfact (19,2) = 0.970
mfact (19,3) = 0.435
mfact (19,4) = 0.902
mfact (19,5) = 0.692
mfact (19,6) = 0.355
tfact (23,1) = temperaturefactor * 0
tfact (23,2) = temperaturefactor * 0.001627
tfact (23,3) = temperaturefactor * 0.005777
tfact (23,4) = temperaturefactor * 0
tfact (23,5) = temperaturefactor * 0
tfact (23,6) = temperaturefactor * 0
```



```
!F6
mfact (24,1) = 1
mfact (20,2) = 0.631
mfact (20,3) = 0.631
mfact (20,4) = 0.510
mfact (20,5) = 0.678
mfact (20,6) = 0.510
tfact (24,1) = temperaturefactor * 0
tfact (24,2) = temperaturefactor * 0.004838
tfact (24,3) = temperaturefactor * 0.004838
tfact (24,4) = temperaturefactor * 0
tfact (24,5) = temperaturefactor * (-0.002817)
tfact (24,6) = temperaturefactor * 0

!F7
mfact (25,1) = 1
mfact (21,2) = 0.435
mfact (21,3) = 0.970
mfact (21,4) = 0.355
mfact (21,5) = 0.692
mfact (21,6) = 0.902
tfact (25,1) = temperaturefactor * 0
tfact (25,2) = temperaturefactor * 0.004838
tfact (25,3) = temperaturefactor * 0.004838
tfact (25,4) = temperaturefactor * 0
tfact (25,5) = temperaturefactor * 0
tfact (25,6) = temperaturefactor * 0

!F8
mfact (26,1) = 1
mfact (20,2) = 0.631
mfact (20,3) = 0.631
mfact (20,4) = 0.510
mfact (20,5) = 0.678
mfact (20,6) = 0.510
tfact (26,1) = temperaturefactor * 0
tfact (26,2) = temperaturefactor * 0.004838
tfact (26,3) = temperaturefactor * 0.004838
tfact (26,4) = temperaturefactor * 0
tfact (26,5) = temperaturefactor * 0.002818
tfact (26,6) = temperaturefactor * 0

!F9
mfact (27,1) = 1
mfact (27,2) = 0.852
mfact (27,3) = 0.852
mfact (27,4) = 0.548
mfact (27,5) = 0.371
mfact (27,6) = 0.548
tfact (27,1) = temperaturefactor * 0
tfact (27,2) = temperaturefactor * 0.004413
tfact (27,3) = temperaturefactor * 0.004413
tfact (27,4) = temperaturefactor * 0
tfact (27,5) = temperaturefactor * 0
tfact (27,6) = temperaturefactor * 0
```

```
! hexagonal array
!F1
  mfact (28,1) = 1
  mfact (28,2) = 0.453
  mfact (28,3) = 0.638
  mfact (28,4) = 0.403
  mfact (28,5) = 0.600
  mfact (28,6) = 0.600
  tfact (28,1) = temperaturefactor * 0
  tfact (28,2) = temperaturefactor * 0.273172
  tfact (28,3) = temperaturefactor * (-0.974487)
  tfact (28,4) = temperaturefactor * 0
  tfact (28,5) = temperaturefactor * 0
  tfact (28,6) = temperaturefactor * 0
!F2
  mfact (29,1) = 1
  mfact (29,2) = 0.655
  mfact (29,3) = 0.577
  mfact (29,4) = 0.599
  mfact (29,5) = 0.505
  mfact (29,6) = 0.505
  tfact (29,1) = temperaturefactor * 0
  tfact (29,2) = temperaturefactor * 0.117534
  tfact (29,3) = temperaturefactor * (-1.192569)
  tfact (29,4) = temperaturefactor * 0.254819
  tfact (29,5) = temperaturefactor * 0
  tfact (29,6) = temperaturefactor * 0
!F3
  mfact (30,1) = 1
  mfact (30,2) = 0.530
  mfact (30,3) = 0.859
  mfact (30,4) = 0.393
  mfact (30,5) = 0.402
  mfact (30,6) = 0.402
  tfact (30,1) = temperaturefactor * 0
  tfact (30,2) = temperaturefactor * 0.073177
  tfact (30,3) = temperaturefactor * (-0.426171)
  tfact (30,4) = temperaturefactor * (-0.000001)
  tfact (30,5) = temperaturefactor * 0
  tfact (30,6) = temperaturefactor * 0
!F4
  mfact (31,1) = 1
  mfact (29,2) = 0.655
  mfact (29,3) = 0.577
  mfact (29,4) = 0.599
  mfact (29,5) = 0.505
  mfact (29,6) = 0.505
  tfact (31,1) = temperaturefactor * 0
  tfact (31,2) = temperaturefactor * 0.117533
  tfact (31,3) = temperaturefactor * (-1.192569)
  tfact (31,4) = temperaturefactor * (-0.254819)
  tfact (31,5) = temperaturefactor * 0
  tfact (31,6) = temperaturefactor * 0
```

```
!F5
mfact (32,1) = 1
mfact (28,2) = 0.453
mfact (28,3) = 0.638
mfact (28,4) = 0.403
mfact (28,5) = 0.600
mfact (28,6) = 0.600
tfact (32,1) = temperaturefactor * 0
tfact (32,2) = temperaturefactor * 0.005585
tfact (32,3) = temperaturefactor * 0.004587
tfact (32,4) = temperaturefactor * 0
tfact (32,5) = temperaturefactor * 0
tfact (32,6) = temperaturefactor * 0

!F6
mfact (33,1) = 1
mfact (29,2) = 0.655
mfact (29,3) = 0.577
mfact (29,4) = 0.599
mfact (29,5) = 0.505
mfact (29,6) = 0.505
tfact (33,1) = temperaturefactor * 0
tfact (33,2) = temperaturefactor * 0.004796
tfact (33,3) = temperaturefactor * 0.005510
tfact (33,4) = temperaturefactor * (-0.000285)
tfact (33,5) = temperaturefactor * 0
tfact (33,6) = temperaturefactor * 0

!F7
mfact (34,1) = 1
mfact (30,2) = 0.530
mfact (30,3) = 0.859
mfact (30,4) = 0.393
mfact (30,5) = 0.402
mfact (30,6) = 0.402
tfact (34,1) = temperaturefactor * 0
tfact (34,2) = temperaturefactor * 0.117533
tfact (34,3) = temperaturefactor * (-0.426178)
tfact (34,4) = temperaturefactor * 0.000001
tfact (34,5) = temperaturefactor * 0
tfact (34,6) = temperaturefactor * 0

!F8
mfact (35,1) = 1
mfact (29,2) = 0.655
mfact (29,3) = 0.577
mfact (29,4) = 0.599
mfact (29,5) = 0.505
mfact (29,6) = 0.505
tfact (35,1) = temperaturefactor * 0
tfact (35,2) = temperaturefactor * 0.117533
tfact (35,3) = temperaturefactor * (-1.192569)
tfact (35,4) = temperaturefactor * (-0.254819)
tfact (35,5) = temperaturefactor * 0
tfact (35,6) = temperaturefactor * 0
```

!F9

```
mfact(36,1) = 1
mfact(36,2) = 0.614
mfact(36,3) = 0.705
mfact(36,4) = 0.498
mfact(36,5) = 0.564
mfact(36,6) = 0.564
tfact(36,1) = temperaturefactor * 0
tfact(36,2) = temperaturefactor * 0.028983
tfact(36,3) = temperaturefactor * (-0.841999)
tfact(36,4) = temperaturefactor * 0
tfact(36,5) = temperaturefactor * 0
tfact(36,6) = temperaturefactor * 0
```